University of Alberta

Geochemical response of a potable aquifer to leakage from geologically sequestered carbon dioxide

by

Kris Draude

A thesis submitted to the Faculty of Graduate Studies and Research in partial fulfillment of the requirements for the degree of Master of Science

in

Geoenvironmental Engineering

Department of Civil and Environmental Engineering

Edmonton, Alberta

Spring 2005

Library and Archives Canada

Published Heritage Branch

395 Wellington Street
Ottawa ON K1A 0N4
Canada

Bibliothèque et Archives Canada

Direction du Patrimoine de l'édition

395, rue Wellington
Ottawa ON K1A 0N4
Canada

0-494-08048-5

Your file *Votre référence*
ISBN:
Our file *Notre reference*
ISBN:

NOTICE:
The author has granted a non-exclusive license allowing Library and Archives Canada to reproduce, publish, archive, preserve, conserve, communicate to the public by telecommunication or on the Internet, loan, distribute and sell theses worldwide, for commercial or non-commercial purposes, in microform, paper, electronic and/or any other formats.

The author retains copyright ownership and moral rights in this thesis. Neither the thesis nor substantial extracts from it may be printed or otherwise reproduced without the author's permission.

AVIS:
L'auteur a accordé une licence non exclusive permettant à la Bibliothèque et Archives Canada de reproduire, publier, archiver, sauvegarder, conserver, transmettre au public par télécommunication ou par l'Internet, prêter, distribuer et vendre des thèses partout dans le monde, à des fins commerciales ou autres, sur support microforme, papier, électronique et/ou autres formats.

L'auteur conserve la propriété du droit d'auteur et des droits moraux qui protège cette thèse. Ni la thèse ni des extraits substantiels de celle-ci ne doivent être imprimés ou autrement reproduits sans son autorisation.

In compliance with the Canadian Privacy Act some supporting forms may have been removed from this thesis.

While these forms may be included in the document page count, their removal does not represent any loss of content from the thesis.

Conformément à la loi canadienne sur la protection de la vie privée, quelques formulaires secondaires ont été enlevés de cette thèse.

Bien que ces formulaires aient inclus dans la pagination, il n'y aura aucun contenu manquant.

Canada

ABSTRACT

Several geochemical changes may arise should geologically sequestered carbon dioxide migrate into an overlying potable aquifer. The objective of this research project was to identify the key short-term changes. This was achieved by conducting a leaching test, a pressurized column study, and geochemical modeling.

Elevated carbon dioxide levels introduced to the groundwater resulted in a reduced pH, despite the buffering effects of the carbonate minerals. Other geochemical changes were observed, including the solubilization and precipitation of various mineral phases present in the sediment. Elements most affected were calcium, magnesium, nickel, iron, strontium, and barium, all of which underwent net dissolution, increasing their concentration in the groundwater.

The elevated bicarbonate levels caused the groundwater to become oversaturated with respect to several carbonate minerals, allowing the formation of precipitates, such as siderite. These precipitates reduced the porosity of the sediment, resulting in a net decrease in hydraulic conductivity.

ACKNOWLEDGEMENTS

I gratefully acknowledge the guidance and encouragement of my supervisor Dr. Robert Donahue, who made sure that I had access to all of the resources I needed and always made sure that I was happy doing my research.

Thank you to Steve Gamble, Gerry Cyre, and Christine Hereygers for their many hours of assistance in setting up the drilling program and especially the pressurized column study.

A special thanks to Wanda Goulden for her generous assistance with the mineralogy, and her ongoing support of my research, and for always asking the right questions.

Thank you also to PTRC for funding this research program.

TABLE OF CONTENTS

1.0 INTRODUCTION 1

1.1 General Background 1

1.2 Objective 3

1.3 Methodology 3

2.0 LITERATURE REVIEW AND BACKGROUND INFORMATION 4

2.1 Carbon Sequestration 4

2.1.1 Geologic Sequestration of Carbon Dioxide 4

2.1.2 The Concept of Geologic Carbon Sequestration 5

2.1.3 The Process of Geologic Carbon Sequestration 6

2.1.4 The Mechanisms of Geologic Carbon Sequestration 7

2.1.5 Carbon Sequestration in Enhanced Oil Recovery Operations 8

2.1.6 Geologic Carbon Sequestration for Enhanced Oil Recovery at Weyburn 8

2.1.7 Necessary Considerations for Geologic Sequestration of Carbon Dioxide 9

2.2 Geology and Mineralogy of the Weyburn Valley Aquifer 10

2.3 Carbon Dioxide 12

2.3.1 Physical Properties 12

2.3.2 Interaction with Various Minerals 13

2.4 The Geochemical Carbon Cycle 15

2.5 The Impact of Sequestered Carbon Dioxide Migration to Overlying Aquifers 20
2.5.1 Iron Mineral Dissolution and Precipitation 22
2.5.2 Aluminum Mineral Dissolution and Precipitation 24
2.6 Geochemical Modeling Using PHREEQC 26
2.6.1 Speciation and Saturation Index Calculations 27
2.6.2 Inverse Modeling 27
3.0 MATERIALS AND METHODS 29
3.1 Introduction 29
3.2 Materials 29
3.2.1 Sediment 29
3.2.2 Reagents 30
3.2.2.1 Groundwater 30
3.2.2.2 Carbonated Water 30
3.3 Methods 30
3.3.1 Drilling Program 31
3.3.1.1 Drilling 31
3.3.1.2 Sample Collection and Analysis 32
3.3.2 Leaching Test 34
3.3.2.1 Preparation of Carbonated Water Solutions 34
3.3.2.2 Preparation of Batch Reaction Systems 35
3.3.2.3 Sample Analysis 36
3.3.3 Column Study 36

3.3.3.1 Experimental Setup 36

3.3.3.2 Sample Analysis 38

3.3.4 Geochemical Modeling 39

4.0 PRESENTATION OF RESULTS 41

4.1 Drilling Program 41

4.2 Leaching Test 48

4.3 Column Study 59

4.4 Geochemical Modeling 81

5.0 SUMMARY AND RECOMMENDATIONS 85

5.1 Drilling Program 85

5.1.1 Key Findings 85

5.1.2 Recommendations 86

5.2 Leaching Test 86

5.2.1 Key Findings 87

5.2.2 Recommendations 87

5.3 Column Study 88

5.3.1 Key Findings 88

5.3.2 Recommendations 89

5.4 Geochemical Modeling 89

5.4.1 Key Findings 89

5.4.2 Recommendations 90

6.0 REFERENCES 91

APPENDIX A – ANALYTICAL METHODS 95

A1.0 Titration for Carbon Dioxide Concentration in Water 96

A2.0 Titration for Alkalinity 99

A3.0 Strong Acid Digestion of Sediments 102

A4.0 Analysis by ICP-MS 106

A5.0 Analysis by Ion Chromatography 109

APPENDIX B – DETAILED MINERALOGY 112

APPENDIX C – ADDITIONAL LEACHING TEST RESULTS 123

C1.0 Leaching Test Results for 600 mg CO_2/L Reactions 124

C2.0 Leaching Test Results for 1200 mg CO_2/L Reactions 125

APPENDIX D - PHREEQC INPUT FILES 126

APPENDIX E – CALCULATIONS 129

E1.0 Buffer Capacity 130

E2.0 Siderite Formation 132

LIST OF TABLES

Table 2.1	Underground carbon dioxide storage sites and their capacities	6
Table 2.2	Relative proportions of carbon-in its various forms	15
Table 2.3	Solubility products for various minerals	17
Table 4.1	Sediment mineralogy	43
Table 4.2	Clay mineralogy and CEC	43
Table 4.3	Acid leachable metals content in sediment	45
Table 4.4	Groundwater properties and composition	46
Table 4.5	CCME Drinking Water Guidelines	47
Table 4.6	Leaching test results for 1800 mg CO_2/L reactions	56
Table 4.7	Relative dissolution of various size fractions	58
Table 4.8	Groundwater composition throughout column study	64
Table 4.9	Elemental composition of various portions of sediment	70
Table 4.10	Mineralogy of fine sediment (before and after column study)	71
Table 4.11	Inverse modeling results	82
Table 4.12	Saturation indices	83
Table 4.13	Speciation results	84

LIST OF FIGURES

Figure 1.1	Carbon dioxide pipeline from Beulah, North Dakota to Weyburn, Saskatchwan	2
Figure 2.1	Phase diagram for carbon dioxide	12
Figure 2.2	Eh-pH diagram for carbonate system	18
Figure 2.3	log concentration-pH diagram for carbonate system	19
Figure 2.4	Solubility diagram for the Fe-H_2O-CO_2 system	24
Figure 2.5	Solubility of aluminum with respect to pH	26
Figure 3.1	Barber Ellis air rotary drilling rig	32
Figure 3.2	Schematic of column study apparatus	37
Figure 4.1	Borehole stratigraphy from drilling site	42
Figure 4.2	Particle size distribution of aquifer sediment	44
Figure 4.3	Change in electrical conductivity during leaching test	49
Figure 4.4	Change in pH during leaching test	50
Figure 4.5	Calcium concentration in solution during leaching test	51
Figure 4.6	Magnesium concentration in solution during leaching test	51
Figure 4.7	Strontium concentration in solution during leaching test	53
Figure 4.8	Barium concentration in solution during leaching test	53
Figure 4.9	Iron concentration in solution during leaching test	54
Figure 4.10	Iron precipitation observed in dilute – strong carbonated water solutions	55
Figure 4.11	Final pH for various size fractions	57

Figure 4.12	Final electrical conductivity for various size fractions	58
Figure 4.13	Carbon dioxide dissipation during leaching test	59
Figure 4.14	Column study apparatus	60
Figure 4.15	pH during column study	61
Figure 4.16	Electrical conductivity during column study	62
Figure 4.17	Bicarbonate concentration during column study	65
Figure 4.18	Calcium concentration during column study	65
Figure 4.19	Magnesium concentration during column study	66
Figure 4.20	Strontium concentration during column study	66
Figure 4.21	Barium concentration during column study	67
Figure 4.22	Iron concentration during column study	67
Figure 4.23	Siderite precipitation formed at column inlet (bottom)	68
Figure 4.24	Change in hydraulic conductivity during column study	73
Figure 4.25	SEM image of bulk sediment before column study [55X magnification]	75
Figure 4.26	SEM image of bulk sediment after column study [55X magnification]	76
Figure 4.27	SEM image of bulk sediment before column study [220X magnification]	77
Figure 4.28	SEM image of bulk sediment from bottom of column after column study [220X magnification]	78
Figure 4.29	SEM image of bulk sediment from top of column after column study [220X magnification]	79

Figure 4.30 SEM images of fine sediment (<75μm) before column study [963X magnification] 80

Figure 4.31 SEM image of fine sediment (<75μm) after column study [963X magnification] 81

1.0 INTRODUCTION

1.1 General Background

The concept of geologic sequestration of carbon dioxide is becoming increasingly attractive as atmospheric carbon dioxide levels continue to escalate.

Carbon dioxide (CO_2) can be stored in geologic formations by displacing other fluids and filling the intergranular pore space, similar to naturally occurring CO_2. The porosity of these formations can be as high as 35%, with the pore spaces typically being interconnected, thus making the rock amenable to fluid flow (Holloway, 2001). Several local factors, including formation thickness, permeability, injectivity, and geochemistry significantly influence the technical feasibility of this technology (Kane and Klein, 2001).

Storage of CO_2 in oil and gas formations is a highly favorable geologic option. These formations represent known stratigraphic traps, because the oil and gas that was originally present in these traps did not escape over geologic time. Therefore, it is conceivable that CO_2 could also be retained in these reservoirs, so long as no pathways to the surface or to adjacent formations are created through over pressurizing the reservoir, or by fracturing, or by leaks around the wells (Reichle et al., 1999). This particular means of sequestration has a double benefit, because it can increase production in nearly depleted wells, thereby extending their economic life by maintaining reservoir pressures for longer than would typically be possible. The CO_2 displaces the oil and brine for pumping, and dissolves into the oil, reducing the viscosity and allowing it to flow more easily.

EnCana is currently employing this technology in its Weyburn Project located in southeastern Saskatchewan, near the town of Weyburn. This project began operation in the fall of 2000, using CO_2 piped from a gas plant in Beulah, North Dakota (Figure 1.1). CO_2 injection in the formation will likely extend the life of this field by approximately 25 years. It is estimated that about 19 million tonnes of CO_2 will be stored, and approximately half of the injected CO_2 will dissolve and become locked up in the oil that remains in the ground (Kane and Klein, 2001).

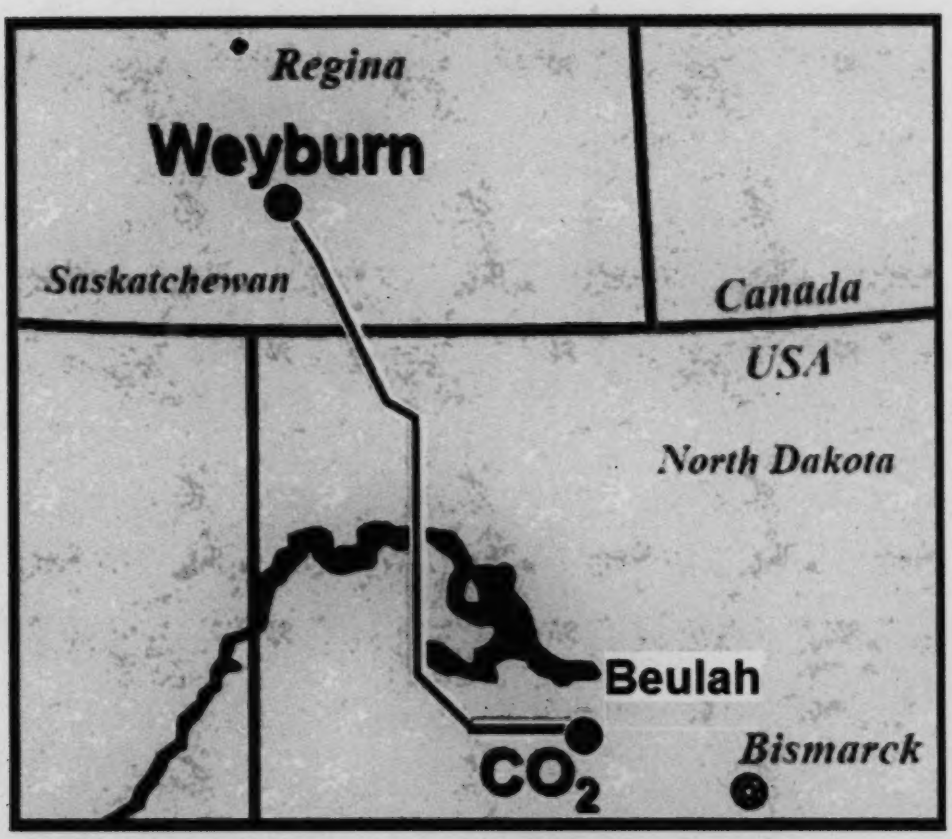

Figure 1.1 Carbon dioxide pipeline from Beulah, North Dakota to Weyburn, Saskatchewan (Modified from www.ieagreen.org.uk)

The question of whether safe and stable storage of CO_2 in the subsurface can be assured is the most important issue currently facing the underground storage of CO_2.

The mechanisms for potential leaks must be understood, in order to avoid or safely handle dangerous situations. The long-term stability of any formation being considered as a reservoir must be assessed. The structural integrity is important to ensure against a gradual return of CO_2 to the atmosphere, or a sudden release. Because CO_2 is heavier than air, a rapid, massive discharge to the surface would displace oxygen, suffocating people and wildlife that may be present (Herzog et al., 2000).

For geologic sequestration, safety has traditionally been considered to be of greater concern than environmental impact (Herzog, 2001), but the consequences to the environment must be better defined and understood. The process of sequestering CO_2 must be less damaging to the environment than its continued gradual release to the atmosphere.

1.2 Objective

The objective of this research program is to characterize the geochemical reactions that may occur in an aquifer as a result of carbon dioxide leakage from an underlying reservoir used for the geologic sequestration of CO_2.

1.3 Methodology

The research consisted of a literature review followed by a drilling program combined with laboratory experiments and some geochemical modeling. The laboratory experiments used the sediment and groundwater obtained during the drilling program and the geochemical modeling was based on the elemental composition of the groundwater before and after being exposed to elevated levels of CO_2. Chapter 2 outlines the key findings of the literature review, while Chapters 3 and 4 describe the methods, results, and interpretation respectively, for the drilling program, laboratory experiments and geochemical modeling.

2.0 LITERATURE REVIEW AND BACKGROUND INFORMATION

2.1 Carbon Sequestration

The concept of carbon sequestration was developed as a response to growing greenhouse gas emissions, of which carbon dioxide is the primary contributor. Carbon sequestration is the capture and secure storage of carbon that would otherwise be emitted to or retained in the atmosphere. This can include direct capture of CO_2 from the exhaust streams of industrial plants, or indirect capture from the atmosphere (Kane and Klein, 2001). Several different types of carbon sequestration exist, including geologic, ocean, terrestrial (soils and vegetation), and advanced biological / chemical processes for sequestration (Reichle et al., 1999).

2.1.1 Geologic Sequestration of Carbon Dioxide

Sequestration of CO_2 in the geosphere is one way of reducing emissions to the atmosphere, without having to reduce the consumption of fossil fuels. The burning of fossil fuels accounts for approximately 80% of the energy consumed worldwide, and results in the emission of about 22×10^9 tonnes of CO_2 per year (Holloway, 2001). A growth in world energy consumption of 2.3% per annum has been estimated by the Energy Information Administration (Lackner, 2002). In order for geologic sequestration of CO_2 to be effective, it must be stable enough to retain CO_2 past the end of the fossil fuel era, in the range of a few hundred to a few thousand years. The study of existing large naturally occurring CO_2 accumulations indicates that under favorable geologic conditions, CO_2 can in fact be retained in the subsurface for millions of years.

2.1.2 The Concept of Geologic Carbon Sequestration

Carbon dioxide is stored in geologic formations by displacing other fluids and filling the intergranular pore space, similar to naturally occurring CO_2. The porosity of these formations can be as high as 35%, with the pore spaces typically being interconnected, thus making the rock amenable to fluid flow (Holloway, 2001). Several local factors, including formation thickness, permeability, injectivity, and geochemistry, significantly influence the technical feasibility of this technology (Kane and Klein, 2001).

The principle of underground storage of CO_2 in reservoir rocks is that wells are drilled into the rock, and CO_2 is then injected. The CO_2 permeates the rock and displaces the fluid that was originally present in the pore spaces. In the case of low permeability, or if barriers to fluid flow exist within the formation (ie. faults that compartmentalize the reservoir), an increase in pore pressure (concentrated around the well) will be realized. This effect will limit the total volume of CO_2 that can be injected into the formation, as well as the rate at which it can be injected. Once injected, a proportion of the CO_2 will mix with and dissolve into the formation fluid. The majority of the gas however, will migrate within the reservoir, particularly towards the top, by buoyancy, until it reaches a permeability barrier or cap rock. It may then become immobilized, or it may migrate laterally if the cap rock is not perfectly horizontal or due to pressure gradients resulting from fluid flow (Holloway, 2001).

The three principle types of underground storage sites for CO_2 include depleted oil and gas fields, deep saline aquifers, and deep coal seams and coalbed methane formations. The global capacity of these storage sites, as outlined in Table 2.1, exceed the annual CO_2 emissions by almost 500 times, indicating the full potential of this method for reducing CO_2 emissions to the atmosphere (Kane and Klein, 2001).

Table 2.1 Underground carbon dioxide storage sites and their capacities

Storage Option	Approximate Global Capacity ($\times 10^9$ tonnes CO_2)
1. Depleted oil and gas fields	400 – 10,000
2. Deep saline aquifers	920
3. Deep coal seams and coalbed methane formations	15

2.1.3 The Process of Geologic Carbon Sequestration

There are three key processes involved with geologic sequestration of CO_2 – capture, purification, and injection into the formation. First, the CO_2 must be captured. It can be captured from stationary sources, such as chemical factories or electric power plants. A typical 500MW conventional coal-fired power plant fitted for CO_2 capture would make approximately 4.3 million tonnes of CO_2 per year available for sequestration (Holloway, 2001). Following capture, CO_2 is separated to at least 90% purity before being transported as a supercritical fluid by pipeline into the geologic formation. This level of purity is desirable in order to reduce the volume of gas being handled, thus reducing the costs for gas compression and transportation, improving the economic feasibility of the process (Herzog, 2001).

The technology for pumping CO_2 into the ground is quite well understood, as it is basically the reverse of pumping oil and gas out of the ground. This practice is currently quite common at many oil fields. It is estimated that in 1998, approximately 43 million tonnes of CO_2 were pumped into the ground in the US, alone (Herzog et al., 2000).

2.1.4 The Mechanisms of Geologic Carbon Sequestration

There are three primary mechanisms by which CO_2 can be sequestered in geologic formations (Benson, 2000):

1. Hydrodynamic trapping, which traps CO_2 as a gas or supercritical fluid under a low-permeability cap rock. Once outside the reach of the injection well, the CO_2 will migrate at the same speed and in the same direction as the natural fluid flow within the formation. If this migration is very slow, and the injection point is distant from the edge of the reservoir, the CO_2 may not reach this edge of the reservoir for millions of years (Holloway, 2001).
2. Solubility trapping, a mechanism which dissolves CO_2 into the fluid phase.
3. Mineral trapping, in which the CO_2 reacts with the minerals and organic matter in the geologic formation to become part of the solid mineral matrix. This is an attractive mechanism, as the safety concerns regarding unexpected leakage of CO_2 to the surface are significantly reduced, due to the stable nature of the formed solids.

The efficiency of solubility trapping depends on many factors, including sweep efficiency (the efficiency of displacement of the original fluid in the formation), the formation of preferential flow paths, and the effects of geologic heterogeneities in the formation. Efficient solubility trapping significantly reduces the likelihood of CO_2 gas returning to the atmosphere. The primary mineral trapping processes in most geologic formations include the precipitation of calcium, magnesium, and iron carbonates (Reichle et al., 1999). It is anticipated that the rates of solubility and mineral trapping to convert CO_2 to less stable and mobile forms can be enhanced, while optimizing hydrodynamic trapping.

2.1.5 Carbon Sequestration in Enhanced Oil Recovery Operations

Storage of CO_2 in oil and gas formations is the most favorable geologic option. These formations represent known stratigraphic traps, because the oil and gas that was originally present in these traps did not escape over geologic time. They are typically well characterized and understood. Therefore, it is conceivable that CO_2 could also be retained in these reservoirs, so long as no pathways to the surface or to adjacent formations are created through over pressurizing the reservoir, or by fracturing, or by leaks around the wells (Reichle et al., 1999). This particular means of sequestration has a double benefit, because it can increase production in nearly depleted wells, thereby extending their economic life by maintaining reservoir pressures for longer than would typically be possible. The CO_2 displaces the oil and brine for pumping. It also dissolves into the oil, reducing the viscosity and allowing it to flow more easily for enhanced oil recovery (EOR).

2.1.6 Geologic Carbon Sequestration for Enhanced Oil Recovery at Weyburn

EnCana's Weyburn CO_2-EOR Project is located in southern Saskatchewan, near the town of Weyburn. This project began operation in the fall of 2000. CO_2 sequestration in this formation will likely extend the life of this field by approximately 25 years. It is estimated that about 19 million tonnes of CO_2 will be stored, and approximately half of the injected CO_2 will dissolve and become locked up in the oil that remains in the ground (Kane and Klein, 2001). The reservoir is largely made up of limestone and dolomite. The average depth of the reservoir is 1400m, and the temperature and pressure conditions are approximately 63°C and 20700kPa (3000psi), respectively (Schempf, 2001).

This thesis is based on the carbon sequestration project at Weyburn, supposing that the injected carbon dioxide will escape the oil and gas reservoir. This could occur via a number of mechanisms, of which leaks around an imperfectly sealed injection well

and leaks through fractures in the cap rock (potentially caused by over-pressurization) will dominate.

2.1.7 Necessary Considerations for Geologic Sequestration of Carbon Dioxide

There are several aspects of geologic sequestration that must be improved upon and better understood, before its use becomes more widespread. Firstly, it is imperative that reliable systems for monitoring CO_2 migration in the subsurface be developed. The hydrodynamics of CO_2 migration (sweep efficiency, preferential flow, and leakage rates) in heterogeneous formations must be better understood. There must also be methods in place for assessing and ensuring the long-term stability of sequestered CO_2. This includes increased knowledge of CO_2 dissolution rates, mineral trapping kinetics, and non-linear feedback processes affecting confinement, for example, mineral dissolution and precipitation that causes changes to rock permeability (Celia and Bachu, 2002).

The influence of stress changes on cap rock and formation integrity must also be better understood (Reichle et al., 1999). Key features considered in assessing a potential sequestration site may include: cap rock characterization, identifying any potential leakage paths, identifying mineral assemblages that will influence mineral trapping and cap rock integrity, and determining initial conditions and anticipating the evolution of joints and fracture networks form stress and chemically induced deformation. Additionally, the cost and energy requirements associated with geologic sequestration of CO_2 must be reduced to make it a more economically attractive process. The energy required for the purification, compression, and transport of CO_2 will provide another source of greenhouse gasses, and this must be balanced such that there is significantly less CO_2 being produced than is being stored.

There are several factors that control the amount of CO_2 that can be injected into a formation. This volume is defined as the amount that can be injected before any undesirable effects occur. These effects could include (Holloway, 2001):

- A substantial rise in reservoir pressure,
- Pollution of potable water by the displacement of the saline/fresh groundwater interface due to increased pressures,
- Pollution of potable water by CO_2 or substances entrained in the migrating CO_2,
- The migration and escape of CO_2 through the cap rock.

The question of whether safe and stable storage of CO_2 in the subsurface can be assured is the most important issue currently facing the underground storage of CO_2. The mechanisms for potential leaks must be understood, in order to avoid or safely handle dangerous situations. The long-term stability of any formation being considered as a storage reservoir must be assessed. The structural integrity is important to ensure against a gradual return of CO_2 to the atmosphere, or a sudden release. Because CO_2 is heavier than air, a rapid, massive discharge to the surface would displace oxygen, suffocating any people and wildlife that may be present (Herzog et al., 2000).

For geologic sequestration, safety is typically of greater concern than environmental impact (Herzog, 2001). The consequences to the environment must be better defined and understood. The process of sequestering CO_2 must be less damaging to the environment than its continued release to the atmosphere.

2.2 Geology and Mineralogy of the Weyburn Valley Aquifer

The groundwater and sediment of the Weyburn Valley Aquifer were used for this research in order to characterize the conditions that may arise from the migration of sequestered CO_2 in the Weyburn CO_2-EOR region. Various geologic formations

make up the Weyburn Valley Aquifer. In ascending order, there is Pierre Shale overlain by the Ravenscrag and Eastend Formations, followed by the Empress Group, which is covered by glacial drift.

The Empress Group is Late Tertiary to Quaternary in age (Whitaker, 1972). Its sediments vary largely, both in terms of mineralogy and texture. Sediments of markedly different age and origin may be included in the Empress group (Glass, 1990), which consists of stratified sediments occupying preglacial valleys and has the potential for producing significant amounts of groundwater (Fulton, 1989).

Preglacial drainage developed on the northeast slope across the interior plains of Canada, from the Rocky Mountains towards the Canadian Shield, carrying debris from the mountains northeastward (Fulton, 1989). The bottom of these preglacial valleys consists primarily of preglacial fluvial sand and gravel, mostly of quartzite and chert composition (Glass, 1990, Simpson, 1993). These deposits are referred to as Saskatchewan Sands and Gravels, and they generally form a belt 1-2km wide along the deepest sections of the valley and tend to be 3-10m thick although they may be as thick as 65m. The deposition of Saskatchewan Sands and Gravels ended when the local drainage was disrupted due to the advance of ice from the direction of the Canadian Shield. Due to the formation of proglacial lakes in many preglacial valleys during ice advance, a layer of silt and clay sporadically overlies the lower layer of sediment in many areas.

The upper proglacial sediment is composed of glacial and fluvial sand and gravel containing granitic clasts from the Precambrian Shield overlying the silt and clay and Saskatchewan Sands and Gravels, filling in the valley (Glass, 1990). Gravels consist of igneous, metamorphic, and carbonate rocks with a small amount of chert and quartzite. The upper sands are largely quartzose with lots of feldspar and carbonate fragments including limestone and dolomite (Whitaker, 1972). Small amounts of wood, coal, and organic rich silts and clays are also common throughout this unit.

2.3 Carbon Dioxide

2.3.1 Physical Properties

An understanding of the physical properties of carbon dioxide, specifically how these properties will change with pressure and temperature is essential to the evaluation of its transport mechanisms. The physical properties of CO_2 will define the density at which it can be sequestered. Because large volume changes are associated with phase changes of CO_2, it is beneficial to store it under physical conditions that are not close to the phase boundary conditions. These conditions are shown in Figure 2.1. Carbon dioxide can exist as a solid, liquid, gas, or super-critical fluid (Holloway, 2001).

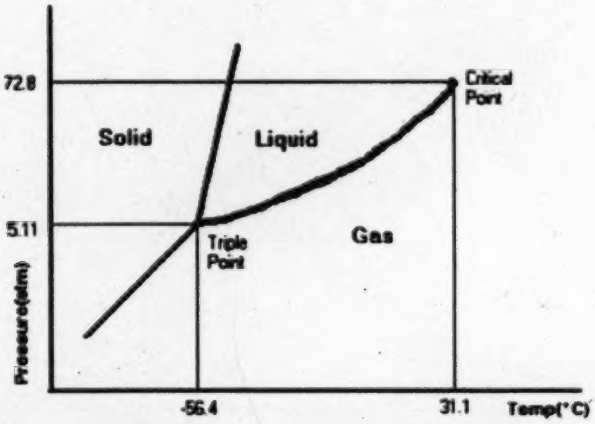

Figure 2.1 Phase diagram for carbon dioxide (modified from Holloway, 2001)

Above its critical temperature of 31.1°C and critical pressure of 72.8 atm, CO_2 exists as a super-critical fluid. A super-critical fluid is a gas-like compressible fluid with liquid-like densities (0.2 – 0.9g/mL). Because CO_2 as a super-critical fluid is much more dense than as a gas and therefore occupies less space, it is desirable to store CO_2 in this form in the subsurface. Under hydrostatic conditions and a geothermal gradient of 25°C, the peak density of CO_2 in the subsurface is approximately 0.72g/mL, compared with a density of less than 0.002g/mL under atmospheric conditions (Holloway, 2001).

On average, the temperature in the subsurface increases by about 30°C per km beneath the surface. The pressure also increases downward within the subsurface; it is typically very close to hydrostatic pressure. Hydrostatic pressure may be exceeded under conditions where the pore space is not connected to the surface (Holloway, 2001). These temperature and pressure effects will determine the state that CO_2 will exist as within the subsurface.

2.3.2 Interaction with Various Minerals

The uptake of CO_2 by water can be increased beyond the typical solubility through interactions with carbonate minerals. The kinetics of reactions with carbonates is considered to be relatively fast (Reichle et al., 1999).

The conversion of CO_2 to stable carbonate minerals, through chemical reaction with groundwater or sediment is a very slow process. However, there are potential chemical and biological additives that could catalyze these reactions (Reichle et al., 1999). While these reactions may be slow, carbon dioxide is chemically reactive and physiologically active. It is the anhydrous form of carbonic acid, which is thermodynamically unstable. Neutralizing this acid with alkaline earth compounds leads to the thermodynamically favored formation of carbonates and bicarbonates (Reaction 2.1). These tend to be relatively stable, and are considered to be environmentally benign (Lackner, 2002). This is the typical, natural interaction of carbon dioxide with the environment.

$$CO_2 + H_2O \leftrightarrow H_2CO_3 \leftrightarrow H^+ + HCO_3^- \leftrightarrow 2H^+ + CO_3^{2-} \qquad \text{(R 2.1)}$$

The aqueous CO_2 (carbonic acid) can also be neutralized through reactions with various oxide and hydroxide minerals. Although calcium is readily available in the geologic formation being considered, and while these reactions should be mentioned, they are not of great significance, because silicates and carbonates tend to have a much higher abundance. These will react with CO_2 by forming carbonates and bicarbonate salts in solution, as shown in Reactions 2.2 – 2.4 (Lackner, 2002). The simplest chemical forms of the minerals are used to demonstrate these reactions.

$$(CaO)(SiO_2)_m + H_2CO_3 \rightarrow CaCO_3 + H_2O + m(SiO_2) \qquad (R\ 2.2)$$

$$(CaO)(SiO_2)_m + 2H_2CO_3 \rightarrow Ca(HCO_3)_2 + H_2O + m(SiO_2) \qquad (R\ 2.3)$$

$$CaCO_3 + H_2CO_3 \rightarrow Ca(HCO_3)_2 \qquad (R\ 2.4)$$

Although the formation of bicarbonates has the benefit of consuming only half of the calcium mineral as the formation of carbonates, the latter are more stable and less mobile as they are not readily soluble. Reactions 2.5 and 2.6 show the likely dissolution reaction mechanisms of calcium carbonate to bicarbonate salt through reaction with carbon dioxide or carbonic acid.

$$H_2CO_3 + CaCO_3 \rightarrow Ca^{2+} + 2HCO_3^- \qquad (R\ 2.5)$$

$$CO_2 + H_2O + CaCO_3 \rightarrow Ca^{2+} + 2HCO_3^- \qquad (R\ 2.6)$$

Recalling the equilibrium kinetics of calcium carbonate in water, it is clear that the presence of CO_2 will have a significant impact, and will in fact change the overall solubility of $CaCO_3$. Calcite will be more readily soluble under an acidic environment, and the enhanced dissolution will actually lead to a neutralization of the carbon dioxide / carbonic acid (Lackner, 2002). While this neutralization effect is desirable, these reactions will also bring about an increase in the overall porosity of the formation, which could enhance the ease of migration of unreacted CO_2.

2.4 The Geochemical Carbon Cycle

The majority of the earth's carbon is stored in sedimentary rocks that contain carbonates and kerogen (Berner et al., 1989). Kerogen is sedimentary organic matter that consists of the remains of soft tissues of ancient plants and animals, and carbonate rocks are composed primarily of the skeletal debris of ancient organisms. The most commonly occurring carbonate minerals include calcite ($CaCO_3$) and dolomite ($CaMg(CO_3)_2$). Table 2.2 indicates the relative amounts of carbon found in various forms on the earth. Clearly, sedimentary minerals and associated matter comprise the majority of the earth's carbon. The weathering of carbonates and other minerals represent a significant portion of the geochemical carbon cycle, wherein CO_2 is consumed.

Table 2.2 Relative proportions of carbon in its various forms

Form	**Carbon Mass** (10^{18} grams)
Calcite	35,000
Dolomite	25,000
Kerogen	15,000
Oceanic aqueous carbonate and bicarbonate	42
Recoverable fossil fuels (coal and oil)	4
Dead surficial carbon (eg. humus)	3
Atmospheric carbon dioxide	0.72
Plants and animals	0.56

(Source: Berner and Lasaga, 1989)

The weathering of carbonate minerals occurs when there are acids present in the groundwater. Carbonic acid is particularly relevant in relating the weathering process within the geochemical carbon cycle. Carbon dioxide can be naturally present in the subsurface due to the carbon dioxide that arises from the decomposition of organic matter in the biological carbon cycle (Berner et al., 1989), or through diffusion from

the atmosphere. The carbon dioxide reacts with water to form carbonic acid, as shown in Reaction 2.1. The carbonic acid then reacts with the carbonate minerals, generating calcium and bicarbonate ions (in the case of calcite), as in Reaction 2.5. Silicate minerals also react in a carbon dioxide rich environment to form carbonates. This is shown in Reaction 2.7, for the simple silicate mineral wollastonite ($CaSiO_3$). The acidic environment that would be brought about by the geologic sequestration of carbon dioxide would be favorable for each of these reactions.

$$2CO_2 + H_2O + CaSiO_3 \rightarrow Ca^{2+} + 2HCO_3^- + SiO_2 \qquad \text{(R 2.7)}$$

Carbonate minerals tend to be amongst the most reactive in subsurface conditions. Dissolution and precipitation reactions play a key role in controlling their composition. These reactions have been extensively studied in laboratory tests, and much information is available for calcite ($CaCO_3$), which is the most commonly occurring carbonate mineral. Dolomite, [$CaMg(CO_3)_2$], the next most common carbonate, is relatively unreactive (Morse, 1983).

The relative weatherabilities of carbonate and silicate minerals are indicated below in Table 2.3. This table provides the solubility products (K_{sp} values) for various minerals. The solubility product for calcite is defined in Equation 2.1. Note that calcite is by far the most soluble mineral on this list. In an acid environment, such as would be generated by the presence of excess carbon dioxide, the solubility of each of these minerals will increase. It has also been shown that dissolution rates are increasingly sensitive to pH at elevated temperatures (Casey and Sposito, 1992). Increased precipitation may also enhance silicate weathering (Berner and Caldeira, 1997). Other factors, such as transport processes and the adsorption of other components such as dissolved magnesium and phosphate ions will also affect the equilibrium relationship, and hence, will also influence the solubility (Morse, 1983). Carbonate rock weathering has been shown to be very sensitive to the partial pressure of carbon dioxide (P_{CO_2}), with an increase in P_{CO_2} resulting in a corresponding increase in carbonate dissolution (Liu and Zhao, 2000). This indicates that carbonate

minerals function as adjustors to atmospheric carbon dioxide, and would do the same for geologically sequestered CO_2. This could lead to significant changes in carbonate dominated formations where carbon dioxide is sequestered.

$$K_{sp} = [Ca^{2+}] [CO_3^{2-}] = 3.3 \times 10^{-9} \text{ (at 25°C)} \qquad \text{(Eq 2.1)}$$

Table 2.3 Solubility products for various minerals

Mineral	**K_{sp}**
Calcite	3.3×10^{-9}
Dolomite	8.13×10^{-18}
Silicates *	1×10^{-30}

(Source: Appelo and Postma, 1996)

* *This is an average value for silicate minerals.*

It is possible for aqueous environments to become so rich in bicarbonate ions that they are considered to be supersaturated, at which point various bicarbonate species will actually begin to precipitate. As the system approaches equilibrium, dissolution reactions will slow down, eventually stopping, allowing precipitation to begin. Saturation is determined by comparison of the Ion Activity Product (IAP, defined for calcite in Equation 2.2) with the equilibrium constant for the dissolution reaction. When the IAP is equal to the equilibrium constant, the system is considered to be in equilibrium, however when this value exceeds the equilibrium constant, the system is then considered to be oversaturated. This is the point at which the dissolution reaction reverses, and precipitation begins.

$$IAP = [Ca^{2+}] [CO_3^{2-}] \qquad \text{(Eq 2.2)}$$

Groundwater is naturally amenable to the presence of bicarbonate ions, as shown in Figure 2.2. This chart shows the Eh-pH diagram for the carbonate system. It is clear that each of the carbonate species will occur readily in a groundwater environment. In most natural environments where the pH is near neutral ($pH \approx 7 \pm 1$) bicarbonate will

dominate. This diagram also shows that these are not redox-sensitive species, the dominant form depends only on pH, regardless of the redox of the environment.

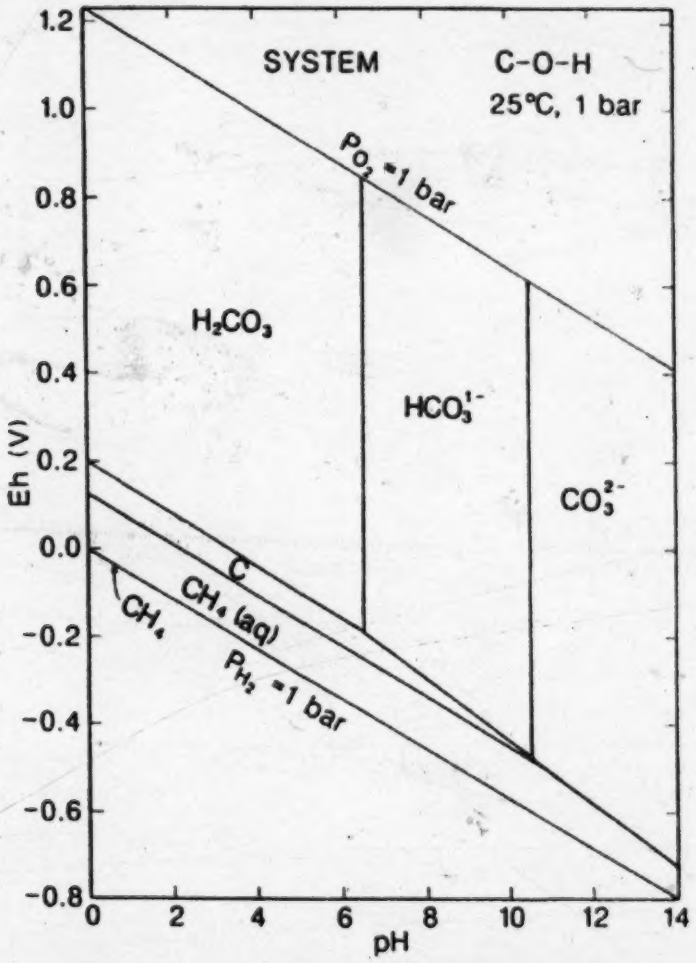

Figure 2.2 Eh-pH diagram for carbonate system (Modified from Brookins, 1988)

Figure 2.3 confirms the prevalence of the bicarbonate ions in an aqueous environment. This is the log concentration – pH diagram for the carbonate system, and it relates all of the equilibrium reactions (Reaction 2.1) and acid constants for these reactions. These reactions occur very fast (~ a few milliseconds), and are taken to be always at equilibrium (White, 1997). By examining a neutral pH of 7, it is clear

that bicarbonate will dominate. This particular diagram is for the case where total carbon dioxide concentration remains constant at 0.01 mol/L.

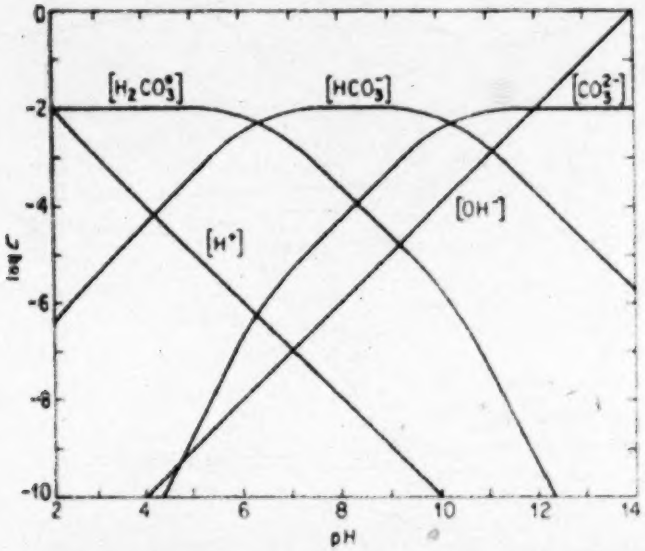

Figure 2.3 log concentration – pH diagram for carbonate system (Modified from Sawyer et al., 1994)

For weathering reactions involving carbonate minerals (Reaction 2.5), half of the generated bicarbonate ions are carried by groundwater to streams, and ultimately to the ocean, where they end up being transformed to calcium carbonate when they are taken up by marine organisms to construct shells and skeletons (Berner et al., 1989). This represents a long-term sink of carbon. The other half of the bicarbonate ions is retransformed into carbon dioxide through the precipitation of other carbonate minerals and ends up back in the atmosphere. The net long-term result of carbonate weathering is that all atmospheric or sequestered carbon dioxide consumed ends up being returned to the atmosphere.

Silicate weathering is much more significant than carbonate weathering as a long-term control on atmospheric carbon dioxide, although it is a much slower process (Appelo and Postma, 1996; Berner and Lasaga, 1989). In this reaction (Reaction 2.8),

two molecules of carbon dioxide are consumed and two bicarbonate ions are produced for each molecule of silicate reacted (K-feldspar is used as an example for this reaction). The bicarbonate ions end up with the same downstream fate as in the carbonate mineral case, however, only one of the two carbon dioxide minerals consumed are returned to the atmosphere through reaction with divalent species such as Ca, Mg, or Fe, resulting in a net loss of half of the carbon dioxide (Reaction 2.9). Thus silicate minerals are more effective than carbonate minerals for reducing atmospheric carbon dioxide.

$$2KAlSi_3O_8 + 2CO_2 + 11H_2O \rightarrow Al_2Si_2O_5(OH)_4 + 2K^+ + 2HCO_3^- \quad \text{(R 2.8)}$$

$$(Ca,Mg,Fe)^{2+} + 2HCO_3^- \rightarrow (Ca,Mg,Fe)CO_3 + H_2CO_3^* \quad \text{(R 2.9)}$$

There are two key mechanisms that restore atmospheric carbon dioxide after the weathering of minerals. One mechanism of release is through volcanic eruptions (Berner and Lasaga, 1989). Or, at depths of several kilometers there is often sufficient heat to cause a reaction between the carbonate and silicate minerals, producing new silicates and carbon dioxide (Reaction 2.10), which may reach the atmosphere via a volcanic eruption or a soda spring. These degassing mechanisms complete the geochemical carbon cycle. They are important, because without them atmospheric carbon dioxide would be completely depleted through the weathering of silicate minerals, and life would cease to exist.

$$CaCO_3 + SiO_2 \rightarrow CaSiO_3 + CO_2 \quad \text{(R 2.10)}$$

2.5 The Impact of Sequestered Carbon Dioxide Migration to Overlying Aquifers

When geologically sequestered CO_2 escapes and migrates to the overlying aquifer, it could impact the groundwater through direct contact, or indirectly through the many potential chemical changes that may first occur in the subsurface during migration to the aquifer.

The most immediate result of direct contact of the CO_2 with the groundwater in the aquifer will be a lowered pH. While carbon dioxide is a normal component of all natural waters, it is typically only introduced through absorption from the atmosphere, which represents significantly lower concentrations than in the case of carbon sequestration. While acidity is of little concern from a public health standpoint, water containing any substantial degree of acidity tends to be quite unpalatable. The greatest concern in terms of the use of acidic water is its corrosive characteristics (Sawyer et al., 1994).

Alkalinity is a measure of the capacity of a water to neutralize acids (Sawyer et al., 1994). Alkalinity can be derived from soluble oxides or hydroxides, which can be extracted from many minerals, or from the salts of weak acids. Such substances act as buffers to resist changes in pH. Bicarbonates tend to provide the major form of alkalinity in many natural systems due to the interactions of CO_2 with minerals. In the geologic sequestration of CO_2, the naturally occurring carbonate minerals can provide a constant and inexhaustible source of alkalinity for the conversion of CO_2 to bicarbonate salts, as shown in Reaction 2.11, which is very similar to Reaction 2.4 (Lackner, 2002).

$$CaCO_3 + CO_2 + H_2O \rightarrow Ca(HCO_3)_2 \qquad \text{(R 2.11)}$$

As was the case with acidity, increased alkalinity is of little significance to public health. Highly alkaline waters also tend to be rather unpalatable (Sawyer et al., 1994).

The release of the alkaline carbonates and bicarbonates in the dissolution reaction results in an equivalent release of calcium ions, which will increase the hardness of the water. Calcium is one of the principle hardness-causing cations. Hard water is no less suitable for human consumption than soft water, indicating the minimal impact of this effect for human use of the water (Sawyer et al., 1994).

As the CO_2 – saturated water migrates towards the surface, it not only has a leaching effect on the carbonate minerals as previously discussed, but also on any metals that may be present in the sediment. This would lead to the mobilization of heavy metals. These acidic waters will be much more efficient in leaching metals out of sediment than neutral or alkaline waters would be (Lackner, 2002).

Studies conducted by Kim et al. (2000) indicated that a major controlling factor in the release of arsenic from mineral rock was strongly related to the bicarbonate concentration in the leaching solution. So even if the CO_2 has been neutralized through the formation of bicarbonate salts, there is still a great risk of mobilizing heavy metals. Bicarbonate was found to be equally effective in leaching arsenic in a deoxygenated reducing environment, suggesting that a non-oxidative leaching process is utilized (Kim et al., 2000).

2.5.1 Iron Mineral Dissolution and Precipitation

Hematite, goethite and $Fe(OH)_3$ are all iron-bearing minerals that are likely present in the aquifer sediment. Hematite is known to occur in tertiary sediments as a result of the weathering and oxidation of ferrous silicate minerals (Langmuir, 1997). Goethite is a commonly occurring weathering product of Fe minerals such as siderite, magnetite, and pyrite (Deer, 1992). It is the most thermodynamically stable oxyhydroxide in water at low temperatures. Amorphous $Fe(OH)_3$ is the most soluble iron-oxide, which is formed as the initial precipitate of the hydrolysis of Fe(III) (Appelo and Postma, 1996).

These common iron bearing minerals are dissolved to produce Fe^{3+} and OH^- ions as shown in Reactions 2.12, 2.13 and 2.14.

Hematite	$\frac{1}{2} Fe_2O_3 + 3/2\ H_2O \leftrightarrow Fe^{3+} + 3OH^-$	(R 2.12)
Goethite	$FeOOH + H_2O \leftrightarrow Fe^{3+} + 3OH^-$	(R 2.13)
$Fe(OH)_3$ (a)	$Fe(OH)_3 \leftrightarrow Fe^{3+} + 3OH^-$	(R 2.14)

The dissolution of these minerals is known to be much faster under suboxic conditions. In an oxidizing environment the mineral surface becomes coated with a layer of FeOOH, which in turn inhibits the dissolution process. The solubility and rate of dissolution of hematite is known to be enhanced in a bicarbonate-rich environment (Bruno et al., 1992). The dependence of the rate of dissolution on the bicarbonate concentration indicates a bicarbonate-promoted dissolution of iron oxides. Various iron bicarbonate complexation species are responsible for the enhanced solubility of iron minerals in a bicarbonate solution.

Under reducing conditions the Fe^{3+} is reduced to Fe^{2+} (Reaction 2.15), which in turn promotes further dissolution of the iron-bearing minerals by lowering the Fe^{3+} saturation levels. The subsequent utilization of Fe^{2+} to form siderite will help to drive these dissolution reactions. The reduction of Fe^{3+} to Fe^{2+} would have to be coupled with an oxidation reaction, most likely the oxidation of dissolved organic carbon (Reaction 2.16).

$$Fe^{3+} + e^- \leftrightarrow Fe^{2+} \qquad \text{(R 2.15)}$$

$$CH_2O \leftrightarrow 0.5CO_2 + 0.5CH_4 \qquad \text{(R 2.16)}$$

In suboxic reducing aqueous environments such as would exist in the aquifer being studied in this research project, Fe(II) is known to combine with CO_2 species to form a siderite precipitate, according to Reaction 2.17 (Langmuir, 1997). Siderite is commonly occurring in sedimentary rocks, and commonly forms along with calcite and dolomite (Appelo and Postma, 1996). In nature, siderite occurs in highly

concentrated Fe^{2+} environments. Aqueous systems where this mineral can be precipitated are typically highly alkaline and rich in dissolved iron(II) (Bruno et al., 1992). The dissolution of Fe(II) bearing minerals (such as magnetite, biotite and smectite) are also potential Fe(II) sources in the aquifer sediment.

$$Fe^{2+} + CO_3^{2-} \rightarrow FeCO_3 \qquad \text{(R 2.17)}$$

Figure 2.4 shows the stability diagram for the Fe-H_2O-CO_2 system. This diagram shows that a suboxic environment is required for the formation of siderite. If any oxygen is present in the system, iron oxyhydroxides will form preferentially. The dotted vertical lines within the siderite stability field indicate the dependence of siderite stability on dissolved iron concentration. The lower the concentration of iron, the smaller the stability field of siderite. Bicarbonate concentration has a similar effect on the stability field of this mineral.

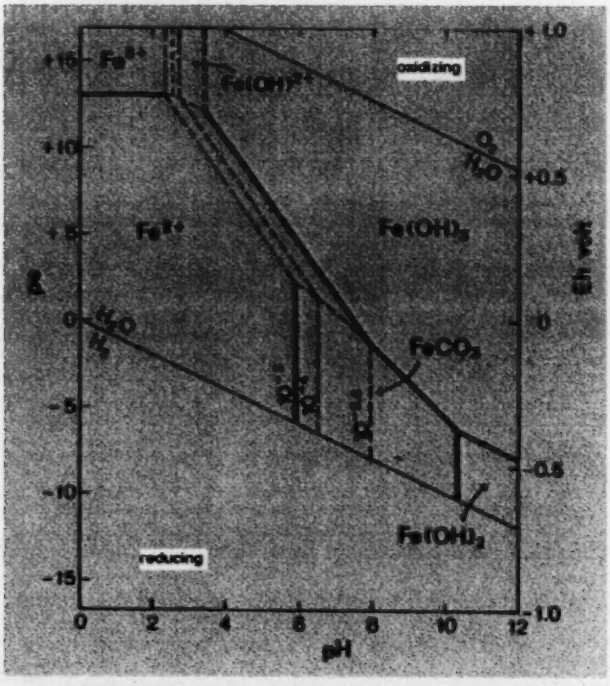

Figure 2.4 Stability diagram for Fe-H_2O-CO_2 system [T=25°C, TIC=$10^{-2.5}$mol/L] (Modified from Appelo and Postma, 1996)

The formation of siderite will likely cause a reduction in the porosity of the formation, with the extra carbon dioxide being added to the mineral matrix. A small decrease in the porosity may in turn lead to a significant decrease in permeability.

2.5.2 Aluminum Mineral Dissolution and Precipitation

Gibbsite [$Al(OH)_3$] is the absolute end product of silicate mineral weathering, as shown in Reactions 2.12 (the dissociation of albite is used as an example) and 2.13 (the subsequent equilibrium equation for gibbsite) (Appelo and Postma, 1996). The equilibrium constant for gibbsite is shown in Equation 2.3. From this equilibrium relationship it is immediately obvious that the activity of aluminum in solution is highly dependent on pH. The development of aluminum-hydroxy complexes may significantly increase the solubility of gibbsite by reducing [Al^{3+}] in solution.

$$NaAlSi_3O_8 + 4H^+ + 4H_2O \rightarrow Na^+ + Al^{3+} + 3H_4SiO_4 \qquad \text{(R 2.12)}$$

$$Al(OH)_3 \leftrightarrow Al^{3+} + 3OH^- \qquad \text{(R 2.13)}$$

$$K_{gibbsite} = [Al^{3+}]\,[OH^-]^3 = 10^{-32.64} \qquad \text{(Eq 2.3)}$$

The albite dissolution rate is strongly pH dependent and is least soluble at neutral pH's (Appelo and Postma, 1996). In a low pH range considerable amounts of aluminum may become solubilized. The dissolution of albite is also influenced by aluminum concentration in solution. Low concentrations of aluminum in solution inhibit the dissolution of albite, however, because the concentration of aluminum also depends on pH, the two rate controlling parameters interact in a complex manner. Given these relationships, it is clear that elevated P_{CO2} in solution will readily bring about the dissolution of albite. A similar effect is observed for feldspars and other alumino-silicate minerals. The adsorption of Al^{3+} onto exchange complexes will also increase the solubility of these minerals by causing the continued dissolution of the

mineral until equilibrium between the mineral phase, exchange complex and solution has been established. Figure 2.5 shows the relationship between pH and aluminum concentration in solution, constrained by gibbsite and aqueous aluminum-hydroxy complexes.

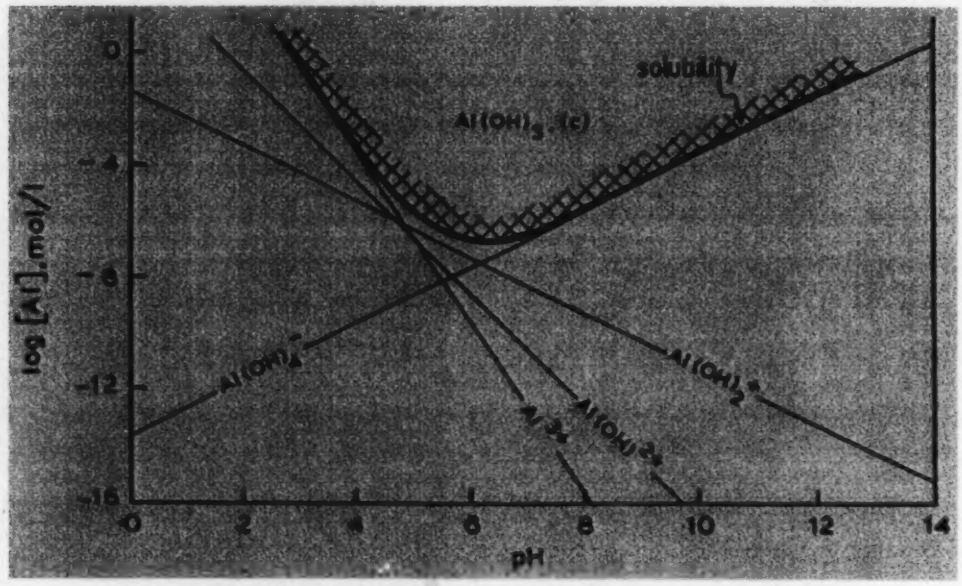

Figure 2.5 Solubility of aluminum with respect to pH (Modified from Appelo and Postma, 1996)

2.6 Geochemical Modeling Using PHREEQC

PHREEQC is a computer program written in the C programming language designed to perform a wide variety of low-temperature aqueous geochemical calculations (Parkhurst and Appelo, 1999). It is based on an ion-association aqueous model and is capable of conducting (1) speciation and saturation-index calculations; (2) batch-reaction and one-dimensional (1D) transport calculations involving reversible reactions, including aqueous, mineral, gas, solid-solution, surface-complexation, and ion-exchange equilibria, and irreversible reactions; and (3) inverse modeling, which finds sets of mineral and gas mole transfers that account for differences in composition between waters, within specified compositional uncertainty limits.

2.6.1 Speciation and Saturation Index Calculations

Speciation calculations use a specified composition for a solution as input and calculate the distribution of aqueous species and saturation indices for relevant phases (Parkhurst and Appelo, 1999). These calculations include equations for mole balance for elements or element valence states, activity of water, and ionic strength.

Saturation index calculations (Eq 2.4) are particularly useful in this research program, to compare the results of the water chemistry before and after the column study. This feature helps to predict which mineral dissolution or precipitation reactions are thermodynamically favorable based on the solution composition data, by comparing the relative saturation indices. A saturation index greater than zero suggests that the solution is oversaturated with respect to that mineral species, and it is likely undergoing precipitation. Whereas a saturation index less than zero indicates that the solution is undersaturated with respect to that species, and is likely being dissolved in the provided conditions.

$$SI = \log \frac{IAP}{K_{eq}} \qquad \text{(Eq 2.4)}$$

2.6.2 Inverse Modeling

Inverse modeling can be used to account for the chemical changes that occur as water undergoes various geochemical reactions (Parkhurst and Appelo, 1999). In inverse modeling, one aqueous solution is assumed to mix with other aqueous solutions and to react with minerals and gases to produce the specified composition of a second aqueous solution. Inverse modeling calculates mixing fractions for the aqueous solutions and mole transfers of the gases and minerals that produce the composition of the second aqueous solution. This takes the approach of comparing saturation indices before and after a specified reaction one step further, by suggesting how many

moles of each mineral phase underwent dissolution or precipitation reactions. The user does need to have an idea of which mineral phases are involved in the dissolution and precipitation reactions, as these minerals must be specified. The program will only find models that are thermodynamically feasible, so if a selected mineral is not undergoing any change, it will not be involved in the model.

Mole-balance equations are included for each element, alkalinity, electrons, water, and each isotope. A charge-balance equation, and an equation that relates uncertainty terms for pH, alkalinity, and total dissolved inorganic carbon are also included for each solution. Inequalities are used to restrict the size of the uncertainty terms, and to limit the sign of the mole transfer of reactants.

The unknowns for the equations and inequalities are the mixing fraction of each aqueous solution, the mole transfers of minerals and gases into or out of the aqueous solution, the aqueous mole transfers between valence states of each redox element, and a set of uncertainty terms that account for uncertainties in the analytical data.

3.0 MATERIALS AND METHODS

3.1 Introduction

The experimental program was designed to measure selected geochemical changes (pH, electrical conductivity, alkalinity, dissolution and/or precipitation of mineral phases) in the sediment and groundwater of the Weyburn Valley Aquifer in a CO_2-enhanced environment.

3.2 Materials

The following sections outline the materials and methods used in the experimental program. Appendix A provides detailed descriptions of the materials and methods used in the experimental program.

3.2.1 Sediment

The sediment used in the experimental program was obtained from the Weyburn Valley Aquifer during a drilling program. The mineralogy of the fine (<75μm) and sandy (75μm – 2000μm) portions of the sediment was determined via XRD (X-ray diffraction) conducted at AGAT Laboratories. For the coarse (>2000μm) sediment, the mineralogy was determined through visual and physical tests. Mineralogy of the sediment is shown in Table 4.1. Additional analyses including semi-quantitative XRD and cation exchange capacity tests were also performed on the fine portion of the sediment and are presented in Table 4.2. Elemental composition of the bulk sediment was determined by Norwest Laboratories and is presented in Table 4.3.

3.2.2 Reagents

3.2.2.1 Groundwater

The water used for the column study was the groundwater obtained from the Weyburn Valley Aquifer during the drilling program. It is carbonate-rich water, with elevated levels of calcium, magnesium and bicarbonate. Elemental composition and routine water properties were determined through testing done at Norwest Laboratories, and are provided in Table 4.4.

3.2.2.2 Carbonated Water

The leaching study used carbonated deionized water. This was prepared by bubbling carbon dioxide into a 20L carboy filled with deionized water to concentrations of ~600, 1200, and 1800mg CO_2/L. The 600 and 1200mg CO_2/L solutions were prepared under ambient temperatures (~22°C). In order to achieve the more concentrated solution of 1800mg CO_2/L, the temperature of the water had to be lowered by placing it in an ice bath as CO_2 is more soluble in water at lower temperatures.

3.3 Methods

The following sections outline the methods used in the research program. Refer to Appendix A for detailed descriptions of the methods used.

3.3.1 Drilling Program

The drilling program was conducted in order to obtain representative sediment and groundwater samples for the laboratory experiments, as well as to characterize the lithology of the sediment overlying the aquifer. No monitoring wells or any instrumentation were installed to characterize in situ geochemical conditions, as this was not an objective of the research program.

3.3.1.1 Drilling

A Barber Ellis air-rotary drill rig (Figure 3.1) using welded steel casing was selected for the collection of the aquifer sediment samples. The selection of appropriate drilling and sampling methods was critical to the collection of high quality geochemical samples. Air rotary was chosen over mud and water drilling methods to avoid contamination of the sediment and pore fluid samples. Fluid drilling methods also tend to wash away fine sediments during drilling. The welded steel casing was required to seal the borehole as it advanced through overlying wet sediment. Samples were collected using a sand bailer to ensure that large grained sediment were not crushed by the drill bit and that sediment samples contained representative pore fluids and fine grained sediment. A sand bailer is a downhole device used to remove sediment from the bottom of a wellbore by use of an atmospheric chamber that is opened to create a surge of fluids and sediment into the chamber for recovery at surface.

Figure 3.1 Barber Ellis air rotary drilling rig

3.3.1.2 Sample Collection and Analysis

Alkalinity, pH, and dissolved oxygen (DO) measurements were made on the water immediately after it was collected. Several samples were also preserved for future analysis. It was important for the samples to be preserved in order to maintain the stability of the samples and to keep them representative of the site, throughout transportation and storage.

Small water samples (500mL) were taken for analysis by Norwest Laboratories. These samples had to be first filtered through a 0.45μm bell-filter to remove all of the sediment and then acidified with nitric acid to keep all of the dissolved species in solution. These samples were then kept in a cooler to maintain the in situ temperature and minimize any chemical changes that could occur at the elevated ambient temperatures.

Several large (20L) mixed sediment and groundwater samples were also taken. Each of these buckets had their headspace purged with argon gas to eliminate the air and reduce the opportunity for oxidation reactions from occurring between the sample and the air. The buckets were fitted with gasketed lids, for tight seals to help prevent the transfer of atmospheric gas into the buckets. These samples were kept cool during transport by depositing blocks of ice around the buckets. Afterwards, they were kept at ~4°C during storage. Cooling was important to help minimize the occurrence (or extent of) reactions that may otherwise have been favored once the samples were removed from the subsurface.

Once the water and sediment samples were obtained, some were sent to Norwest Laboratories for elemental analysis. The sediment samples underwent a strong acid digestion as part of a qualitative and quantitative elemental analysis, to determine the composition. XRD analyses were also conducted on the sand (75μm – 2000μm) and fines (<75μm) portions of the sediment to determine the mineralogy. The gravel portion (>2000μm) of the sediment underwent visual and physical tests to determine the mineralogy. The water samples were tested for major cations and anions, trace metals, alkalinity, hardness, total dissolved solids (TDS), dissolved organic carbon (DOC), and total organic carbon (TOC).

Additional sediment samples were taken approximately every 3m throughout the drilling process in order to generate a borehole log and characterize the lithology of the sediment overlying the aquifer.

3.3.2 Leaching Test

The leaching study was a preliminary test conducted to determine the potential for mineral dissolution of the sediment phase due to elevated carbon dioxide levels in water. This was a batch experiment where a known mass of sediment and carbonated water were combined in Nalgene (HDPE) bottles, and sealed for a specific length of time after which they were opened for analysis. The two key experimental variables included initial CO_2 concentration in the water and residence time. Temperature and pressure remained constant.

3.3.2.1 Preparation of Carbonated Water Solutions

The carbonated water was prepared by bubbling carbon dioxide through deionized water. The carbon dioxide was applied at approximately 70kPa (10psig), a sufficient pressure to efficiently dissolve CO_2 into the aqueous phase, but not so high as to promote turbulent conditions. Turbulence could have made the open system more amenable to CO_2 dissipation from the aqueous phase rather than dissolution into the water.

Three concentrations of carbonated water were prepared (~600, 1200 and 1800mg CO_2/L). The weakest concentration of 600mg CO_2/L was similar to the actual in situ carbon dioxide levels in the aquifer. The 1200mg CO_2/L solution was the highest concentration that could be achieved under ambient temperature and pressure conditions in the laboratory (22°C, 101.3kPa). In order to achieve a more concentrated solution of 1800mg CO_2/L, the water had to be cooled to increase the solubility of CO_2. The deionized water was immersed in an ice bath while the CO_2 was bubbled into it, allowing for the production of a more concentrated solution.

3.3.2.2 Preparation of Batch Reaction Systems

A known mass of wet sediment (600 – 700g) was added to 0.47L (16oz) HDPE bottles. The bottles were topped up with a known volume of a specific concentration of carbonated water. The bottles were very carefully filled in order to minimize any headspace and the lid was sealed with Teflon tape before being placed in a 7-8°C cooler. It was important to minimize any atmospheric interactions with these experimental systems. One system was prepared for each set of experimental conditions (ie. 600, 1200, 1800mg CO_2/L carbonated water, and 1, 2, 4, 8, 16, 32, 64 days retention time).

Wet sediment was used in order to minimize any chemical or physical changes of the sediment that could potentially occur as a result of atmospheric exposure in the drying process. The use of wet sediment created two issues that had to be considered during data analysis. The first of these was that the actual mass of dry sediment was not known. In order to deal with this, several moisture content measurements were made on the wet sediment, and the average value was taken as a representative estimate. This value was then used to calculate an approximate mass of dry sediment used. The second problem associated with using wet sediment was that the water remaining with the sediment phase contained dissolved mineral species, in sufficient quantity to impact the interpretation of the analytical results. This was quantified by creating a blank system, where a known mass of sediment was added to a bottle, topped up with deionized water and then given a quick swirl for a couple of seconds, prior to removing the water to be analyzed as a blank.

An experiment was also set up to compare the extent of some of these observed geochemical effects between the various size fractions in the sediment. This was done to determine to what extent the observed changes were attributable to the fines, sand, or gravel portion of the sediment under elevated CO_2 conditions. The sediment was divided into three size fractions for this test – gravel (>2000μm), sand (75μm – 2000μm) and fines (<75μm). A separate reaction bottle was set up for each of these

size fractions, using the strong carbonated water (~1800mgCO_2/L). These reactions ran for the duration of the experiment, and were then tested for resultant pH, electrical conductivity, and elemental composition as indicators of the extent of reaction that occurred in each case.

3.3.2.3 Sample Analysis

The resulting water from each of the bottles underwent immediate pH and electrical conductivity (EC) measurements at the time of sampling. Some of this water was also filtered and preserved for ion chromatography (IC) and ICP/MS analysis to measure major ions, and trace metals, respectively. Carbon dioxide concentration in blank samples was also measured at each sampling interval to quantify carbon dioxide dissipation to atmosphere.

3.3.3 Column Study

The column study utilized a pressurized column, designed to generate information on the mineral-water-CO_2 interactions under conditions more representative of those found in situ. This study utilized a pressurized continuous flow-through reactor, packed with aquifer sediment and groundwater. The groundwater was spiked with carbon dioxide prior to flowing through the pressurized column. Pressure within the system was held constant at approximately 690kPa (100psig), which corresponds to in situ pore water pressures. Operating under elevated pressures similar to in situ aquifer pressure yields more representative results than the leaching tests, because the solubility of carbon dioxide is increased which should enhance mineral dissolution effects.

3.3.3.1 Experimental Setup

The experimental setup is shown in Figure 3.2.

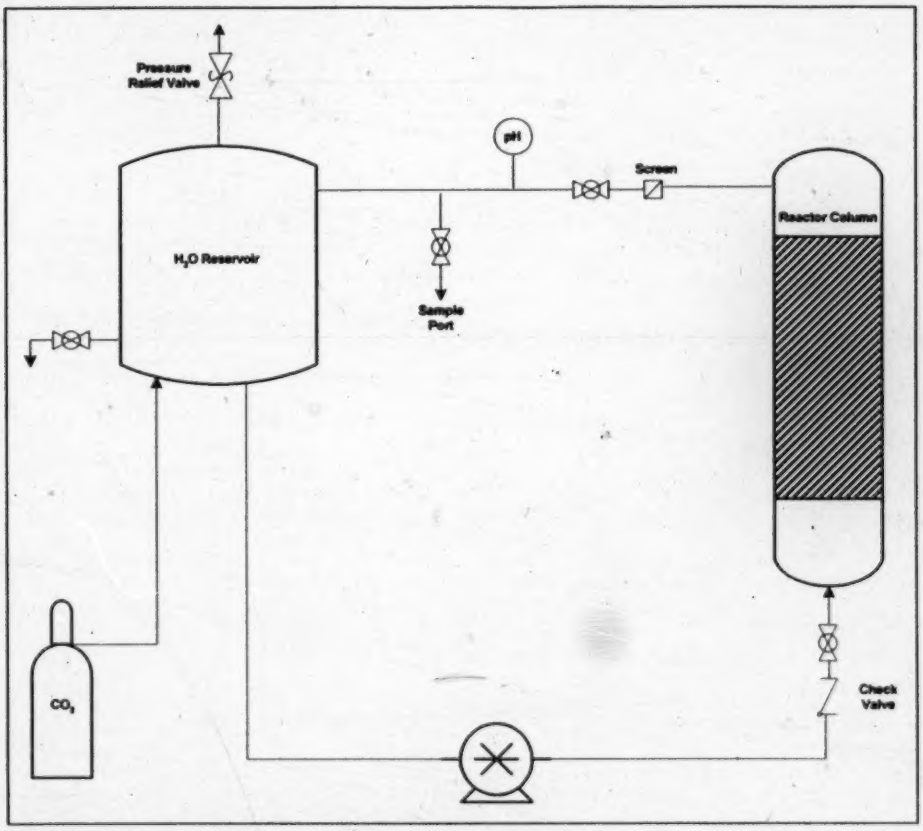

Figure 3.2 Schematic of column study apparatus

The water reservoir (H = 61cm, ID=12.7cm, V=7722mL) held the volume of water required for regular sampling throughout the duration of the experiment without draining the reactor column. The carbon dioxide was bubbled directly into this reservoir, through a diffuser for optimal dispersion of the bubbles. The CO_2 was added such that the pressure in the system was maintained at ~690kPa (100psig), close to in situ conditions. In order to ensure that pressure did not exceed the desired level, the reservoir was equipped with a pressure relief valve set to vent should this level be exceeded. The bottom of the reservoir was equipped with a sample port, in order to draw off water samples for analysis.

The carbonated water was transferred from the reservoir to the reaction column via a high performance peristaltic pump (Masterflex model 77250-62), at a volumetric flow

rate of 3700mL/day, corresponding to approximately one pore volume per day (based on an estimated porosity of 0.25 of the sediment in the column). This feed line was also equipped with an in-line pH probe. The water then passed through a check valve, (to prevent any backflow from the column) prior to entering the reaction column.

The reaction column was 117cm high with an ID of 12.7cm, for a total volume of 14.8L. Both ends of the column were equipped with two layers of geotextile (Terrafix 240R) on either side of a high-permeability gravel bed in order to diffuse the flow radially throughout the column rather than having channel flow through the center between the 0.64cm (¼") holes where the water enters and exits the column. A 0.22μm filter paper (nylon, hydrophilic) was also fitted to both ends (between the geotextile and sediment) in order to ensure that all sediment remained in the column and was not carried out with the water.

After passing through the column, the water was then recycled back to the reservoir. The return line was also equipped with an in-line pH probe to compare the pH before and after residing in the column. A sample port was also included on the outlet line to measure the chemical species that have leached out of the sediment. The outlet line was roughly 4m long, ensuring sufficient sample volume, since the column and reservoir were closed off during sampling.

All construction materials were selected to be as chemically inert as possible, in order to minimize system interferences with the mineral-water-CO_2 chemistry. Both the water reservoir and the reaction column were made of acrylic. The lines were ½" (1.27cm) Teflon, and the valves and connection fittings were PVC and nylon.

3.3.3.2 Sample Analysis

Water samples were taken at various times throughout the 30 day duration of the experiment (Days 0, 1, 2, 3, 5, 7, 9, 13, 16, 20, 23, and 30). This water underwent immediate pH, EC, and alkalinity measurements at the time of sampling.

Approximately 50mL of this water was also filtered and preserved (by adding 0.3mL of concentrated nitric acid) for IC and ICP/MS analysis to measure major ions and trace metals, respectively. The samples had to be acidified in order to keep the dissolved species in solution until the time of analysis.

The sediment was tested at the start and finish of the column study. Strong acid digestion was conducted on the bulk sediment and on the fines portion of the sediment before the column study. The resultant leachate was then analyzed via IC and ICP/MS for elemental composition. Sediment samples were taken at the end of the experiment and analyzed in a similar manner for comparison. Bulk sediment samples were taken from the bottom, middle and top of the column. A sample of the fine sediment was also taken for analysis at the end of the column study. The fines also underwent semi-quantitative XRD analysis (conducted at AGAT Laboratories, Calgary, Alberta) at the start and finish of the column study to observe what mineralogical changes may have occurred over the 30-day study. Scanning electron microscopy (SEM) was performed on various fractions of the sediment before and after the column study in order to observe any physical changes that may have occurred at the sediment surfaces. An environmental SEM was used for this analysis (Philips FEI, Model XL30).

3.3.4 Geochemical Modeling

Geochemical modeling was conducted using PHREEQC Interactive (Version 2.8) to help determine the geochemical changes that were observed in the column, and therefore would likely be observed in the aquifer, under elevated CO_2 conditions. PHREEQCI was used to predict reaction pathways of key geochemical changes that were observed in the column study, specifically the formation of an iron precipitate. This required using the inverse modeling function.

The original groundwater properties and those measured at the end of the column study were entered as Solutions 1 and 2, respectively. Mineral phases that were

thought to be primary contributors to the dissolution and precipitation reactions were selected. Elements that were not considered in the selected mineral phases but were present in the groundwater were entered in the balances section, so as to be balanced by the software. The input file is included in Appendix D.

After the model had been run, the output indicated how many moles of each phase would be either dissolved or precipitated. Since there could theoretically be more than one reaction pathway that occurs for the given data, some discretion had to be used in selecting which scenario best fit the reactions that occurred in the column, based on observations and assumptions that were made based on the knowledge of the conditions in the system.

4.0 PRESENTATION & DISCUSSION OF RESULTS

The following section presents and discusses results from the drilling program and the experimental program conducted for this thesis. A brief experimental overview, as well as observations, raw data, results, general trends, remarks on the quality of data and a discussion of the results are provided.

4.1 Drilling Program

The drilling program was conducted in order to obtain representative sediment and groundwater samples to use in the experimental program. It also yielded information on the lithology of the site (Figure 4.1). This fit with what was expected, based on research conducted on the geology of the region (presented in Section 2.2); the sand and gravel aquifer (Empress Formation) was overlain by glacial drift.

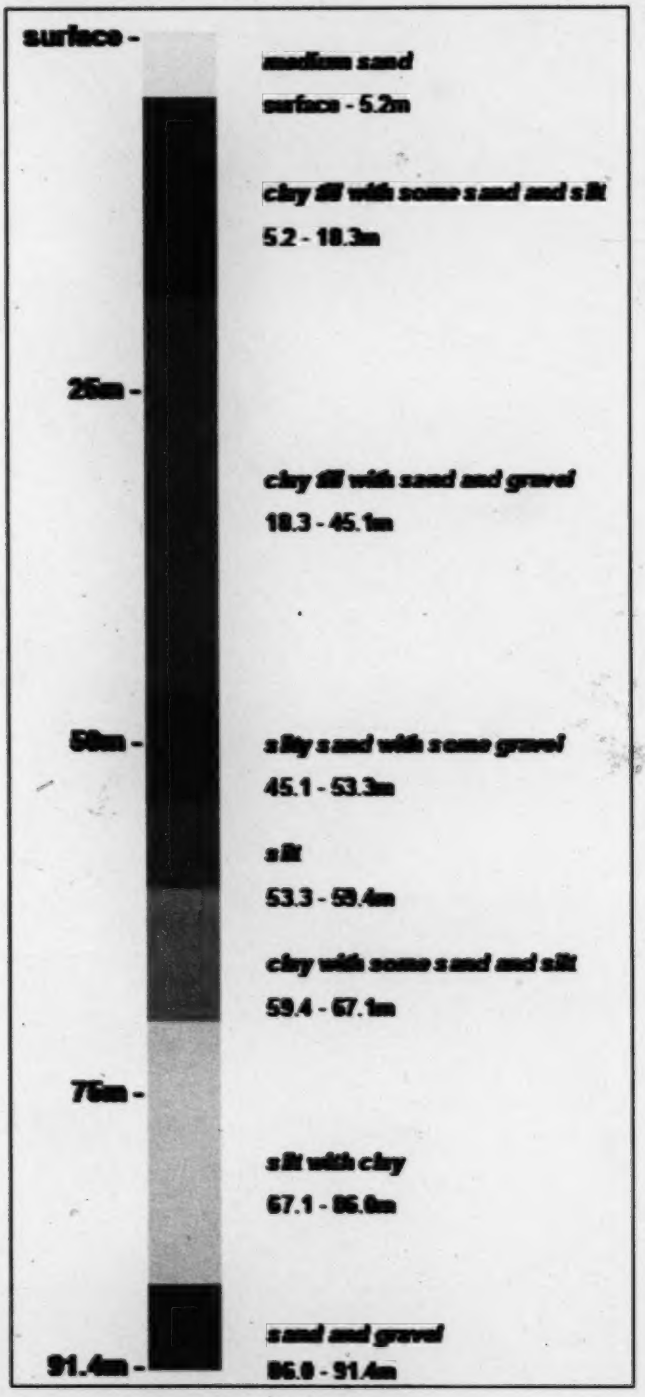

Figure 4.1 Borehole stratigraphy from drilling site

The mineralogy of the sediment was determined by XRD for fines and sand, and by visual and physical tests for the more coarse gravel material. These results are shown in Tables 4.1 and 4.2. The strong presence of calcite and dolomite are responsible for the high concentration of calcium and magnesium in the sediment, similarly the feldspars are the cause of the high aluminum levels. The mineralogy of the aquifer sediment was consistent with what the literature available on the Empress Formation indicates.

Table 4.1 Sediment mineralogy

Fines *(<75μm)*	**Sand** *(<2000μm)*	**Gravel** *(>2000μm)*
Quartz	Quartz	Quartz
Calcite	Calcite	Calcite
Dolomite	Dolomite	Dolomite
Feldspar	K-Feldspar	K-Feldspar
Smectite	Na-Feldspar	Na-Feldspar
Illite		Granite
Kaolinite		Chert
Chlorite		Coal

Table 4.2 Clay mineralogy and CEC

Mineral	**Composition** *[%]*
Smectite	44
Illite	20
Kaolinite	19
Chlorite	17
Total CEC	*38.6 meq/100g*

The sediment was of varied size, ranging from fine silt and clay minerals to sands to coarse gravelly sediment. This is shown in the size distribution diagram in Figure 4.2. Mineralogical analysis indicated an abundance of quartzite, calcite, dolomite, chert, feldspar, plagioclase, and granite minerals, as well as some coal. The lower sands and gravels (Saskatchewan Sands and Gravels) are derived from preglacial drainage from the Rocky Mountains in the west. The upper sediment was deposited by the advance

of ice from the Canadian Shield. This accounts for the presence of carbonate and granite minerals.

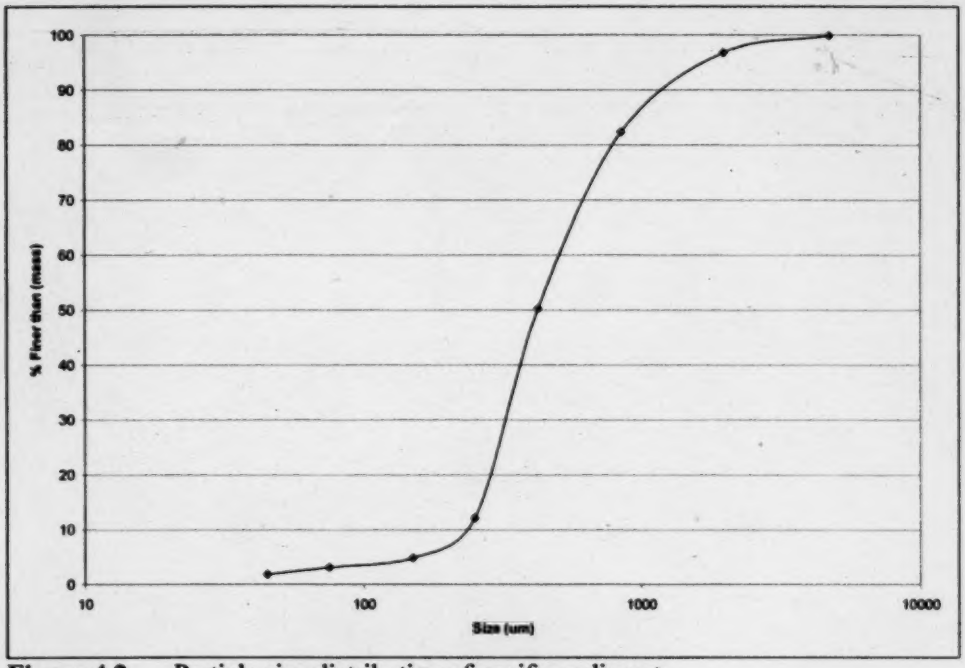

Figure 4.2 Particle size distribution of aquifer sediment

Sediment composition is shown in Table 4.3, which lists the extractable metals concentrations. The sediment is rich in calcium and magnesium because of the carbonate minerals. The iron levels are also high, indicating the presence of iron-rich minerals, and the high aluminum content indicates the presence of aluminosilicates. Several trace metals are also present in sufficient quantities to be of concern, should they become solubilized. Most notable are arsenic, barium, chromium, cobalt, copper, lead, nickel, strontium, titanium, vanadium, and zinc.

Table 4.3 Acid leachable metals content in sediment.

	Average Composition *[ug/g]*	Maximum Compostion *[ug/g]*	Minimum Composition *[ug/g]*	Standard Deviation *[ug/g]*
aluminum	3650	6290	1930	1543
antimony	0.5	1.6	<0.2	0.45
arsenic	3.7	4.8	1.4	1.4
barium	81.5	233	35.7	59.9
beryllium	0.28	0.86	0.10	0.24
bismuth	<0.3	<0.3	<0.3	N/A
cadmium	0.19	0.78	<0.02	0.25
calcium	27011	32600	22900	3079
chromium	7.34	11.2	4.18	2.43
cobalt	4.90	15.5	1.97	4.31
copper	4.68	8.28	2.05	1.86
iron	8942	12200	6210	2174
lead	4.18	8.10	1.90	2.02
magnesium	7073	9080	4080	1499
manganese	232	310	136	56.8
molybdenum	0.82	3.57	0.06	1.07
nickel	10.3	30.5	5.15	8.03
phosphorus	224	344	126	71.3
selenium	<0.25	0.5	<0.2	N/A
silicon	215	248	164	23.8
silver	<0.05	0.07	<0.05	N/A
strontium	32.0	64.9	19.6	14.8
sulfur	866	3040	129	910
thallium	<0.2	<0.2	<0.2	N/A
tin	1.32	2.4	0.6	0.51
titanium	131	238	106	41
vanadium	14.8	36.4	6.6	8.9
zinc	25.5	42.3	10.3	11.8

The primary properties and composition of the groundwater are listed in Table 4.4. The water chemistry indicates that this is a calcium, magnesium, and bicarbonate rich water, indicative of the high carbonate content of the aquifer.

Table 4.4 Groundwater properties and composition

		Average Values	Maximum Value	Minimum Value	Standard Deviation
routine water properties					
pH		8.07	8.15	7.86	0.09
electrical conductivity	[uS/cm @ 25°C]	3053	3090	2830	90.2
temperature of observed pH and EC	[°C]	18.3	18.7	18.0	0.2
calcium	[mg/L]	66.0	71.1	58.6	4.9
magnesium	[mg/L]	26.7	32.3	23.1	3.4
sodium	[mg/L]	584	646	514	42
potassium	[mg/L]	6.6	9.3	5.1	1.8
iron	[mg/L]	<0.05	<0.05	<0.05	N/A
manganese	[mg/L]	0.20	0.26	0.08	0.06
chloride	[mg/L]	633	664	594	25
nitrate-N	[mg/L]	<0.02	<0.02	<0.02	N/A
nitrite-N	[mg/L]	<0.01	<0.01	<0.01	N/A
nitrate and nitrite-N	[mg/L]	<0.03	<0.03	<0.03	N/A
sulphate	[mg/L]	49.7	60.0	49.2	5.8
hydroxide	[mg/L]	<5	<5	<5	N/A
carbonate	[mg/L]	<6	<6	<6	N/A
bicarbonate	[mg/L]	849	873	802	22
P-alkalinity	[mg/L]	<5	<5	<5	N/A
T-alkalinity	[mg/L]	696	716	658	18
TDS	[mg/L]	1785	1890	1650	76
hardness	[mg/L]	267	310	242	23
ionic balance	[%]	95	102	90	4
silicon	[mg/L]	8.6	10.8	7.1	1.5
sulphur	[mg/L]	16.6	20.0	12.9	1.9
aluminum	[mg/L]	<0.025	<0.025	<0.03	N/A
antimony	[mg/L]	<0.001	<0.001	<0.001	N/A
arsenic	[mg/L]	0.004	0.006	0.002	0.002
barium	[mg/L]	0.138	0.264	0.101	0.054
beryllium	[mg/L]	<0.0005	<0.0005	<0.0005	N/A
bismuth	[mg/L]	<0.003	<0.003	<0.003	N/A
boron	[mg/L]	0.530	0.553	0.464	0.028
cadmium	[mg/L]	<0.00005	<0.00005	<0.00005	N/A
chromium	[mg/L]	0.0065	0.0074	0.0057	0.0008
cobalt	[mg/L]	0.0032	0.0054	0.0014	0.0016
copper	[mg/L]	<0.005	<0.005	<0.005	N/A
lead	[mg/L]	<0.0005	<0.0005	<0.0005	N/A
lithium	[mg/L]	0.07	0.07	0.06	0.003
molybdenum	[mg/L]	0.024	0.031	0.021	0.003
nickel	[mg/L]	0.0048	0.0057	0.0040	0.0006
selenium	[mg/L]	0.0029	0.0031	<0.001	0.0002
silver	[mg/L]	<0.0005	<0.0005	<0.0005	N/A
strontium	[mg/L]	0.540	0.612	0.492	0.042
thallium	[mg/L]	<0.0003	<0.0003	<0.0003	N/A
tin	[mg/L]	<0.005	<0.005	<0.005	N/A
titanium	[mg/L]	<0.003	<0.003	<0.003	N/A
uranium	[mg/L]	<0.003	<0.003	<0.003	N/A
vanadium	[mg/L]	0.0045	0.0083	0.0006	0.0026
zinc	[mg/L]	<0.025	0.093	<0.005	N/A

As many properties as could be were measured in the field at the time of sampling. This was important to determine representative groundwater conditions. These, as well as the laboratory analyses conducted immediately upon return from the field were useful to compare with the conditions of the water eight months later, when it was used in the column study. Most of the components in the water were stable and remained relatvely constant throughout storage. A few elements (Al, As, Ba, Sr) however, were not entirely stable in solution and underwent substantial changes in concentration from the time of sampling to the time of beginning the column study. With the exception of aluminum, all of these elements decreased in concentration in the groundwater between the two sample periods. A small extent of this difference could be attributable to the analyses being conducted in different laboratories (initial – external, column study – in-house). Aluminum however is known to be relatively unstable, and changes with pH. The change in pH from 8.1 at the time of sampling to 7.6 at the time of the column study could account for some of the difference. The other elements which decreased in concentration likely underwent some precipitation or adsorption reactions.

The CCME Drinking Water Guidelines are provided in Table 4.5. If these levels should be exceeded in the groundwater, a serious risk assessment on the fate of the aquifer should be conducted, in the event of carbon dioxide migration.

Table 4.5 CCME Drinking Water Guidelines

Element	**Maximum Acceptable Concentration** *(µg/L)*
Al	100
Fe	≤300*
Zn	≤5000*
As	25
Pb	10
Cu	≤1000*
Ba	1000
U	20

* *These values are not guidelines. They represent aesthetic objectives.*

4.2 Leaching Test

The leaching study was conducted to determine the potential for mineral dissolution of the sediment phase due to elevated carbon dioxide levels in water. A series of tests were conducted, with varying carbon dioxide levels (dilute – 600 mg CO_2/L, medium – 1200 mg CO_2/L, and strong – 1800 mg CO_2/L) and residence time. Several properties of the resulting solutions were measured in order to characterize the changes that had taken place in each reaction system. These properties included electrical conductivity, pH, elemental composition, and final carbon dioxide concentration (in the blank systems). These results are shown in Figures 4.3 – 4.9, with the conditions of the original groundwater included for comparison.

The change in electrical conductivity over time is shown in Figure 4.3. The rapid increase in EC implies the rapid dissolution of some of the sediment into the aqueous phase. It appears that the EC stabilized to some sort of equilibrium or saturation point after ~16 days. The equilibrium point was only about one half of the EC in the original groundwater, suggesting that either additional time is required to reach those equilibrium values or that the different chemistry due to the lack of dissolved species in the deionized water alters the solubility of the mineral phases. Lower concentrations of complex species reactions would contribute to lower mineral solubility. The error related to the measured EC values is ±100μS/cm.

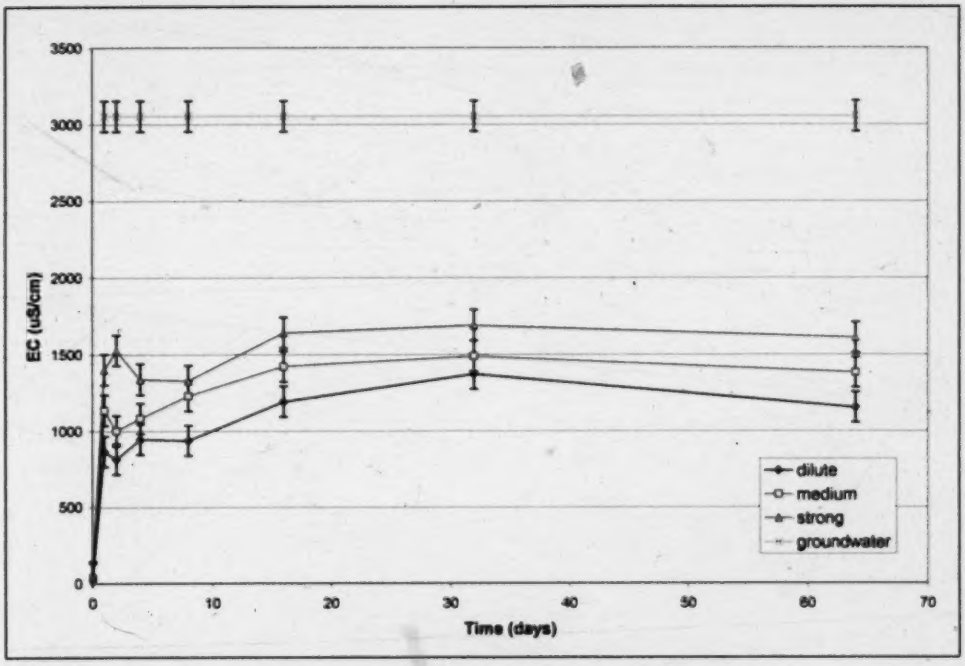

Figure 4.3 Change in electrical conductivity during leaching test

The initial pH of the carbonic acid added to each of the bottles was ~3.9 – 4.2, decreasing with increasing acid concentration. Measurements taken on the Day 1 samples indicated that the pH had rapidly increased to near neutrality, as shown in Figure 4.4. An error of ±0.1pH unit is associated with these values. With the resultant pH in the range of 6 – 7 and the quickness of this pH increase, it was inferred that a carbonate mineral dissolution reaction was neutralizing the carbonic acid to form bicarbonate ions.

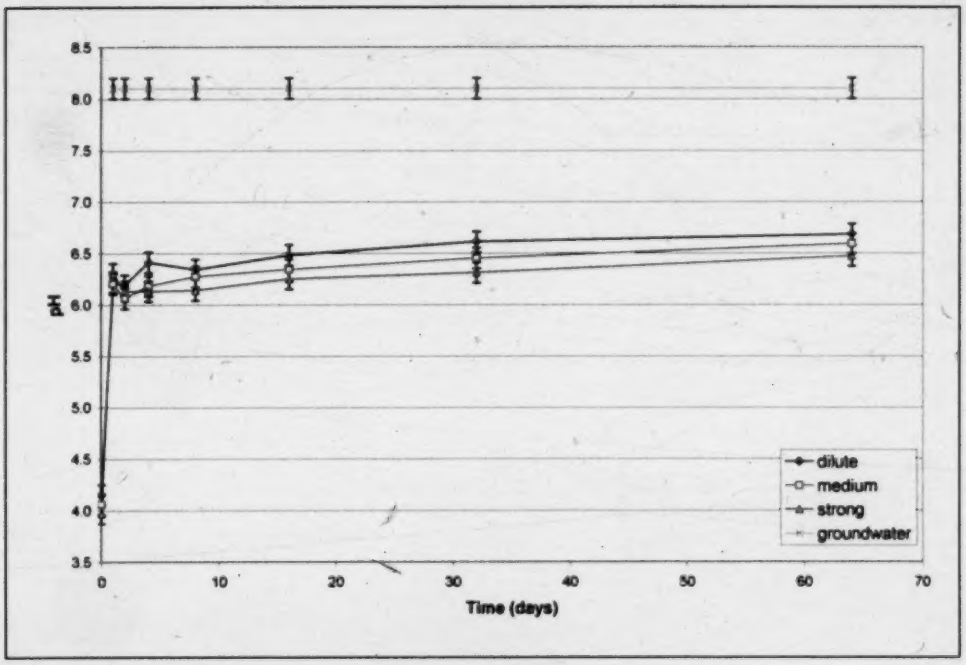

Figure 4.4 Change in pH during leaching test

Further evidence in support of this theory is provided in Figures 4.5 and 4.6, which show the increasing calcium and magnesium levels in solution, indicating that carbonate minerals such as calcite and dolomite were dissolved. The general reaction for the dissolution of carbonate minerals in a carbon dioxide rich aqueous environment is shown in Reaction 2.6. When this type of weathering reaction occurs, the pH increases. The dissolution of clay minerals such as smectite also likely contributed to the increase in magnesium concentration in solution.

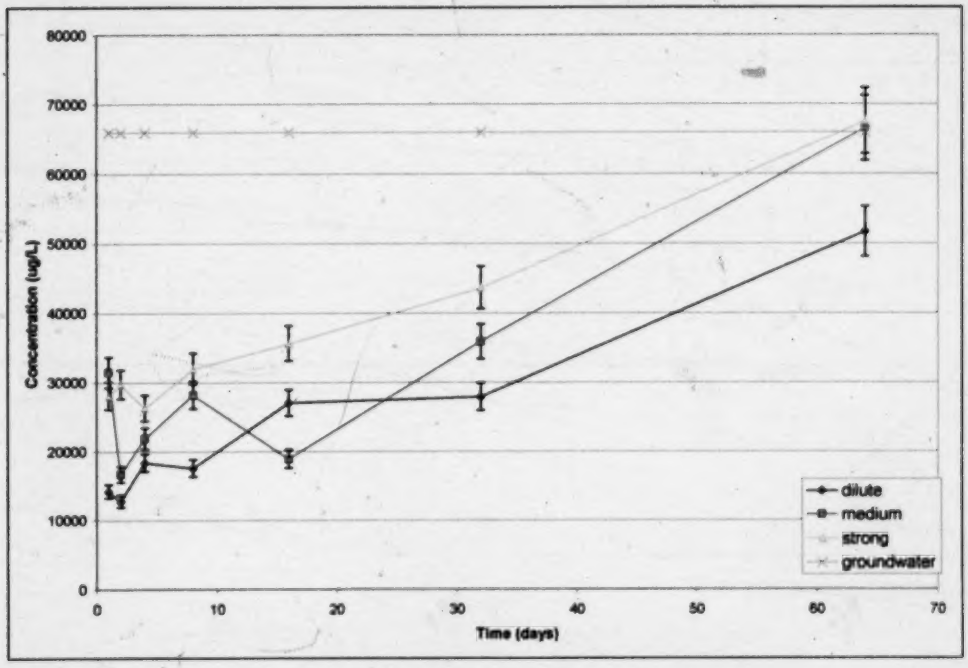

Figure 4.5 Calcium concentration in solution during leaching test

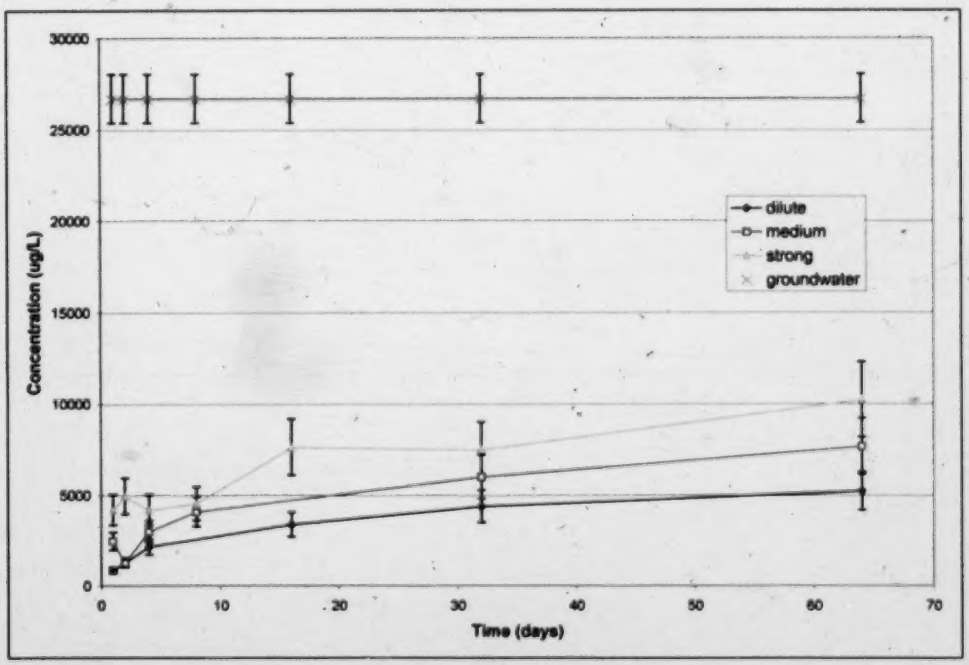

Figure 4.6 Magnesium concentration in solution during leaching test

The standard deviation for calcium and magnesium concentrations is 7% and 20%, respectively. The increase in calcium ions in solution was much more dramatic than that of magnesium ions. By the end of the experiment, the resultant medium and strong carbonated solutions had calcium concentrations roughly equivalent to the original groundwater levels. The magnesium levels approached approximately one third of the original groundwater levels. This can be explained by the relative solubilities of calcite and dolomite. Calcite is more readily soluble in a weak acid solution as compared to dolomite, and rapidly approaches equilibrium concentrations. Despite the smaller increase in dissolved magnesium concentration as compared to calcium, the fact that the concentration increased suggests that perhaps some dolomite was also solubilized, or that it was released through cation exchange reactions on the clay minerals.

Other than calcium and magnesium, only strontium, barium and iron showed a distinct trend of dissolution, as shown in Figures 4.7, 4.8, and 4.9. The standard deviation for these metals was 6% for strontium, 4% for barium, and 8% for iron. These elements are known to readily substitute for calcium in carbonate minerals. Analysis of some of the carbonate rocks present in the sediment yielded strontium levels approximately 147% of those found in the bulk sediment (29.4ug/g), confirming this substitution effect. The enhanced dissolution of strontium is to be expected, on account of how prone it is to substitution in carbonate minerals combined with the large extent of carbonate dissolution that was observed. Strontium was most susceptible to dissolution under elevated dissolved CO_2 concentration; however the trend was also quite distinct for barium and iron, albeit to a lesser extent.

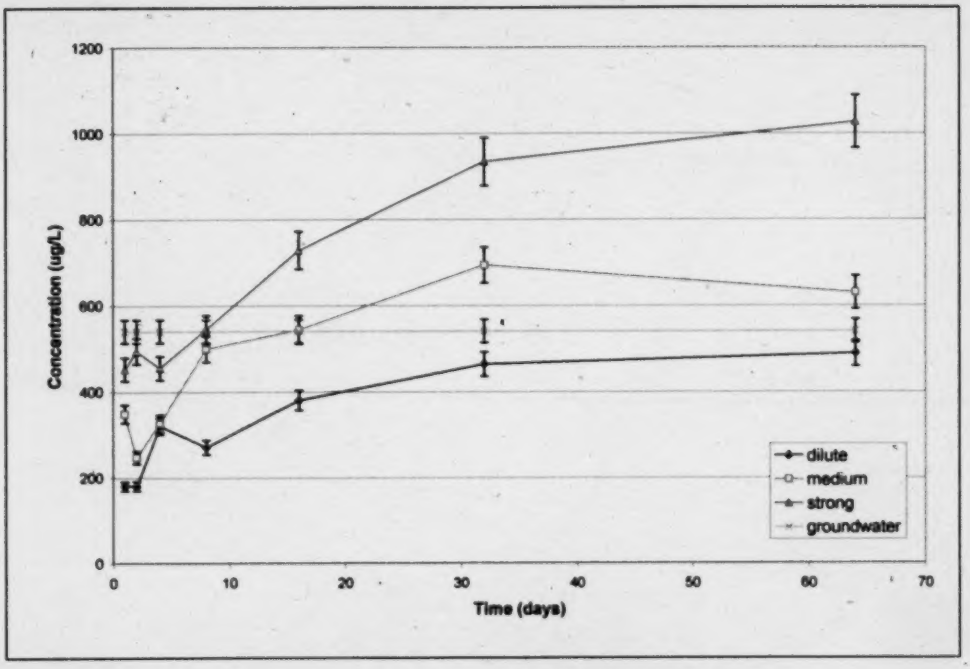

Figure 4.7 Strontium concentration in solution during leaching test

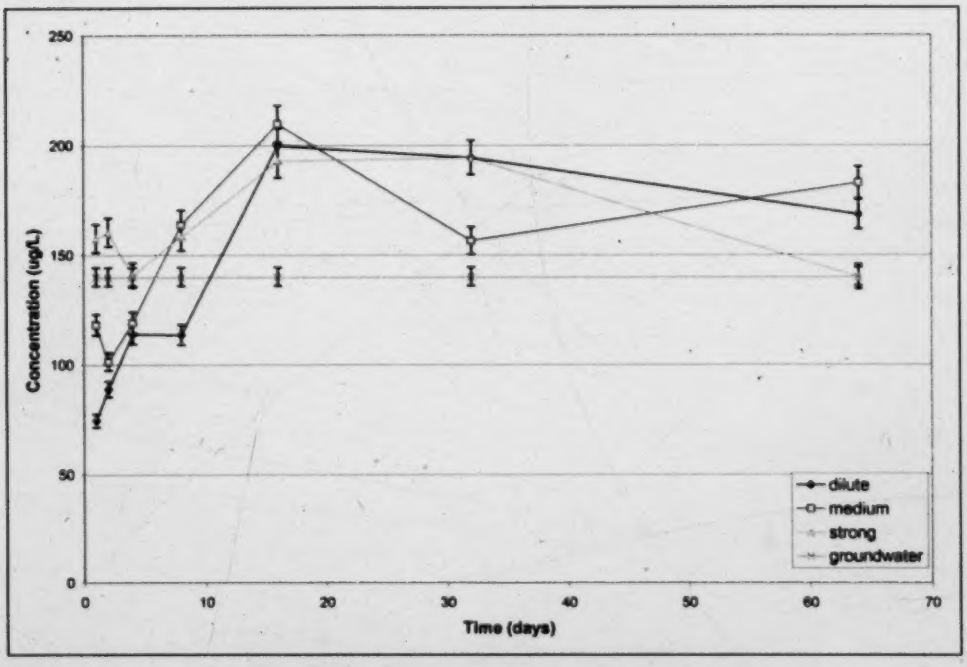

Figure 4.8 Barium concentration in solution during leaching test

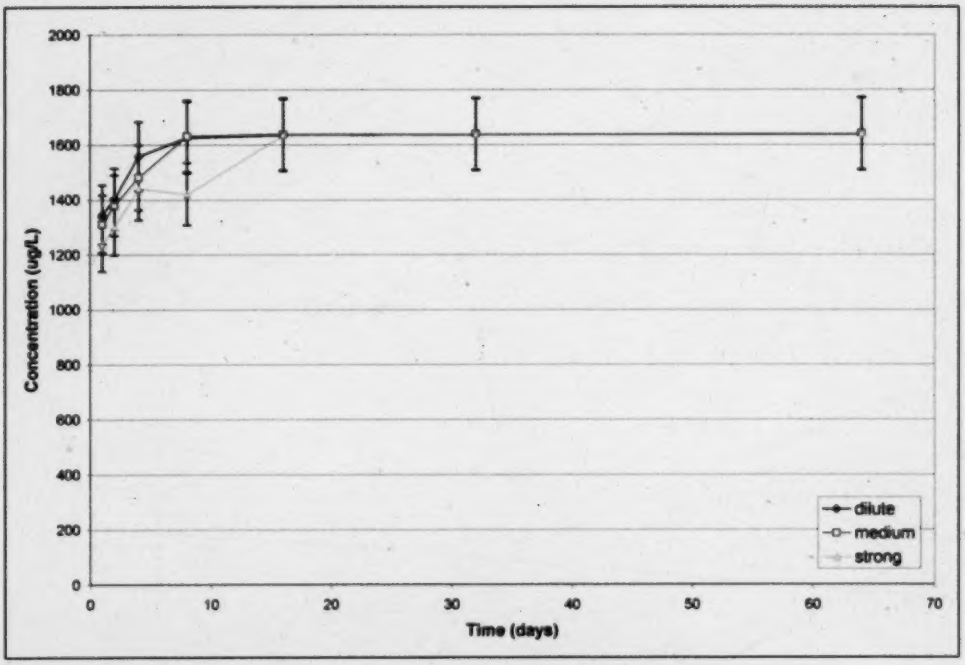

Figure 4.9 Iron concentration in solution during leaching test

Iron levels in the aqueous phase appeared to reach a saturation point, as indicated by the asymptotic nature of the curves, shown in Figure 4.9. When the concentration reached this saturation point, iron precipitates began to form, likely enabled by oxygen that was able to diffuse into the bottles and oxidize the iron, causing it to precipitate. This precipitation is shown in Figure 4.10, which shows a typical set of samples from the experiment. The iron precipitation can be seen clearly, particularly in the strong carbonated water solution. The effect is probably most obvious in this case because the more acidic conditions brought about by higher levels of carbon dioxide could more readily cause the further dissolution of iron to maintain equilibrium concentrations as the original dissolved iron formed precipitates.

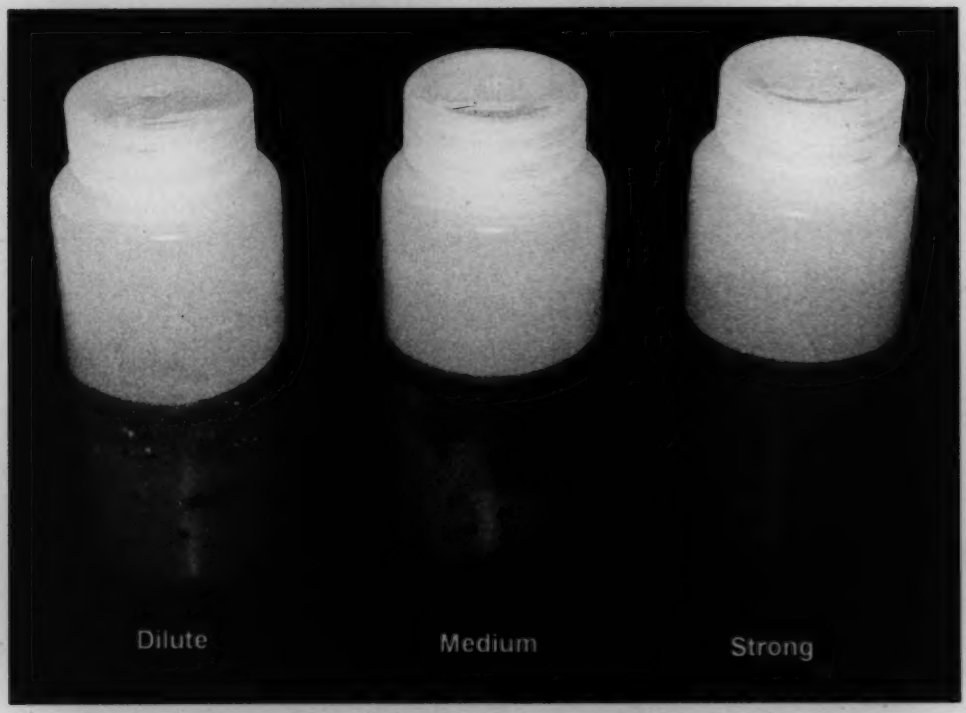

Figure 4.10 Iron precipitation observed in dilute – strong carbonated water solutions

In the presence of fugitive oxygen, the iron would be oxidized and preferentially form iron hydroxides. The iron precipitate would not have been siderite due to the low dissolved iron concentrations and the presence of oxygen due to atmospheric interactions. The siderite stability field is highly dependent on $[Fe^{2+}]$, and at the low concentrations observed in this experiment the stability field would disappear completely.

Table 4.6 shows the resultant water composition for each sampling interval (1800mg CO_2/L). A negative value indicates that the measured levels were less than in the blank. The results for the 600 mg CO_2/L and the 1200 mg CO_2/L are provided in Appendix C.

Table 4.6 Leaching test results for 1800mg CO_2/L reactions

		Concentration [ug/g]						
		Day 1	2	4	8	16	32	64
Calcium	Ca	1.25E+01	1.30E+01	1.21E+01	1.54E+01	1.58E+01	2.05E+01	3.17E+01
Magnesium	Mg	2.01E+00	2.28E+00	2.09E+00	2.42E+00	3.51E+00	3.71E+00	4.98E+00
Sodium	Na	5.93E+00	6.84E+00	7.42E+00	7.24E+00	7.99E+00	9.01E+00	-4.90E+00
Potassium	K	4.04E-01	0.00E+00	0.00E+00	0.00E+00	2.60E-01	4.44E-01	0.00E+00
Carbonate	CO3	0.00E+00	0.00E+00	0.00E+00	0.00E+00	0.00E+00	0.00E+00	0.00E+00
Bicarbonate	HCO3	0.00E+00	0.00E+00	0.00E+00	0.00E+00	0.00E+00	0.00E+00	0.00E+00
Sulphate	SO4	-1.18E+00	-1.07E+00	-4.48E-01	-5.38E-01	-1.43E-01	5.44E+00	5.17E+00
Chloride	Cl	9.64E+00	1.37E+01	2.18E+01	2.01E+01	2.61E+01	2.79E+01	5.31E+01
Nitrate - Nitrite	NO3, NO2 +	0.00E+00	0.00E+00	0.00E+00	0.00E+00	0.00E+00	0.00E+00	0.00E+00
Total Iron	Fe	-6.96E-02	-5.13E-02	3.90E-02	6.18E-02	1.03E-01	1.46E-01	1.46E-01
Aluminum	Al	-8.31E-02	-7.88E-02	-7.48E-02	-7.50E-02	-7.62E-02	-7.49E-02	-5.56E-02
Antimony	Sb	-1.06E-04	-1.52E-04	-1.02E-04	-1.43E-04	-1.51E-04	-1.46E-04	-1.46E-04
Arsenic	As	8.58E-04	6.09E-04	5.87E-04	8.31E-05	-2.58E-04	-2.69E-04	-3.63E-04
Barium	Ba	7.28E-02	7.23E-02	6.77E-02	8.07E-02	8.78E-02	9.48E-02	6.93E-02
Berryllium	Be	0.00E+00	0.00E+00	0.00E+00	0.00E+00	0.00E+00	0.00E+00	0.00E+00
Bismuth	Bi	0.00E+00	0.00E+00	0.00E+00	0.00E+00	0.00E+00	0.00E+00	0.00E+00
Cadmium	Cd	4.62E-06	3.84E-06	5.88E-06	8.14E-06	4.36E-06	6.90E-06	6.86E-06
Cesium	Cs	0.00E+00	0.00E+00	0.00E+00	0.00E+00	0.00E+00	0.00E+00	0.00E+00
Chromium	Cr	0.00E+00	0.00E+00	0.00E+00	0.00E+00	0.00E+00	0.00E+00	0.00E+00
Cobalt	Co	0.00E+00	0.00E+00	0.00E+00	0.00E+00	0.00E+00	0.00E+00	0.00E+00
Copper	Cu	-2.79E-04	-2.36E-04	-1.42E-04	3.93E-04	1.63E-04	1.03E-03	5.15E-04
Gallium	Ga	4.45E-05	4.37E-05	0.00E+00	1.92E-04	0.00E+00	0.00E+00	0.00E+00
Lead	Pb	-1.20E-04	-1.20E-04	-1.20E-04	-1.20E-04	-1.20E-04	-1.20E-04	-2.62E-05
Lithium	Li	1.42E+00	2.22E+00	3.22E+00	2.55E+00	3.98E+00	4.16E+00	-1.05E+01
Manganese	Mn	7.57E-04	3.94E-04	2.29E-04	1.92E-04	0.00E+00	0.00E+00	0.00E+00
Molybdenum	Mo	-5.54E-03	-5.49E-03	-4.52E-03	-5.67E-03	-6.62E-03	-6.84E-03	-7.08E-03
Nickel	Ni	3.84E-03	3.71E-03	2.28E-03	6.38E-03	1.38E-03	2.16E-03	1.13E-03
Phosphorus	P	0.00E+00	0.00E+00	0.00E+00	0.00E+00	0.00E+00	0.00E+00	0.00E+00
Rubidium	Rb	1.28E-04	1.13E-04	1.52E-04	2.43E-04	2.11E-04	3.58E-04	3.10E-04
Selenium	Se	2.23E-04	3.06E-04	8.24E-04	1.20E-03	0.00E+00	0.00E+00	4.67E-04
Silicon	Si (soluble)	-4.11E-03	-4.11E-03	-4.11E-03	-4.11E-03	-4.06E-03	-4.11E-03	-3.78E-03
Silver	Ag	0.00E+00	0.00E+00	0.00E+00	0.00E+00	0.00E+00	0.00E+00	0.00E+00
Strontium	Sr	2.07E-01	2.21E-01	2.16E-01	2.72E-01	3.28E-01	4.46E-01	4.89E-01
Sulfur	S	2.49E+01	2.24E+01	2.90E+01	3.66E+01	2.42E+01	3.28E+01	3.27E+01
Tellurium	Tl	0.00E+00	0.00E+00	0.00E+00	0.00E+00	0.00E+00	0.00E+00	0.00E+00
Titanium	Ti	-1.25E-03	-1.54E-03	-4.41E-04	2.03E-03	4.48E-04	-5.11E-04	-4.84E-04
Uranium	U	4.88E-04	5.54E-04	5.69E-04	5.87E-04	2.16E-04	1.31E-04	3.68E-05
Vanadium	V	0.00E+00	0.00E+00	0.00E+00	0.00E+00	0.00E+00	0.00E+00	0.00E+00
Zinc	Zn	2.75E-02	2.91E-02	3.15E-02	3.63E-02	1.61E-02	1.23E-02	3.75E-03

A series of tests were also conducted in order to determine which size fraction of the sediment would be most reactive/leachable under elevated carbon dioxide conditions. The sediment was divided into three size fractions for this test – gravel (>2000μm), sand (75 - 2000μm) and fines (<75μm). These tests used the strong carbonated water (~1800mgCO_2/L). The reactions ran for the duration of the experiment, and were then tested for resultant pH, electrical conductivity, and elemental composition as indicators of the extent of reaction that occurred in each case. The pH and EC results

show significantly higher resultant values (Figures 4.11 and 4.12), indicating that the fine sediment is much more reactive than the sand and gravel fractions.

The higher pH (near neutrality) indicates the relatively high buffering capacity of the fine sediment, which directly correlates with higher reactivity/leachability. The higher EC values indicate that more mineral species have gone into solution, which is confirmed by the elemental composition of the resulting leachates as shown in Table 4.7. These results show that the concentration of most elements is approximately two orders of magnitude higher for the fines, as compared to the sand or gravel. This result is to be expected, due to the higher surface area per mass of fines as compared to coarser sediment. Note that no blank was used to account for the minerals in the pore fluid associated with these samples, therefore the values are slightly elevated relative to those in Table 4.6.

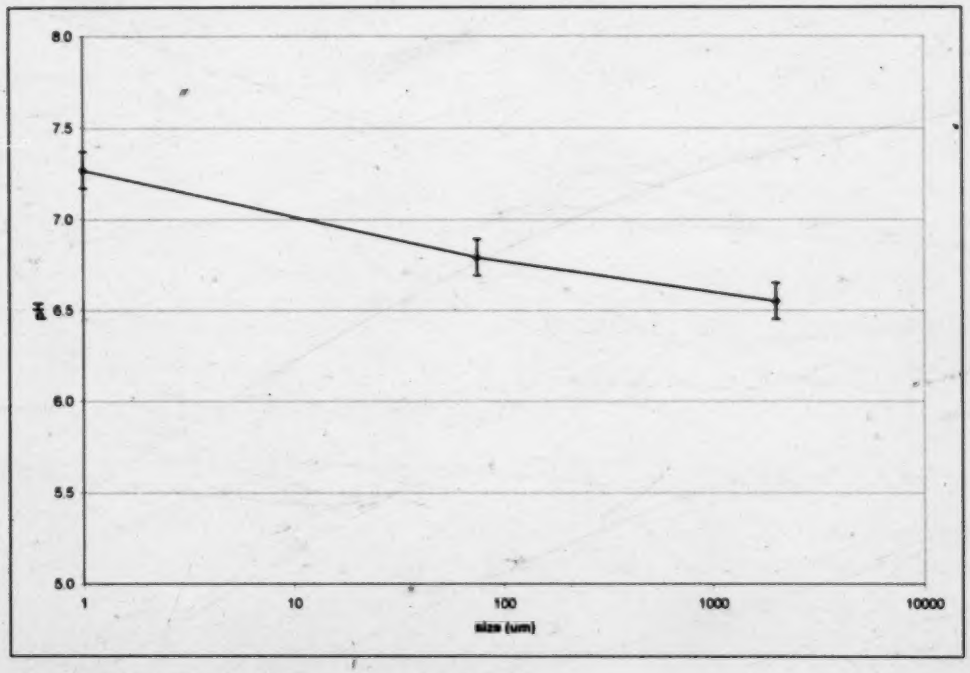

Figure 4.11 Final pH for various size fractions

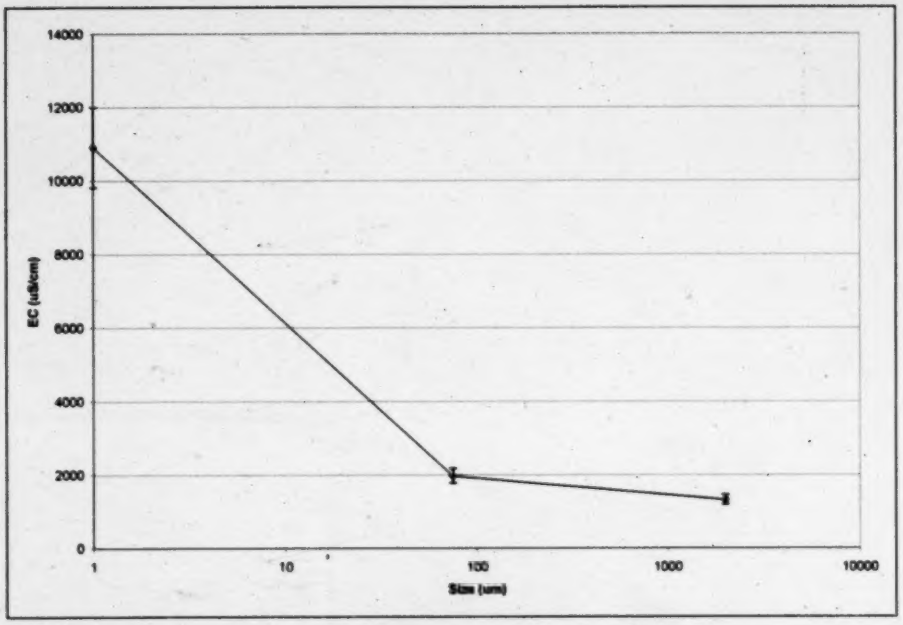

Figure 4.12 Final electrical conductivity for various size fractions

Table 4.7 Relative dissolution of various size fractions

	Fines *[ug/g]*	Sand *[ug/g]*	Gravel *[ug/g]*
Calcium	825	122	67.2
Magnesium	1179	22.1	17.5
Sodium	27298	120	74.5
Potassium	233	3.0	1.8
Bicarbonate	25271	529	430
Sulphate	3006	90.2	18.3
Chloride	12715	88.9	22.5
Total Iron	11.4	0.76	0.54
Aluminum	19.9	0.18	0.18
Antimony	2.71E-02	3.19E-04	1.47E-04
Arsenic	1.43E-01	8.49E-04	2.70E-04
Barium	3.62	0.11	0.06
Cadmium	3.46E-03	9.21E-05	2.27E-05
Copper	5.52E-01	3.47E-03	1.91E-03
Lead	1.61E-03	9.89E-05	2.23E-05
Molybdenum	1.05	2.15E-03	3.48E-04
Nickel	2.22E-01	9.55E-03	1.88E-03
Rubidium	6.03E-02	1.72E-03	8.21E-04
Selenium	1.13E-01	1.11E-03	0
Silver	3.09E-03	1.22E-05	5.32E-06
Strontium	10.9	0.55	0.40
Titanium	6.15E-02	3.39E-03	2.42E-03
Uranium	4.72E-01	4.27E-03	2.01E-03
Zinc	7.70E-02	9.21E-03	3.05E-03

The resulting carbon dioxide concentrations in each of the blank systems are shown in Figure 4.13. The experimental error associated with this titrimetric measurement is ±50mg CO_2/L. This figure suggests that not all of the carbon dioxide was actually consumed through weathering reactions, but that some of it escaped to the atmosphere, causing the water to go "flat". This effect was likely less pronounced in the actual test bottles however, due to the rapid geochemical reactions occurring between the carbonated water and the sediment very early in the experiment.

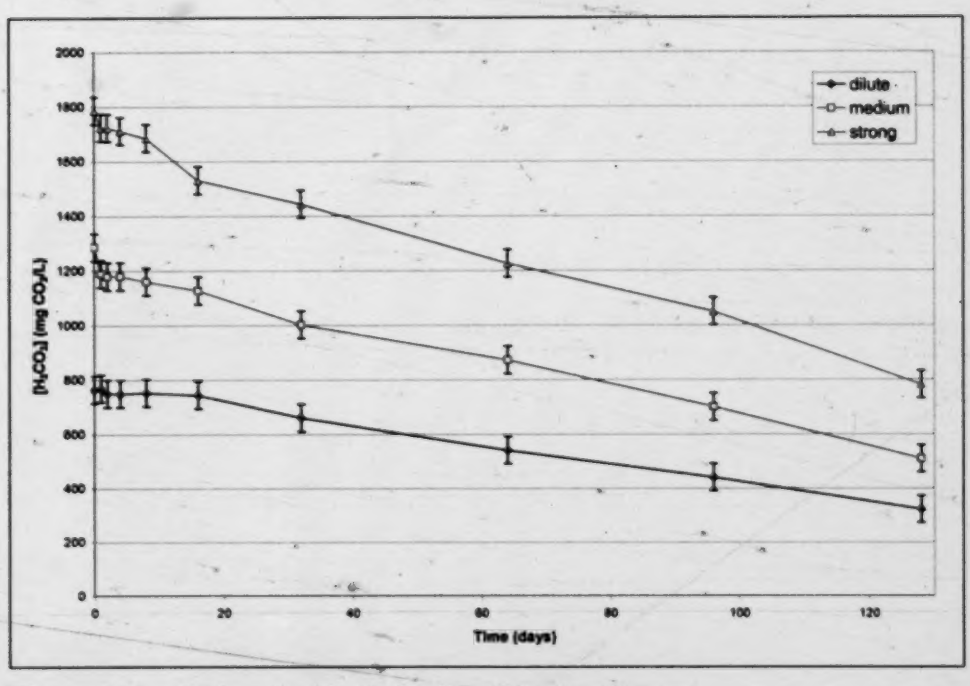

Figure 4.13 Carbon dioxide dissipation during leaching test

4.3 Column Study

The column study expanded on the initial findings of the leaching study, yielding results more representative of the potential geochemical changes that may occur in an aquifer impacted by carbon dioxide. The apparatus used for the column study is shown in Figure 4.14. The tall column (on the right) was packed with sediment and

the carbonated groundwater from the water reservoir (left) was pumped through it from the bottom up. This study built on the leaching experiment by using groundwater which was already at equilibrium with the sediment and by providing a constant CO_2 supply at a pressure corresponding to in situ pore pressures in the aquifer.

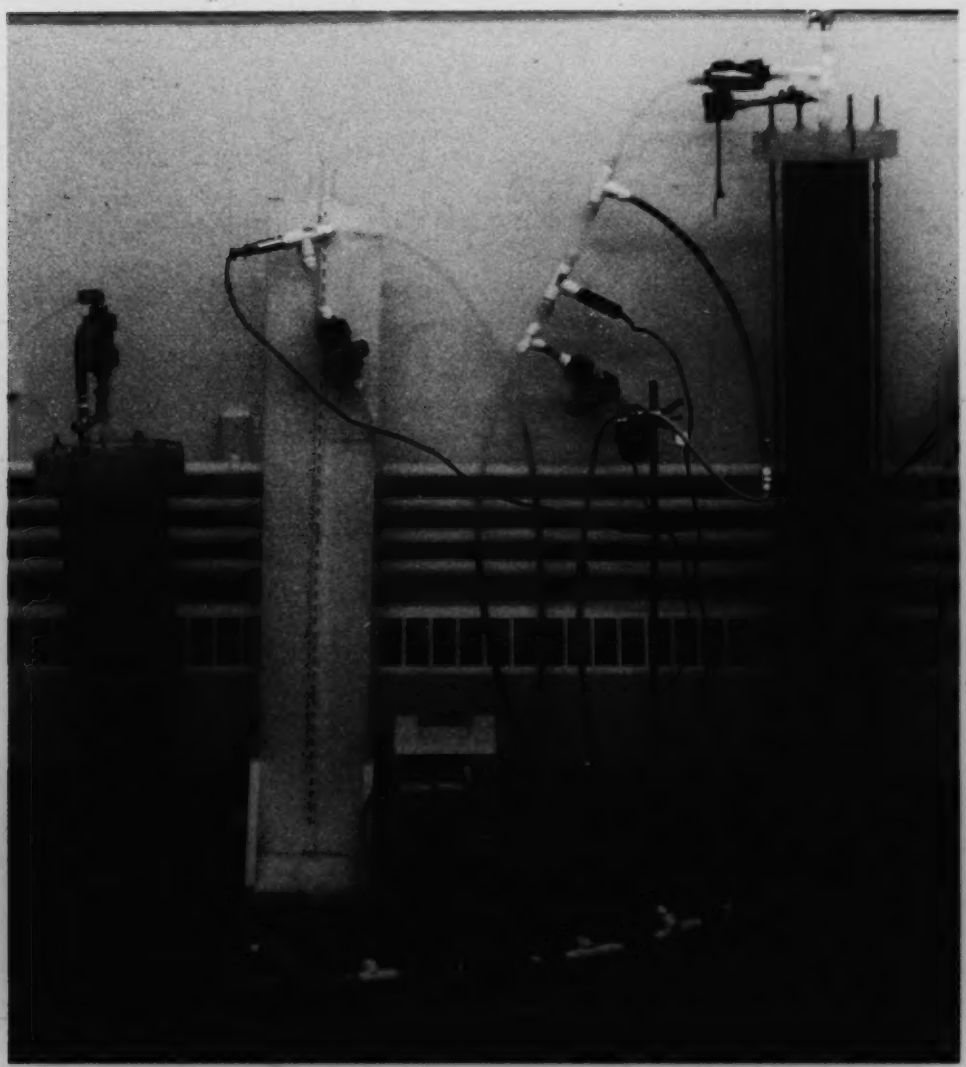

Figure 4.14 Column study apparatus

Although the groundwater was initially at equilibrium with the sediment in the column, it took roughly three days for the system to re-equilibrate after elevating the carbon dioxide levels. At this time, the pH at the outlet of the column was the same as at the inlet, as shown in Figure 4.15. The short-term buffering capacity of the water and the long-term buffering capacity of the carbonate and clay (illite ↔ kaolinite) minerals countered the acidifying effect of the carbon dioxide by converting it into bicarbonate ions. This was likely due to the migration of many fine particles into the water reservoir during initial start up, when the flow rates were higher than during operation. The presence of the fines in the reservoir would have an immediate buffering effect on the carbonated water, prior to it even entering the column. The pH was lowered from its original value of 7.6 to 5.5, despite the buffering effects that were encountered.

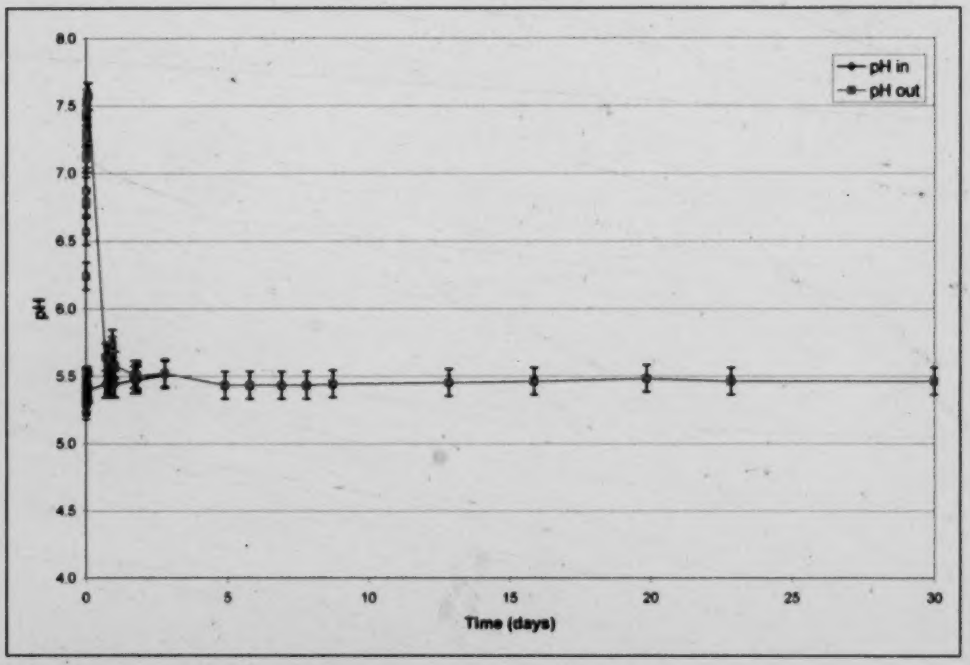

Figure 4.15 pH during column study

The ready dissolution of calcite in the presence of elevated CO_2 levels provided a long-term buffering capacity. Reactions between clay minerals also provide

significant buffering capacity, and although they are much slower than calcite dissolution they can provide up to 10 times more buffer capacity (Langmuir, 1997). Using equations for buffering capacity provided in Langmuir, the buffer capacity of the original groundwater and the column water-sediment system in equilibrium with calcite and clay minerals can be determined for comparison. The unreacted groundwater has a buffering capacity of 1.6meq/L pH, compared to 11.2meq/L pH and 23.0meq/L pH for calcite saturation and clay mineral equilibrium respectively. Calculations of these buffer capacities are shown in Appendix E. For comparison, the buffering capacity of pure water at the corresponding pH (5.5) is 0.01meq/L pH.

The electrical conductivity measurements are shown in Figure 4.16. Upon addition of CO_2, a significant increase in EC was observed when compared with the original groundwater level of 3.6mS/cm (Day 0). Measurements reached as high as 5.4mS/cm near the end of the experiment. As in the case of pH, EC values seem to have become roughly equilibrated within the first week of the experiment.

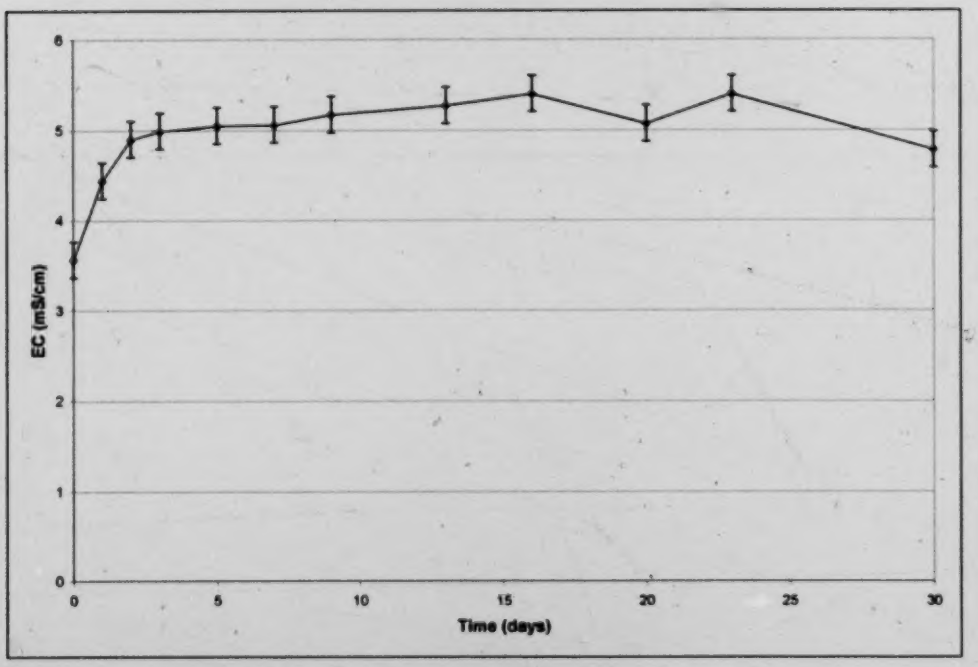

Figure 4.16 Electrical conductivity during column study

Elemental composition of the resulting groundwater was determined at each sampling interval. These results are summarized in Table 4.8. Some of the elements that underwent relatively dramatic changes in concentration are also shown graphically in Figures 4.14 – 4.22. In most cases where a particular element underwent a significant change in concentration from the original groundwater, it was an increase. However, a few elements decreased either immediately, or after an initial increase (eg. aluminum, nickel, zinc, arsenic, and barium). It should be noted that the aqueous concentrations of aluminum, arsenic, barium and strontium at the start of the study had varied (beyond reasonable experimental error) from those measured when the samples were first obtained. Although every effort was made to preserve the samples in their original condition and maintain the composition, these few elements were less stable than the others, and likely underwent various geochemical reactions during storage.

The bicarbonate concentration was proportional to the dissolved carbon dioxide levels, because the dissolved carbon dioxide is metastable and was quickly converted to bicarbonate ions under ambient conditions. The solubilization of various carbonate minerals would also contribute to the overall bicarbonate concentration. Figure 4.17 shows that with the constant applied P_{CO2}, the bicarbonate levels remained relatively constant once they reached equilibrium with the system. Bicarbonate concentrations exceeded four times the levels originally found in the groundwater (Day 0).

Figures 4.18 – 4.21 show the aqueous concentrations of calcium, magnesium, strontium and barium respectively, throughout the experiment. The significant increase in these levels (especially calcium) from the original groundwater levels indicates the dissolution of carbonate minerals. In each of these plots it appears as though the system has equilibrated itself with respect to these minerals, by the asymptotic nature of the lines.

Aqueous iron levels showed a sudden increase almost immediately after the system was carbonated (Figure 4.22). Early in the experiment (~7days), a reddish brown iron precipitate was observed to be forming in the sediment around the bottom of the column (Figure 4.23), suggesting that the water was saturated in iron with respect to some mineral phase.

Table 4.8 Groundwater composition throughout column study

Day	Anions [mg/L]					Cations [mg/L]			
	carbonate	bicarbonate	chloride	sulfate	bromide	calcium	magnesium	sodium	potassium
0	0	711	687.1	121.1	3.78	73.9	31.9	579.9	6.6
1	0	3355	646.0	112.7	3.43	503.5	71.3	587.9	21.7
2	0	2928	644.0	114.6	3.24	466.8	83.6	591.1	17.7
3	0	2959	645.2	115.8	3.22	421.4	85.3	607.1	19.2
5	0	2971	643.5	114.0	3.27	467.6	86.0	604.8	19.2
7	0	2989	649.1	110.6	3.45	504.9	85.8	597.8	18.9
9	0	3050	644.2	115.9	3.56	520.2	88.5	606.1	19.4
13	0	3050	644.6	114.9	3.43	512.1	86.2	596.1	19.6
16	0	3050	642.6	115.5	3.32	518.0	87.0	596.8	19.2
20	0	2952	651.8	114.5	3.41	521.4	86.8	599.8	19.9
23	0	3010	651.0	113.4	3.27	519.2	86.5	596.4	19.9
30	0	2928	649.2	118.1	3.45	517.0	86.4	596.1	19.0

Day	Trace Metals [ug/L]									
	aluminum	titanium	manganese	iron	nickel	copper	zinc	arsenic	selenium	rubidium
0	645.2	5	0.00	330	3.1	0.96	0.58	0.31	1.04	0.31
1	218.2	5	3.78	215000	84.1	1.78	6.95	2.19	1.04	0.83
2	270.4	5	5.85	199000	71.1	1.21	13.12	2.02	0.89	0.85
3	260.7	5	6.96	191000	86.2	1.47	15.20	1.64	1.41	0.83
5	256.1	4	6.05	196000	79.6	1.02	17.31	1.41	1.62	0.81
7	263.2	5	8.09	201000	77.4	1.32	16.48	1.28	1.73	0.89
9	254.0	5	9.24	211000	97.2	1.33	15.94	1.17	1.77	0.87
13	252.0	5	8.16	200000	84.4	0.58	10.69	1.19	2.04	0.82
16	251.3	5	8.09	199000	89.0	1.45	10.87	1.07	1.75	0.81
20	243.2	5	5.05	196000	91.0	0.00	9.39	1.05	1.48	0.85
23	244.0	5	2.94	183000	71.9	1.20	9.23	0.99	1.38	0.89
30	238.8	4	1.70	147000	48.6	0.96	9.78	0.96	1.41	0.91

Day	Trace Metals (con't) [ug/L]										
	strontium	molybdenum	silver	cadmium	antimony	cesium	barium	tellurium	lead	bismuth	uranium
0	64.8	2.44	0.005	0.010	0.258	0.001	11.6	0.010	0.020	0.016	0.430
1	233.1	0.82	0.045	0.008	0.075	0.003	116.8	0.002	0.047	0.014	0.462
2	234.8	0.48	0.015	0.009	0.062	0.003	102.2	0.002	0.035	0.014	0.386
3	235.5	0.36	0.011	0.011	0.058	0.003	91.1	0.002	0.025	0.011	0.371
5	229.7	0.34	0.008	0.008	0.041	0.002	90.6	0.001	0.010	0.010	0.352
7	242.9	0.32	0.007	0.008	0.039	0.002	93.5	0.001	0.018	0.008	0.327
9	242.9	0.29	0.026	0.003	0.041	0.002	96.2	0.001	0.013	0.030	0.310
13	229.8	0.26	0.009	0.015	0.033	0.002	87.2	0.001	0.006	0.015	0.311
16	236.1	0.21	0.007	0.004	0.039	0.002	87.5	0.001	0.016	0.010	0.288
20	235.8	0.23	0.005	0.005	0.035	0.002	84.2	0.000	0.009	0.009	0.292
23	237.0	0.21	0.004	0.005	0.023	0.002	80.7	0.000	0.012	0.007	0.275
30	233.3	0.20	0.003	0.003	0.021	0.002	70.7	0.000	0.005	0.005	0.276

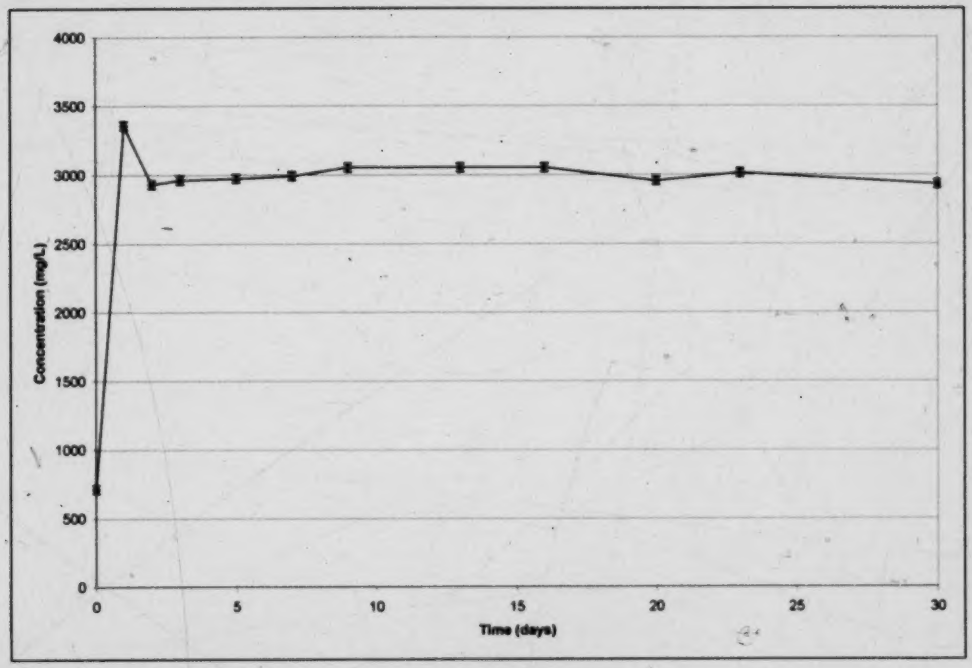

Figure 4.17 Bicarbonate concentration during column study

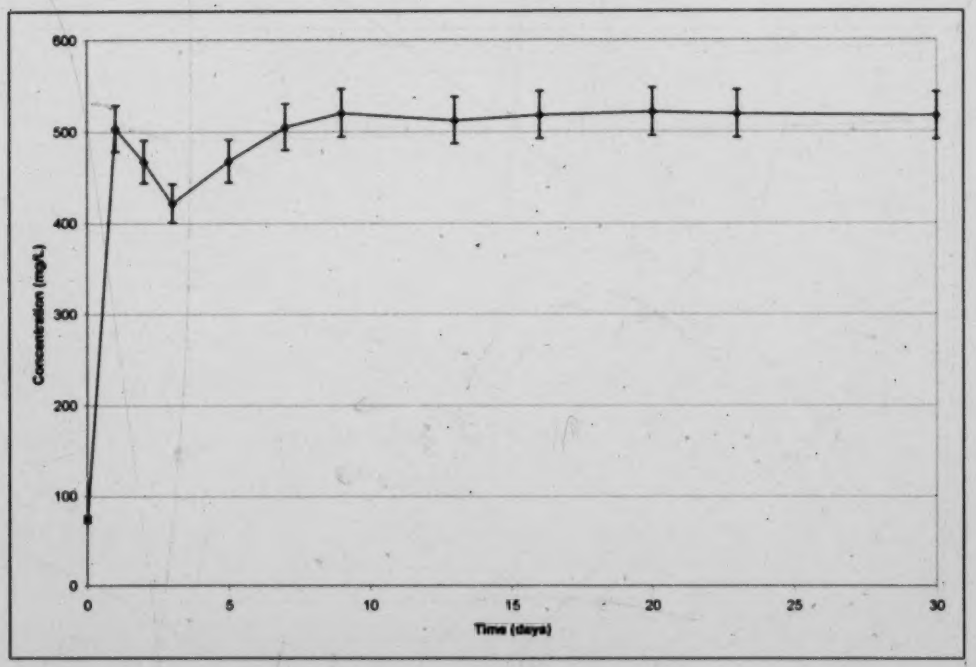

Figure 4.18 Calcium concentration during column study

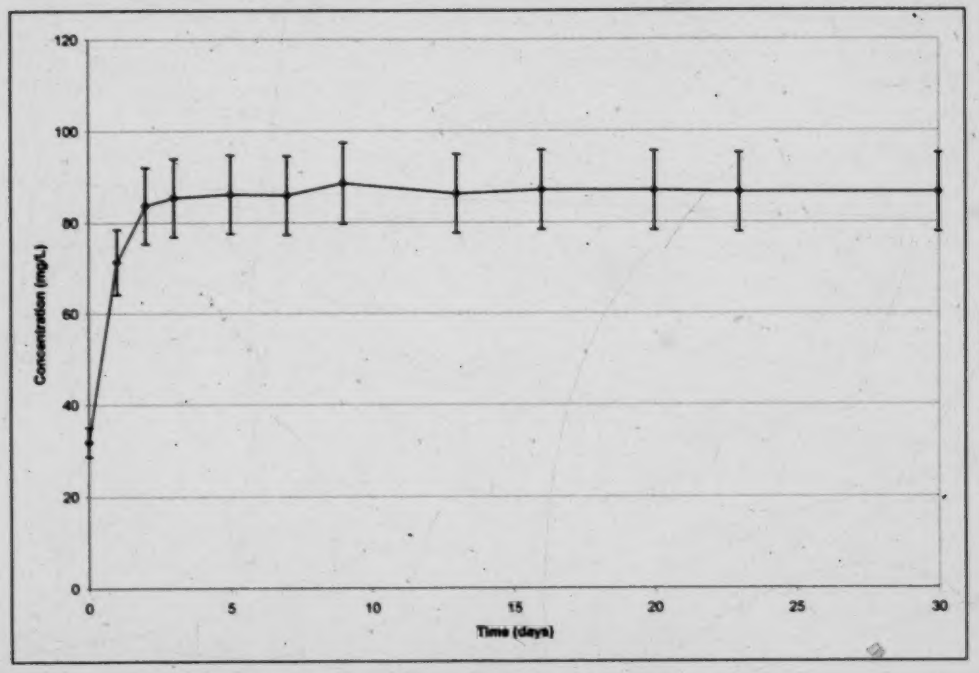

Figure 4.19 Magnesium concentration during column study

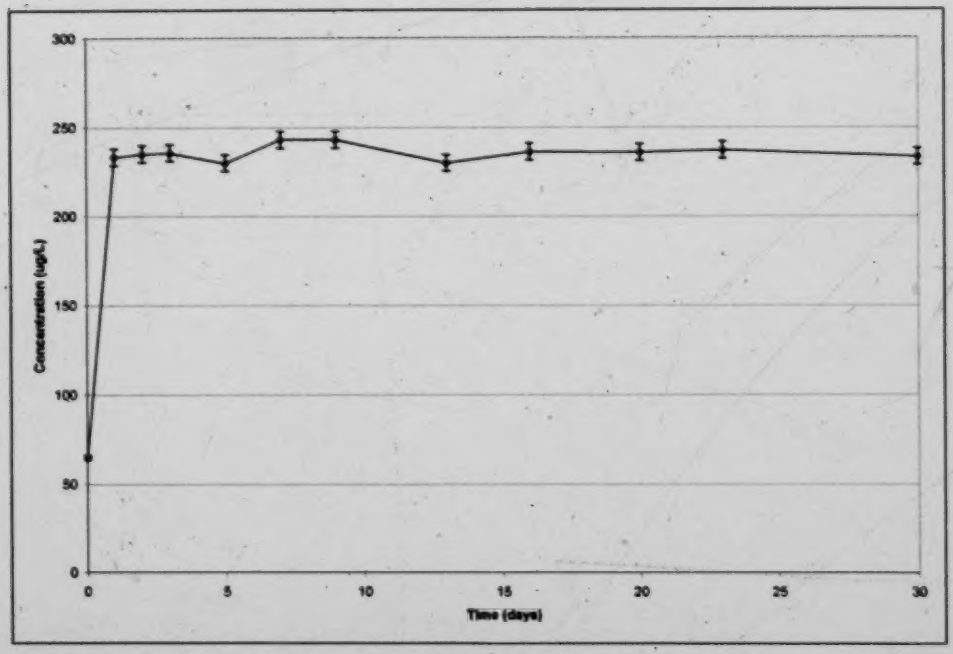

Figure 4.20 Strontium concentration during column study

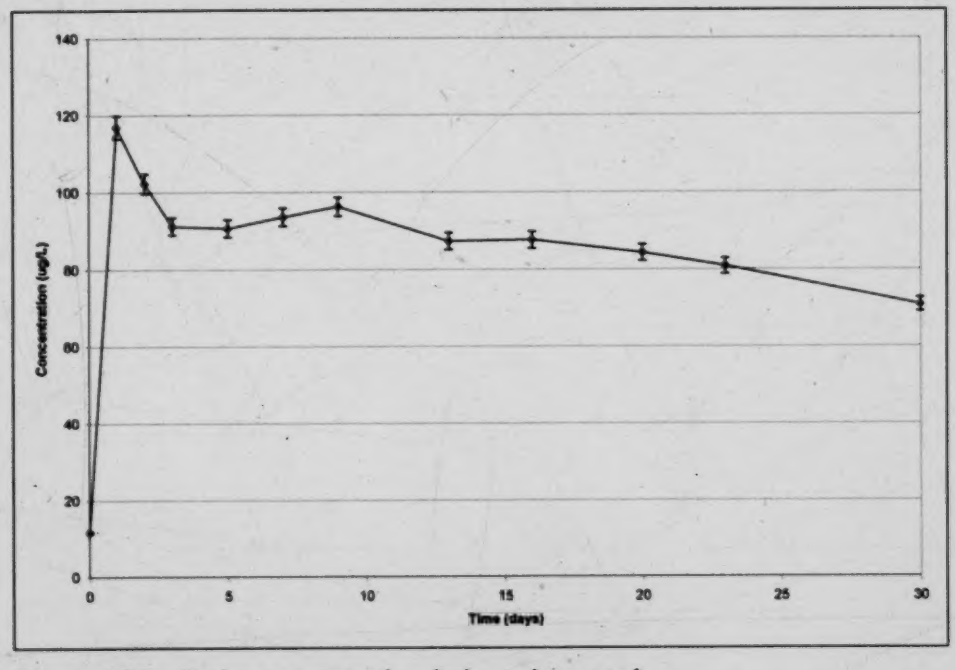

Figure 4.21 Barium concentration during column study

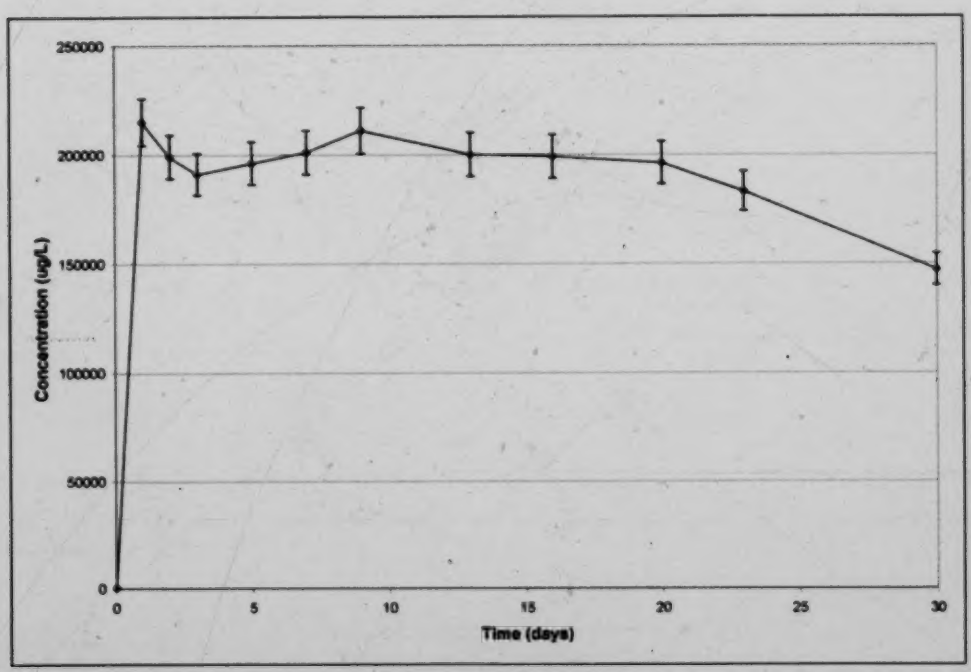

Figure 4.22 Iron concentration during column study

Figure 4.23 Siderite precipitate formed at column inlet (bottom)

While the results presented in Table 4.8 indicate that the groundwater concentration of several of the metal ions (manganese, iron, nickel, copper, zinc, arsenic, selenium, rubidium, strontium, barium, lead, uranium) increased under elevated CO_2 conditions, none of these exceeded the Drinking Water Quality Guidelines presented by CCME (Table 4.5) throughout the duration of the experiment. In fact, for those metals (arsenic, selenium, barium, lead, uranium) that CCME listed a Maximum Acceptable Concentration (MAC), the observed experimental water levels all remained at least an order of magnitude lower than the MAC's. Some of the other metals (nickel, rubidium, strontium) had no guidelines, while others (manganese, iron, copper, zinc)

were listed as Aesthetic Objectives (AO). With the exception of iron, these metals remained well under AO's. Iron exceeded the AO of 300μg/L by a significant amount, with peak dissolved iron levels at 215000μg/L early in the experiment.

Tests were also conducted in order to determine the change in sediment composition before and after the column study. Strong acid digestions in Aqua Regia were performed in order to solubilize the minerals for elemental analysis via IC and ICP/MS. Semi-quantitative XRD analysis was also performed on the fine portion of the sediment to determine the mineralogical changes.

Table 4.9 shows the elemental composition of the sediment. This test was performed on the bulk sediment and the fines portion of the sediment before the column study. After the column study, bulk sediment samples were analyzed from the bottom, middle and top of the column (to compare any geochemical differences in the sediment along the length of the column), as well as the fines. The concentrations of nearly all of the elements decreased after the column study as compared to before. This effect was common to the bulk sediment and the fines. Comparison of the bulk and fine sediment composition shows without doubt the importance of the fine portion of the sediment to the geochemical changes occurring under elevated carbon dioxide levels. The fines contained elevated levels of all trace metals compared to the bulk composition, and in the majority of samples, a larger proportion of metals leached out of the fines compared to the bulk sediment. For example, the decrease in iron levels in the fine sediment is sufficient to account for all of the iron in solution.

Table 4.9 Elemental composition of various portions of sediment

	Bulk Sediment				Fines	
	before	after - bottom	after - middle	after - top	before	after
	[ug/g]	[ug/g]	[ug/g]	[ug/g]	[ug/g]	[ug/g]
calcium	33113	22898	26779	18040	30360	71607
magnesium	12993	7171	10708	6059	14963	28458
aluminum	18679	12734	16490	12053	23933	25497
titanium	181.4	153.1	150.6	155.4	239.9	216.2
manganese	81.7	127.6	20.2	146.6	887.9	197.4
iron	16099	9643	7208	6623	47282	33774
nickel	118.3	95.9	153.5	116.4	214.9	167
copper	3.8	8.5	7.2	5.1	57.7	36.2
zinc	13.7	19.7	9.4	18.3	137.6	73.1
arsenic	9.9	6.7	5.6	5.7	21.9	16.1
selenium	6.0	3.6	9.2	2.3	17.7	11.6
rubidium	4.7	3.3	2.6	3.0	40.4	26.7
strontium	29.4	18.5	18.1	19.8	99.6	84.8
molybdenum	2.8	2.9	1.9	2.0	3.5	2.9
silver	0.05	0.04	0.01	0.02	0.22	0.11
cadmium	0.07	0.05	0.04	0.02	0.43	0.4
antimony	0.20	0.06	0.08	0.07	0.75	0.52
cesium	0.16	0.14	0.14	0.15	3.27	1.76
barium	77.7	49.9	32.1	37.7	268.7	186.9
tellurium	0.03	0.03	0.02	0.02	0.33	0.22
lead	4.08	1.53	2.00	1.85	20.39	12.14
bismuth	0.15	0.14	0.08	0.06	0.44	0.21
uranium	0.30	0.33	0.29	0.31	1.50	1.06

The mineralogical composition of the fines (before and after the column study) are provided in Table 4.10. As mentioned previously, the proportion of iron-rich clay minerals decreased during the column study, as did the total clay levels in the sample. It is important to keep in mind when analyzing this data that the test is semi-quantitative, and is subject to 10% margins of error. A significant source of error, particularly for the fine sediment after the column study, is the effect of the pore water chemistry. Due to the small amount of fines that could be collected after the column study, the water was decanted from the sample as much as was possible without losing any sample prior to being oven-dried. The impact of the drying of this mineral-rich water with the sample was that the abundance of minerals such as calcium, magnesium, and bicarbonate caused elevated levels of calcite and dolomite to be reported. The same effect was observed in the measurement of elemental composition (Table 4.10), where the levels of calcium and magnesium are higher in

the sediment after the column study than before. This cannot be the case, as it was shown in the groundwater measurements (which do not have this type of error associated with them) that there is an increase in calcium, magnesium and bicarbonate, which corresponds to a net dissolution of the carbonate minerals calcite and dolomite. While the overestimation of mineral phase was significant for carbonate minerals, it was greatly reduced for the others where there was not such an abundance of dissolved species in the resultant groundwater.

Table 4.10 Mineralogy of fine sediment (before and after column study)

	Before	After
	% of Sample	
quartz	27	29
plagioclase	4	7
K-feldspar	4	7
calcite	6	11
dolomite	9	25
kaolinite	9	9
chlorite	9	3
illite	19	5
smectite	13	4
% clay	*50*	*22*

Elemental analysis conducted on the fine sediment indicated that ~3% of the total mass was iron (Table 4.9). While some of this iron is present in iron-bearing clay minerals, it is likely that some other iron-bearing mineral(s) were present in the fine sediment. Unfortunately due to the relatively low abundance of these minerals (as compared with silicates and carbonates) they were not detected in the XRD analysis (a particular mineral phase must make up at least 3 – 5% of the sample in order to be detected) that was conducted (Table 4.10). It is likely that hematite, goethite and $Fe(OH)_3$ are present in the aquifer sediment. The dissolution of these minerals would have been favored in the low pH, high bicarbonate environment.

The decomposition of clay minerals such as smectite and chlorite were also sources of Fe(II). As can be seen in Table 4.10, the fine portion of the sediment prior to the column study was rich in these iron-bearing minerals, whereas in the fines collected

after the column study had reduced iron levels. In fact, the overall percentage of clay minerals in the fines dropped from 50% of total sample before the column study to only 22% after the experiment (some of this may have been due to the initial migration of fines into the reservoir). Calculations of aqueous Fe levels based on the decrease in iron concentration in the fines (from Table 4.9) yields a net contribution of Fe(II) for the formation of siderite. These calculations are shown in Appendix E.

The CEC (cation exchange capacity) of the fine sediment was determined to be 38.6meq/100g. Surface exchange processes in the column study were deemed to be insignificant however, relative to changes in solution due to the large extent of mineral dissolution that occurred.

Pressure differential measurements were taken across the column throughout the experiment in order to determine any change in hydraulic conductivity that may occur during this experiment. Figure 4.24 shows hydraulic conductivity plotted over time. These values are only included for the first half of the experiment, because after that time a minor leak developed at the top of the column which had a significant impact on the pressure differential readings. A distinct drop in hydraulic conductivity values can be observed, from ~4×10^{-4} to 1.7×10^{-4}cm/s indicating that the precipitates formed throughout the experiment were beginning to have a noticeable plugging effect.

While this effect was slight for this short experiment, it is conceivable that over geologic time scales the accumulation of mineral precipitates could lead to a significant decrease in porosity, which would adversely affect the permeability and fluid flow in the aquifer. This effect would be observed to somewhat of a lesser extent due to the ongoing dissolution of calcite and dolomite, which would increase the hydraulic conductivity. A net loss in porosity is observed however, due to the uptake of the carbon dioxide mass into the mineral matrix.

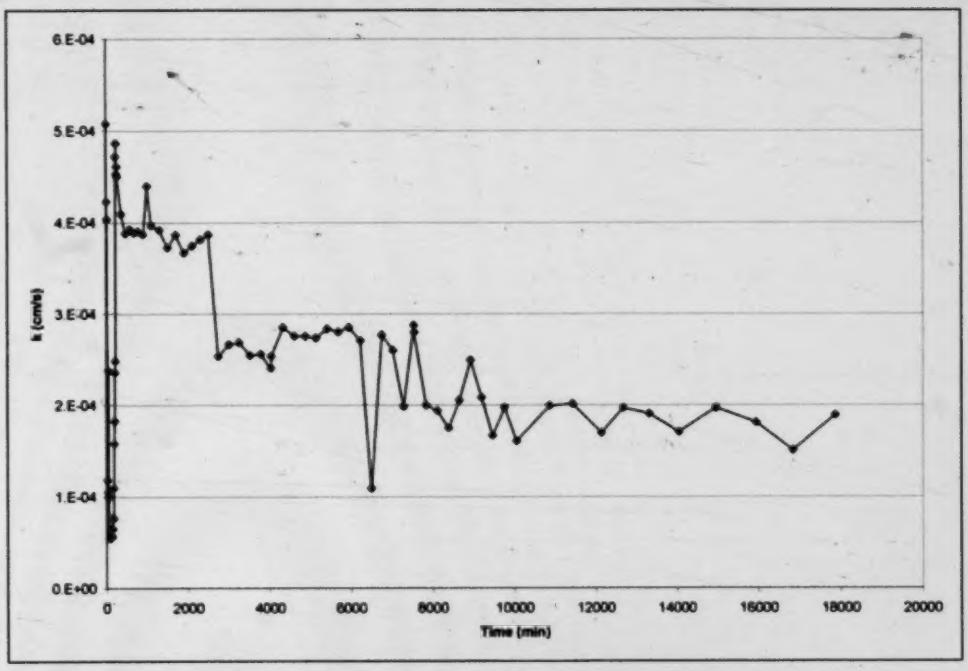

Figure 4.24 Change in hydraulic conductivity during column study

(*Note that values are not included for the second half of study, due to a minor leak at top of column, which skewed the pressure differential readings and yielded unrepresentative and falsely high k values)

Numerical simulations to determine potential impacts of CO_2 sequestration through mineral trapping were conducted at Lawrence Berkeley National Laboratory at the University of California (Xu et al, 2003). Results indicated that the precipitation of siderite occurred (at rates dependent on the rate of reduction of Fe(III) from sources such as goethite) and led to a considerable decrease in porosity of the formation. This suggests that the initial observed decrease in hydraulic conductivity may become significant in the long term.

Scanning electron microscopy (SEM) was performed on various fractions of the sediment before and after the column study in order to observe any physical changes that may have occurred at the sediment surfaces.

Figures 4.25 and 4.26 show the bulk sediment (before and after the column study, respectively) at 55X magnification. The initial sediment sample is coated with a nebulous film, which is the fine particles present in the sample coating the sand grains. This is further shown in Figures 4.27 – 4.29, which show the bulk sediment before the column study, and after the study from the bottom and the top of the column respectively. These are at a magnification of 220X. In Figure 4.27 (before the column study) it can again be seen that the sediment is coated with fines. Figures 4.28 and 4.29 (after column study) do not exhibit a similar coating, even at the increased magnification.

The unique feature of the sediment particles after the column study is that they show the deposition of tiny discrete particles on the sediment surface. This effect is more obvious for the sediment taken from the bottom (Figure 4.28) of the column than at the top (Figure 4.29), suggesting that it could be the iron precipitate which was visually much more evident at the bottom of the column than at the top.

It should also be noted that there is no apparent "rounding" of the bulk sediment surface after the column study that would provide evidence of mineral weathering. Most of the sediment that is observable in these images is silicate sand. Due to the relatively slow weathering rates of silicate minerals and the short duration of this experiment, it is not surprising that weathering effects were not visible on these grains.

Figures 4.30 and 4.31 show SEM images for the fine sediment (ie. silt and clay less than 75μm) before and after the column study, respectively. In Figure 4.30a, the branching between the particles can be seen, whereas in part b the particles appear to be discrete and unconnected. In the fine sediment sample observed after the column study (Figure 4.31), it appears that all of the particles are branched and connected. These particles also appear to have more of a plate-like structure, indicative of kaolinite, a common by-product of feldspar weathering.

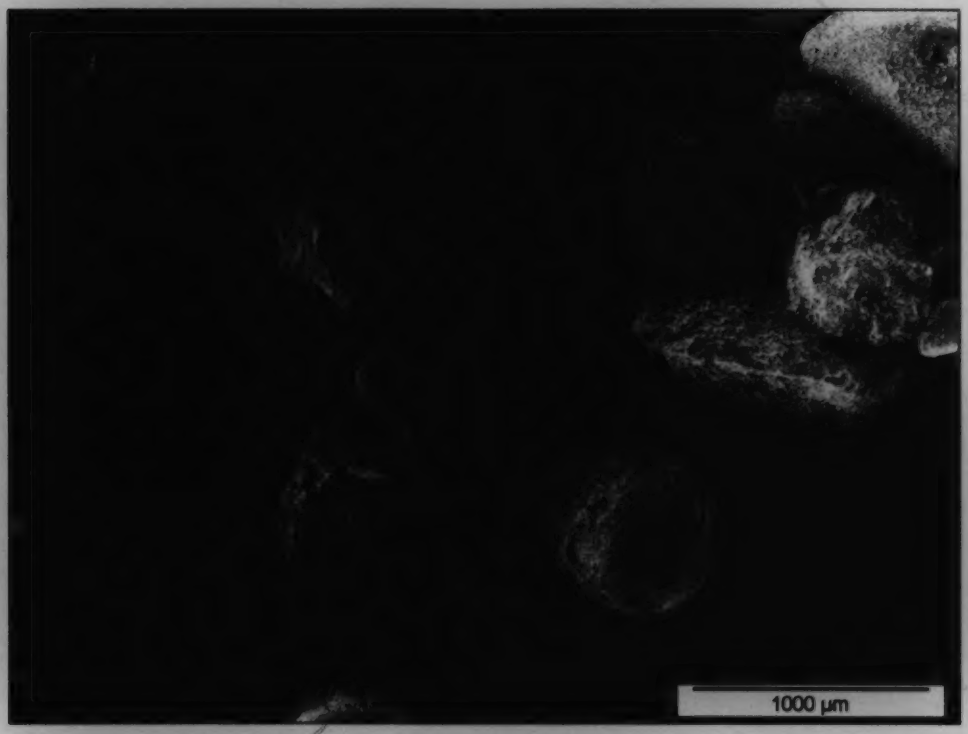

Figure 4.25 SEM image of bulk sediment before column study [55X magnification]

Figure 4.26 SEM image of bulk sediment after column study [55X magnification]

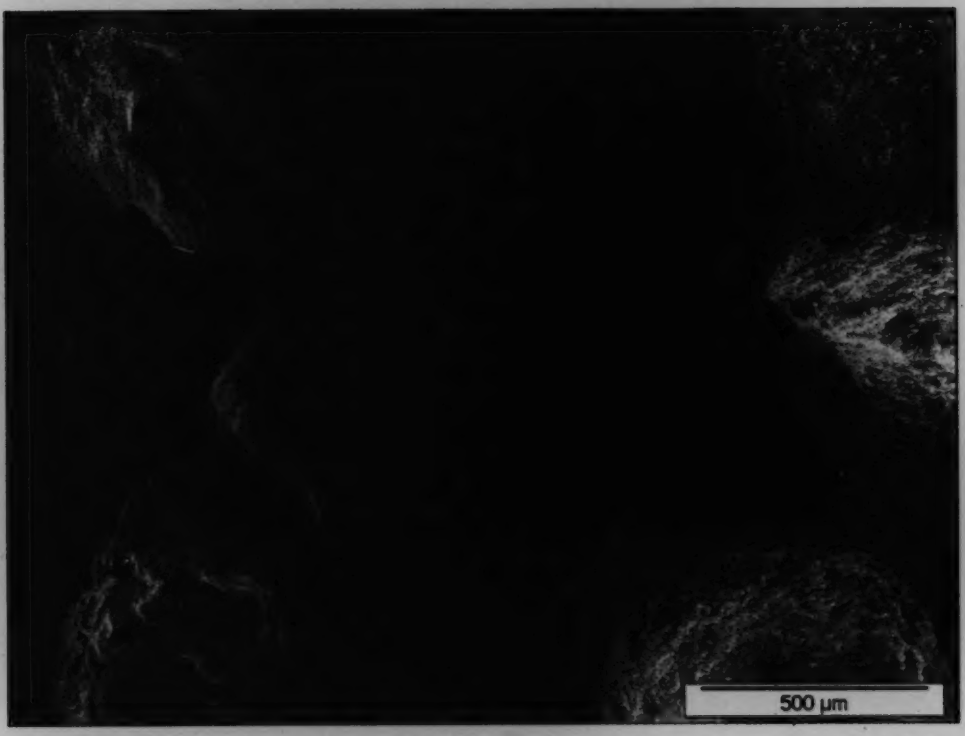

Figure 4.27 SEM image of bulk sediment before column study [220X magnification]

Figure 4.28 – SEM image of bulk sediment from bottom of column after column study [220X magnification]

Figure 4.29 – SEM image of bulk sediment from top of column after column study [220X magnification]

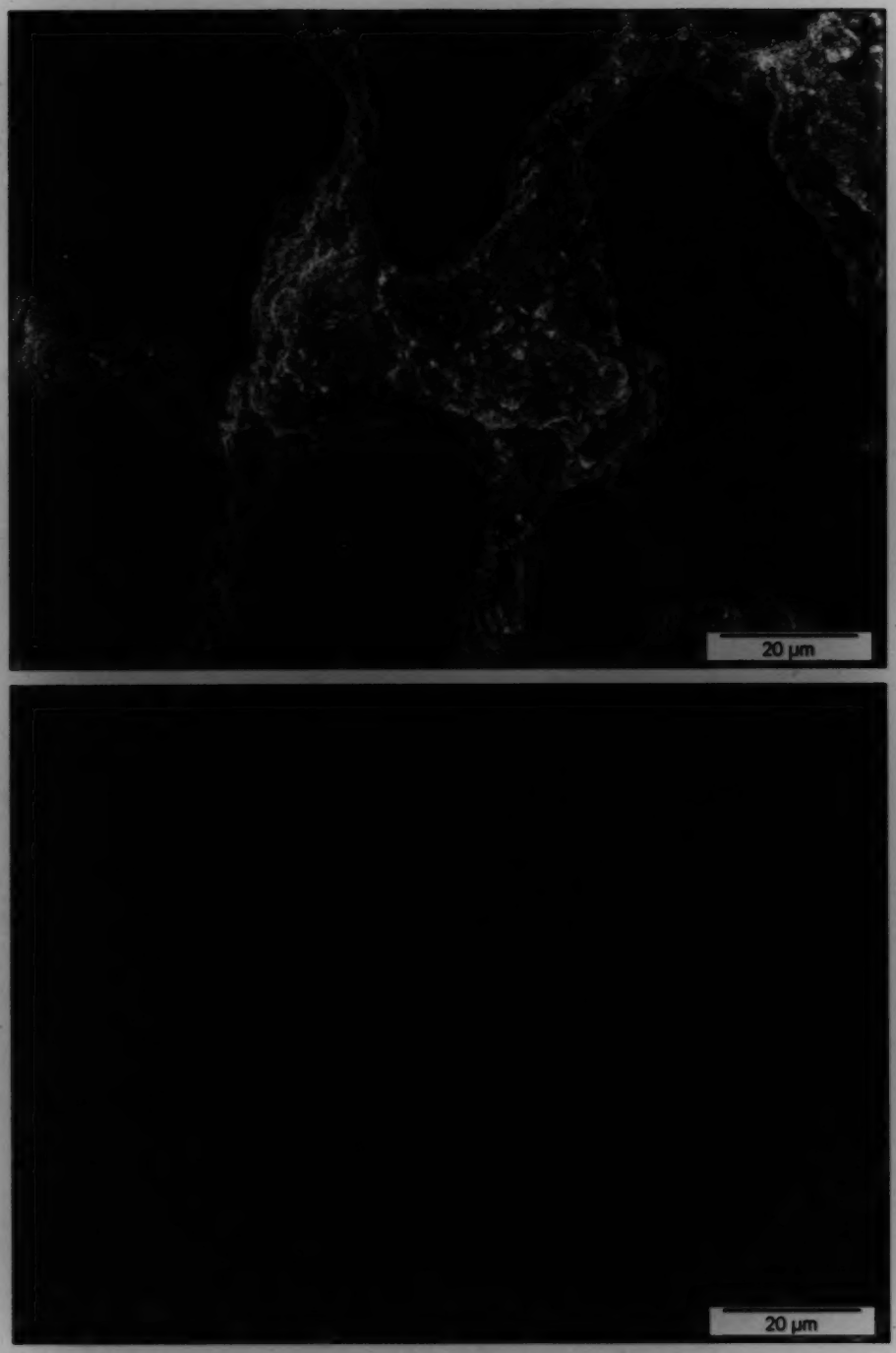

Figure 4.30 (a, b) SEM images of fine sediment (<75µm) before column study [963X magnification]

Figure 4.31 SEM image of fine sediment (<75µm) after column study [963X magnification]

4.4 Geochemical Modeling

Geochemical modeling was conducted using PHREEQC in order to characterize the geochemical changes that were observed in the column and therefore would likely be observed in the aquifer, under elevated CO_2 conditions. Additionally, with the aid of inverse modeling techniques, PHREEQC was used to predict reaction pathways of key geochemical changes that were observed in the column. Of particular interest was the mechanism of siderite formation (ie. which mineral species were becoming solubilized to generate sufficient Fe(II) in solution for the formation of siderite). The input file is provided in Appendix D.

The results of the inverse modeling indicated that the dissolution of the common iron-bearing minerals goethite, hematite and $Fe(OH)_3$ and the subsequent formation of siderite would be thermodynamically favorable under the conditions of the column study. These results are shown in Table 4.11.

Table 4.11 Inverse modeling results

Fe(OH)$_3$ (a) Dissolution		
Phase mole transfers:		
Calcite	9.507e-003	CaCO3
Dolomite	2.311e-003	CaMg(CO3)2
Siderite	-8.950e-001	FeCO3
CO2(g)	9.757e-001	CO2
CH2O	2.247e-001	CH2O
Fe(OH)3(a)	8.988e-001	Fe(OH)3
Redox mole transfers:		
C(-4)	1.124e-001	
Fe(3)	8.988e-001	

Goethite Dissolution		
Phase mole transfers:		
Calcite	9.507e-003	CaCO3
Dolomite	2.311e-003	CaMg(CO3)2
Siderite	-2.093e+000	FeCO3
CO2(g)	1.875e+000	CO2
Goethite	2.097e+000	FeOOH
CH2O	5.243e-001	CH2O
Redox mole transfers:		
C(-4)	2.622e-001	
Fe(3)	2.097e+000	

Hematite Dissolution		
Phase mole transfers:		
Calcite	9.507e-003	CaCO3
Dolomite	2.311e-003	CaMg(CO3)2
Siderite	-6.288e+000	FeCO3
CO2(g)	5.020e+000	CO2
CH2O	1.573e+000	CH2O
Hematite	3.146e+000	Fe2O3
Redox mole transfers:		
C(-4)	7.865e-001	
Fe(3)	6.292e+000	

A positive phase mole transfer indicates that the mineral was dissolving, while a negative phase mole transfer (as for siderite) indicates mineral precipitation. Also included are calcite and dolomite, whose dissolution was required to generate the necessary bicarbonate ions for siderite precipitation. It was necessary to include the organic carbon (CH_2O) as the redox couple for the reduction of Fe(III) to Fe(II), as shown under the redox mole transfers heading. Using the measured DOC values from the groundwater, it was determined that approximately 1.4 moles of carbon were available for reaction, exceeding the amount required for the redox couple, according to the results of the model, shown in Table 4.11.

Although the results of the inverse modeling indicate that it is thermodynamically feasible for any of these three iron-bearing minerals to become solubilized under the specified conditions, it is most likely that the $Fe(OH)_3$ was the primary mineral phase going into solution. Analysis of the saturation indices of each of these minerals in solution (Table 4.12) suggests that only $Fe(OH)_3$ became undersaturated (negative value) in the carbon dioxide enhanced environment. Hematite and goethite remained heavily oversaturated, although to a lesser extent than in the original solution. Table

4.12 also shows the dissolution of calcite and dolomite, which were somewat soluble in the weakly acidic environment.

Table 4.12 Saturation indices

Day	Calcite	Dolomite	$Fe(OH)_3(a)$	Goethite	Hematite	Siderite	$CO_2(g)$
0	0.58	1.09	2.47	8.18	18.35	-0.24	-1.84
1	-0.11	-0.78	-0.56	5.15	12.29	1.38	0.80
2	-0.27	-0.99	-0.79	4.92	11.83	1.25	0.82
3	-0.30	-0.99	-0.78	4.93	11.84	1.25	0.82
5	-0.34	-1.13	-1.04	4.67	11.32	1.17	0.91
7	-0.31	-1.10	-1.04	4.68	11.34	1.18	0.91
9	-0.29	-1.04	-0.99	4.72	11.43	1.21	0.90
13	-0.28	-1.04	-0.98	4.73	11.45	1.20	0.90
16	-0.27	-1.01	-0.96	4.76	11.50	1.20	0.89
20	-0.25	-0.99	-0.89	4.82	11.63	1.21	0.85
23	-0.27	-1.01	-0.99	4.72	11.44	1.17	0.88
30	-0.27	-1.03	-1.08	4.64	11.26	1.07	0.87

Additional useful information in the PHREEQC output file is the speciation data (Table 4.13). The Day 0 values present the original conditions, prior to the carbon dioxide levels being elevated. With the exception of Fe(III), each of the species increased in total concentration in solution. The decreased levels of Fe(III) are to be expected on account of the reduction of Fe(III) to Fe(II) as previously discussed. Each of the other species included in this table are present predominantly as the free ion or as bicarbonate complexes. Each species is also present as carbonate and sulfate complexes, although to a much lesser extent.

Table 4.13 Speciation results

	Day 0	Day 1	Day 2	Day 3	Day 5	Day 7	Day 9	Day 13	Day 16	Day 20	Day 23	Day 30
Ba	8.8E-08	8.6E-07	7.5E-07	6.7E-07	6.7E-07	6.9E-07	7.0E-07	6.4E-07	6.4E-07	6.1E-07	5.9E-07	5.2E-07
Ba^{+2}	7.4E-08	7.0E-07	6.2E-07	5.5E-07	5.5E-07	5.7E-07	5.8E-07	5.2E-07	5.3E-07	5.1E-07	4.9E-07	4.3E-07
$BaSO_4$	9.8E-09	4.5E-08	4.1E-08	3.8E-08	3.6E-08	3.5E-08	3.7E-08	3.4E-08	3.4E-08	3.3E-08	3.1E-08	2.9E-08
$BaHCO_3^+$	3.4E-09	1.1E-07	8.9E-08	8.1E-08	8.1E-08	8.3E-08	8.6E-08	7.8E-08	7.9E-08	7.3E-08	7.2E-08	6.2E-08
$BaCO_3$	2.7E-10	8.4E-11	5.5E-11	5.1E-11	4.1E-11	4.2E-11	4.4E-11	4.1E-11	4.3E-11	4.2E-11	3.9E-11	3.4E-11
Ca	1.9E-03	1.3E-02	1.2E-02	1.1E-02	1.7E-03	1.3E-02	1.3E-02	1.3E-02	1.3E-02	1.3E-02	1.3E-02	1.3E-02
Ca^{+2}	1.6E-03	9.9E-03	9.4E-03	8.4E-03	2.1E-03	1.0E-02	1.0E-02	1.0E-02	1.0E-02	1.1E-02	1.0E-02	1.0E-02
$CaHCO_3^+$	1.1E-04	2.4E-03	2.0E-03	1.9E-03	2.1E-03	2.2E-03	2.3E-03	2.3E-03	2.3E-03	2.3E-03	2.3E-03	2.3E-03
$CaSO_4$	8.5E-05	2.5E-04	2.5E-04	2.3E-04	2.5E-04	2.5E-04	2.7E-04	2.6E-04	2.7E-04	2.7E-04	2.6E-04	2.6E-04
$CaCO_3$	2.0E-05	4.1E-06	2.9E-06	2.7E-06	2.4E-06	2.6E-06	2.7E-06	2.8E-06	2.9E-06	2.9E-06	2.9E-06	2.8E-06
Fe(II)	1.8E-06	3.9E-03	3.6E-03	3.4E-03	3.5E-03	3.6E-03	3.8E-03	3.6E-03	3.6E-03	3.5E-03	3.3E-03	2.6E-03
Fe^{+2}	1.0E-06	1.3E-03	1.3E-03	1.2E-03	1.2E-03	1.3E-03	1.3E-03	1.3E-03	1.3E-03	1.3E-03	1.2E-03	9.4E-04
$FeHCO_3^+$	5.7E-07	2.5E-03	2.3E-03	2.2E-03	2.2E-03	2.3E-03	2.4E-03	2.3E-03	2.3E-03	2.2E-03	2.1E-03	1.7E-03
$FeCO_3$	1.9E-07	7.8E-06	5.8E-06	5.8E-06	4.8E-06	4.9E-06	5.3E-06	5.1E-06	5.2E-06	5.3E-06	4.8E-06	3.8E-06
$FeSO_4$	4.3E-08	2.6E-05	2.8E-05	2.7E-05	2.6E-05	2.6E-05	2.8E-05	2.6E-05	2.6E-05	2.6E-05	2.4E-05	2.0E-05
$FeCl^+$	1.3E-08	1.3E-05	1.3E-05	1.2E-05	1.3E-05	1.3E-05	1.3E-05	1.3E-05	1.3E-05	1.3E-05	1.2E-05	9.6E-06
$FeOH^+$	5.2E-09	5.4E-08	4.5E-08	4.4E-08	3.7E-08	3.8E-08	4.0E-08	3.9E-08	3.9E-08	4.2E-08	3.7E-08	3.0E-08
Fe(III)	4.1E-06	9.6E-08	6.7E-08	6.7E-08	4.5E-08	4.6E-08	5.0E-08	5.0E-08	5.2E-08	5.7E-08	4.8E-08	3.9E-08
$Fe(OH)_3$	3.1E-06	2.8E-09	1.7E-09	1.7E-09	9.3E-10	9.5E-10	1.1E-09	1.1E-09	1.1E-09	1.3E-09	1.1E-09	8.6E-10
$Fe(OH)_2^+$	9.0E-07	9.1E-08	6.4E-08	6.3E-08	4.3E-08	4.4E-08	4.8E-08	4.7E-08	4.9E-08	5.4E-08	4.6E-08	3.7E-08
$Fe(OH)_4^-$	1.1E-07	1.0E-12	5.1E-13	5.3E-13	2.4E-13	2.4E-13	2.7E-13	2.8E-13	3.1E-13	3.8E-13	2.9E-13	2.3E-13
$FeOH^{+2}$	1.4E-10	1.7E-09	1.4E-09	1.4E-09	1.2E-09	1.2E-09	1.3E-09	1.2E-09	1.2E-09	1.3E-09	1.2E-09	9.3E-10
$FeSO_4^+$	2.3E-15	1.5E-12	1.5E-12	1.5E-12	1.5E-12	1.4E-12	1.5E-12	1.5E-12	1.5E-12	1.5E-12	1.3E-12	1.1E-12
Fe^{+3}	1.7E-15	2.9E-12	2.8E-12	2.6E-12	2.8E-12	2.9E-12	3.0E-12	2.8E-12	2.8E-12	2.8E-12	2.6E-12	2.1E-12
Mg	1.3E-03	2.9E-03	3.5E-03	3.5E-03	3.6E-03	3.6E-03	3.7E-03	3.6E-03	3.6E-03	3.6E-03	3.6E-03	3.6E-03
Mg^{+2}	1.2E-03	2.3E-03	2.8E-03	2.8E-03	2.8E-03	2.8E-03	2.9E-03	2.8E-03	2.9E-03	2.9E-03	2.9E-03	2.8E-03
$MgHCO_3^+$	7.9E-05	5.7E-04	6.1E-04	6.3E-04	6.3E-04	6.3E-04	6.6E-04	6.4E-04	6.5E-04	6.3E-04	6.4E-04	6.3E-04
$MgSO_4$	6.7E-05	6.6E-05	8.2E-05	8.6E-05	8.3E-05	7.9E-05	8.3E-05	8.1E-05	8.2E-05	8.2E-05	8.0E-05	8.4E-05
$MgCO_3$	8.5E-06	5.6E-07	5.0E-07	5.3E-07	4.3E-07	4.3E-07	4.6E-07	4.6E-07	4.7E-07	4.8E-07	4.7E-07	4.6E-07
Sr	7.4E-07	2.7E-06	2.7E-06	2.7E-06	2.6E-06	2.8E-06	2.8E-06	2.6E-06	2.7E-06	2.7E-06	2.7E-06	2.7E-06
Sr^{+2}	6.6E-07	2.1E-06	2.1E-06	2.1E-06	2.1E-06	2.2E-06	2.2E-06	2.1E-06	2.1E-06	2.1E-06	2.1E-06	2.1E-06
$SrHCO_3^+$	4.9E-08	5.6E-07	5.1E-07	5.2E-07	5.0E-07	5.3E-07	5.3E-07	5.1E-07	5.2E-07	5.1E-07	5.2E-07	5.0E-07
$SrSO_4$	3.3E-08	5.1E-08	5.5E-08	5.7E-08	5.3E-08	5.3E-08	5.4E-08	5.2E-08	5.3E-08	5.3E-08	5.2E-08	5.4E-08
$SrCO_3$	3.0E-09	3.1E-10	2.4E-10	2.5E-10	2.0E-10	2.1E-10	2.1E-10	2.1E-10	2.2E-10	2.2E-10	2.2E-10	2.1E-10

5.0 SUMMARY AND RECOMMENDATIONS

The objective of this research program was to characterize the geochemical reactions that may occur in an aquifer as a result of carbon dioxide leakage from an underlying reservoir being used for the geologic sequestration of CO_2. The following sections present an overview of the key findings from the work conducted, and recommendations for future research.

5.1 Drilling Program

The drilling program was conducted to obtain representative groundwater and sediment samples for the laboratory experiments while determining the lithology of the overlying sediment.

5.1.1 Key Findings

- The groundwater is rich in calcium, magnesium, and bicarbonate, indicative of the high carbonate content of the aquifer. Strontium was also present at elevated levels.

- The sediment is also high in calcium and magnesium, because of the carbonate minerals. The iron levels are also high, indicating the presence of iron-rich minerals, and the high aluminum content indicates the presence of aluminosilicates. Several trace metals are also present in relatively high concentrations including arsenic, barium, chromium, cobalt, copper, lead, nickel, strontium, titanium, vanadium, and zinc.

- The fines were the most geochemically reactive portion of the sediment, therefore it was very important that care was taken to ensure that they were obtained as part of the bulk sample, in order to achieve representative results.

5.1.2 Recommendations

- The precautions taken to preserve the samples with minimal geochemical changes during storage were effective. For future projects of this nature, every key property of the water should be measured, even if it is not thought to be important at the time. While most important properties were determined either at the time of sampling or upon return to the lab, the redox potential of the water, which turned out to be significant for the reduction of Fe(III) to Fe(II), was never determined. While in situ redox can be measured, it can be very difficult and it was beyond the scope of this study.

- For samples sent to an external laboratory for analysis, it should be confirmed beforehand that the methods used will be consistent with in-house methods. For example, the strong acid digestion conducted be Norwest was actually a much milder method than the Aqua Regia Microwave Digestion used in-house. This created some difficulties for the comparison of these data.

5.2 Leaching Test

The leaching study was conducted to determine the potential for mineral dissolution of the sediment phase due to elevated carbon dioxide levels in water.

5.2.1 Key Findings

- The pH of the water in the reaction systems rapidly increased from ~4 to near neutrality, due to the rapid buffering ability of the carbonate minerals in the sediment.

- Calcium and magnesium concentrations in the water rapidly increased, suggesting that carbonate minerals such as calcite and dolomite were dissolved. Exchange reactions on the clay minerals could also account for the increase in magnesium concentration.

- Strontium, barium and iron also showed a distinct trend of dissolution. Strontium was most susceptible to dissolution under elevated dissolved CO_2 concentration; the trend was also distinct for barium and iron, although to a lesser extent.

- Iron levels in the aqueous phase appeared to reach a saturation point, at which time iron precipitates began to form. It is supposed that a sufficient quantity of oxygen was able to diffuse into the bottles and oxidize the iron, causing it to precipitate.

- The fine sediment is much more reactive than the sand and gravel fractions. The fines yielded significantly higher resultant pH and EC values, and the resultant concentration of most elements in the water was approximately two orders of magnitude higher for the fines, as compared to the sand or gravel.

5.2.2 Recommendations

- The leaching test should be conducted with groundwater rather than deionized water, in order to yield more representative results.

- Bottles that would be less susceptible to atmospheric interactions should be used for this type of test. If this were not feasible, the experiment should be conducted in an isolated carbon dioxide atmosphere.

5.3 Column Study

The column study expanded on the initial findings of the batch leaching study, yielding results more representative of the potential geochemical changes that may occur in an aquifer impacted by carbon dioxide.

5.3.1 Key Findings

- The carbon dioxide caused the pH of the groundwater to drop from approximately 7.6 to 5.5. This decrease in pH was buffered by the many carbonate species present in the formation. It is conceivable that over a longer period of time than was observed during this experiment, these pH values could be further decreased.

- The presence of carbon dioxide and the lower pH allowed for many metals present in the sediment to become dissolved into the aqueous phase. Most notable of these metals was iron, which then proceeded to form siderite, an iron carbonate precipitate.

- The formation of siderite was shown to cause a decrease in the hydraulic conductivity of the sediment.

- Other metals that were dissolved did not approach the Drinking Water Quality Guidelines outlined by the CCME, for the short-term duration of this experiment.

5.3.2 Recommendations

- The column study should be run for a longer period of time in order to determine some of the geochemical changes that may be observed beyond the very short term.

- In order to facilitate a longer test run, the construction of the apparatus should be changed. While the use of chemically inert materials helped to generate the most representative results, they do not have the durability or safety that would be gained by using stainless steel components. Although using metal parts would present charged surfaces which may have some impact on the final results, the apparatus surface relative to the sediment surface area is relatively insignificant. This would help to minimize the occurrence of leaks, which would enable continued accuracy for the monitoring of hydraulic conductivity while adding to the longevity of the experiment.

5.4 Geochemical Modeling

Geochemical modeling was conducted using PHREEQC to help determine the geochemical changes that were observed in the column, and therefore would likely be observed in the aquifer, under elevated CO_2 conditions.

5.4.1 Key Findings

- The model confirmed the dissolution of calcite and dolomite.
- Modeling results suggested that goethite, hematite, and $Fe(OH)_3$ were the geochemical source of the elevated iron levels in solution.
- Results from this analysis indicated that the iron precipitate formed in the column was in fact siderite.

5.4.2 Recommendations

- Measures should be taken to ensure that all major chemical species are analyzed and can be inputted into the model. Since silicate results were not available, many mineral species could not be considered in the model. Specifically, the extent of the clay mineral weathering could not be determined.

6.0 REFERENCES

Appelo, C.A.J., and Postma, D. 1996. Geochemistry, groundwater and pollution. A.A. Balkema, Rotterdam, Netherlands.

Benson, S.M. 2000. An overview of geologic sequestration of CO_2. ENERGEX 2000: Proceedings of the 8th International Energy Forum. Las Vegas, NV: 1219 – 1225.

Berner, R.A., and Caldeira, K. 1997. The need for mass balance and feedback in the geochemical carbon cycle. Geology.955 – 956.

Berner, R.A., and Lasaga, A.C. 1989. Modeling the geochemical carbon cycle. Scientific American. 74 – 81.

Brookins, D.G. 1988. Ef-pH diagrams for geochemistry. Springer-Verlag, Berlin.

Bruant, R.G., Giannar, D.E., Myneni, S.C.B., and Peters, C.A. 2002. Effect of pressure, temperature, and aqueous carbon dioxide concentration on mineral weathering as applied to geologic storage of carbon dioxide. Princeton University.

Bruno, J., Stumm, W., Wersin, P., and Brandberg, F. 1992. On the influence of carbonate in mineral dissolution:I. The thermodynamics and kinetics of

hematite dissolution in bicarbonate solutions at T=25°C. Geochimica et Cosmochimica Acta, **55**: 1139 – 1147.

Bruno, J., Stumm, W., Wersin, P., and Brandberg, F. 1992. On the influence of carbonate in mineral dissolution:II. The solubility of $FeCO_3$ (s) at 25°C and 1atm total pressure. Geochimica et Cosmochimica Acta, **56**: 1149 – 1155.

Butler, J.N. 1982. Carbon dioxide equilibria and their applications. Addison-Wesley.

Casey, W.H. and Sposito, G. 1992. On the temperature dependence of mineral dissolution rates. Geochimica et Cosmochimica Acta. **56**: 3825-3830.

Celia, M.A., and Bachu, S. 2002. Geological sequestration of CO_2: Is leakage unavoidable and acceptable? Princeton University.

Deer W.A., Howie, R.A. and Zussman, J. 1966. An introduction to the rock-forming minerals, 2nd Edition. Addison Wesley Longman Limited, England.

Fulton, R.J. 1989. Quaternary geology of Canada and Greenland. Geological Survey of Canada, Ottawa, Ontario.

Glass, D.J. 1990. Lexicon of Canadian stratigraphy: Volume 4 Western Canada. Canadian Society of Petroleum Geologists, Calgary, Alberta.

Herzog, H.J. 2001. What future for carbon capture and sequestration? Environmental Science & Technology. April: 148A – 153A.

Herzog, H., Eliasson, B. and Kaarstad, O. 2000. Capturing greenhouse gases. Scientific American. February: 72 – 77.

Holloway, S. 2001. Storage of fossil fuel-derived carbon dioxide beneath the surface of the earth. Annual Reviews, Energy and the Environment. **26**: 145-66.

Hossner, L.R. 1996. Dissolution for total elemental analysis. In Methods of Soil Analysis. Part 3. Chemical Methods. Soil Science Society of America and American Society of Agronomy, Madison, WI.

IEA Greenhouse Gas R&D Programme: Weyburn CO_2-EOR Project. Retrieved March 7, 2004, from http://www.ieagreen.org.uk

Kane, R.L. and Klein, D.E. 2001. Carbon sequestration: An option for mitigating global climate change. Chemical Engineering Progress, **97**(6): 45 – 52.

Kim, M., Nriagu, J. and Haack, S. 2000. Carbonate ions and arsenic dissolution by groundwater. Environmental Science and Technology. **34**: 3094 – 3100.

Lackner, K.S. 2002. Carbonate chemistry for sequestering fossil carbon. Annual Reviews, Energy and the Environment. **27**: 193-232.

Lackner, K.S., and Wendt, C.H. 1995. Carbon dioxide disposal in carbonate minerals. Energy, **20**(11): 1153 – 1170.

Langmuir, D. 1997. Aqueous environmental geochemistry. Prentice Hall, Upper Saddle River, New Jersey.

Liu, Z. and Zhao, J. 2000. Contribution of carbonate rock weathering to the atmospheric CO_2 sink. Environmental Geology. **39**(9): 1053-1058.

Morse, J.W. 1983. Carbonates: Mineralogy and chemistry. Mineralogical Society of America, Washington, D.C.

Pacala, S.W. 2002. Global constraints on reservoir leakage. Princeton University.

Parkhurst, D.L. and Appelo, C.A.J. 1999. Users guide to PHREEQC (Version 2) – A computer program for speciation, batch-reaction, one-dimensional transport, and inverse geochemical calculations. U.S. Geological Survey, Denver, CO.

Rau, G.H., and Caldeira, K. 1999. Enhanced carbonate dissolution: A means of sequestering waste CO_2 as ocean bicarbonate. Energy Conversion and Management, **40**: 1803 – 1813.

Reichle, D.R., Houghton, J., Kane, B. and Eckmann, J. 1999. Carbon sequestration research and development. A U.S. Department of Energy Report.

Sawyer, C.C., Parkin, G.F. and McCarty, P.L. 1994. Chemistry for environmental engineering, 4th Edition. New York: McGraw-Hill.

Schempf, F.J.,2001. Weyburn project plays double role. Hart's Energy & Petroleum, September: 75 – 77.

Whitaker, S.H. and Christiansen, E.A. 1972. The Empress Group in southern Saskatchewan. Canadian Journal of Earth Sciences, Volume 9, No.4, pp. 353-360.

White, W.B. 1997. Thermodynamic equilibrium, kinetics, activation barriers, and reaction mechanisms for chemical reactions in karst terrains. Environmental Geology. **30**: 46-58.

Xu, T., Apps, J.A. and Pruess, K. 2004. Numerical simulation of CO_2 disposal by mineral trapping in deep aquifers. Applied Geochemistry, Volume 19, pp. 917-936.

APPENDIX A

ANALYTICAL METHODS

A1.0 Titration for Carbon Dioxide Concentration in Water

A1.1 Introduction

This research project extensively makes use of carbonated water. In order to determine the concentration of carbon dioxide in water, a titration with sodium hydroxide (NaOH) must be performed. The titration reaction is as shown below in Reaction #1 (note that dissolved carbon dioxide exists as the metastable carbonic acid species).

$$H_2CO_3^* + NaOH \rightarrow H_2O + Na^+ + HCO_3^- \qquad (R.A1)$$

The titration can be conducted colorimetrically or potentiometrically. The colorimetric titration uses a phenolphthalein indicator to determine the endpoint, whereas the potentiometric titration utilizes a pH meter to determine the endpoint at a specific pH. For this measurement, potentiometric titration will be used since is known to be considerably more precise than colorimetric titration (Greenberg, 1995).

A1.2 Objective

The objective of this analytical procedure is to determine the amount of dissolved carbon dioxide in a water sample.

A1.3 Materials

The following reagents, glassware and equipment are required to complete this analytical procedure:

- 1N NaOH
- Deionized water
- Buffer solutions (pH=4.0, 7.0 and 10.0, for calibration of pH meter)

- 1L volumetric flask
- 100mL pipette
- Pipette bulb
- 32oz Nalgene LDPE container (with lid)
- 50mL burette
- Burette stand and clamp
- 100mL graduated cylinder
- 250mL beaker
- 100mL beaker
- Magnetic stirring plate (+ magnetic stir bar)
- pH meter

A1.4 Method

1. Prepare a solution of 0.1N NaOH by pipetting 100mL of 1N NaOH into a 1L volumetric flask and topping it up to the mark with deionized water. Transfer this solution into a labeled 32oz LDPE container for storage.
2. Perform a three-point calibration on the pH meter, using the pH=4.0, 7.0 and 10.0 buffer solutions. (The titration will range from pH ≈ 4 to 8.3)
3. Use the 100mL beaker to fill the burette with 0.1N NaOH to the 0.00mL mark.
4. Measure 100mL of carbonated water using the graduated cylinder. Transfer this water into the 250mL beaker with the magnetic stir bar.
5. Insert the pH probe into the beaker of water and wait for the initial reading to stabilize.
6. Start the magnetic stirrer. Be sure the speed of stirring is quite low so as to minimize turbulence in the system, and hence atmospheric interferences.
7. Begin adding the NaOH in small additions (~1mL) until the pH approaches the endpoint. When the pH is approximately 8.0, add the NaOH in a drop wise manner until the desired endpoint of pH=8.3 is reached. Record the total volume of titrant required.

8. Repeat Steps 3 – 7 at least once, or until agreement (±10%) in the results is achieved.

A1.5 Results

In order to determine the concentration of dissolved carbon dioxide in the water, the following calculation should be performed:

$$[CO_2] = \frac{V_t \times N \times 44{,}000}{V_s}$$

where: V_t = the volume (L) of NaOH titrant required
N = the normality of the NaOH titrant (0.1N)
V_s = the volume (L) of water being titrated (0.10L)

A1.6 References

Greenberg, A.E., L.S. Clesceri and A.D. Eaton, editors. (1995) *Standard Methods for the Examination of Water and Wastewater*, 18th Edition. Washington, D.C.: American Public Health Association.

A2.0 Titration for Alkalinity

A2.1 Introduction

Alkalinity is the capacity of a water to neutralize acids (Sawyer et al., 1994). The presence of salts of weak acids, as well as weak or strong bases may cause alkalinity in natural waters. Hydroxide, carbonate, and bicarbonate are the chemical species that contribute most of the alkalinity in natural waters. The mineral content results primarily from dissolving limestone or dolomite minerals in the aquifer. Carbon dioxide is closely related to alkalinity as shown in Reaction A2.

$$CO_2 + H_2O \leftrightarrow H_2CO_3^- + H^+ \leftrightarrow CO_3^{2-} + 2H^+ \qquad \text{(R.A2)}$$

The alkalinity titration with H_2SO_4 can be conducted colorimetrically or potentiometrically. The colorimetric titration uses a phenolphthalein indicator to determine the conversion of carbonate ion to bicarbonate ion or hydroxide to water, and a bromcresol green indicator for the conversion of bicarbonate to carbonic acid. The potentiometric titration utilizes a pH meter to determine the endpoints at a specific pH (pH=8.3, 4.5). For this measurement, a combination of potentiometric and colorimetric titration will be used. The color changing indicators will be used to determine when the endpoint is near (these inflection points are very abrupt potentiometrically), and the potentiometric method will be used to determine the exact endpoint since it is known to be a considerably more precise technique than colorimetric titration (Greenberg, 1995).

A2.2 Objective

The objective of this analytical procedure is to determine the alkalinity of a water sample.

A2.3 Materials

The following reagents, glassware and equipment are required to complete this analytical procedure:

- 1N H_2SO_4
- Deionized water
- Phenolphthalein indicator
- Bromcresol Green indicator
- Buffer solutions (pH=4.0 and 7.0, for calibration of pH meter)
- 1L volumetric flask
- 50mL burette
- Burette stand and clamp
- 100mL graduated cylinder
- 250mL beaker
- 100mL beaker
- Magnetic stirring plate (+ magnetic stir bar)
- pH meter

A2.4 Method

1. Prepare a solution of 0.01N H_2SO_4 by pipetting 10mL of 1N H_2SO_4 into a 1L volumetric flask and topping it up to the mark with deionized water.
2. Perform a two-point calibration on the pH meter, using the pH=4.0 and 7.0 buffer solutions. (The titration will range from pH $\approx$ 5.5 to 4.0)
3. Use the 100mL beaker to fill the burette with 0.01N H_2SO_4 to the 0.00mL mark.
4. Measure 50mL of carbonated water using the graduated cylinder. Transfer this water into the 250mL beaker with the magnetic stir bar.
5. Insert the pH probe into the beaker of water and wait for the initial reading to stabilize.

6. Start the magnetic stirrer. Be sure the speed of stirring is quite low so as to minimize turbulence in the system, and hence atmospheric interferences.
7. Add the phenolphthalein indicator to the water. If there is any pink coloration on addition of this indicator, titrate with the H_2SO_4 to a colorless endpoint. Record the volume of titrant required to reach this endpoint (P-alkalinity).
8. Add the bromcresol green indicator to the water. This will turn the water green, if there is any alkalinity present.
9. Begin adding the H_2SO_4 in small additions (~1mL) until the pH approaches approximately 5.0. Continue to add the H_2SO_4, in a drop wise manner until the desired endpoint of pH=4.5 is reached. Record the total volume of titrant required. At this pH the color indicator should be a grayish pink color.
10. Perform Steps 3 – 9 in duplicate (provided that a sufficient volume of water is available) to determine the precision in the analytical procedure.

A2.5 Results

In order to determine the alkalinity of the water, the following calculation should be performed:

$$alkalinity = \frac{V_t \times N \times 50{,}000}{V_s}$$

where: V_t = the volume (mL) of H_2SO_4 titrant required
N = the normality of the H_2SO_4 titrant (0.01N)
V_s = the volume (mL) of water being titrated (50mL)

A2.6 References

Greenberg, A.E., L.S. Clesceri and A.D. Eaton, editors. (1995) *Standard Methods for the Examination of Water and Wastewater*, 18th Edition. Washington, D.C.: American Public Health Association.

A3.0 Strong Acid Digestion of Sediments

A3.1 Objective

A strong acid digestion is carried out in order to determine the elemental composition of sediment samples. The strong acids digest the minerals into aqueous phase, which can then be easily analyzed by instrumental techniques such as Inductively Coupled Plasma Mass Spectroscopy (ICP-MS) and Ion Chromatography (IC).

A3.2 Materials

The following reagents, glassware and equipment are required to complete this analytical procedure:

- Concentrated (68-71%) HNO_3
- Concentrated (35-38%) HCl
- Deionized (DI) water
- Weighing boats
- Digital pipettor (1 – 10mL)
- 1oz Nalgene LDPE containers with lids
- Parafilm
- Drying oven
- Analytical balance
- Rock grinding mill
- Ethos Sel Microwave Extraction Unit

A3.3 Method

1. Begin by drying the sediment samples in the oven overnight at 80°C (or longer, as required).
2. After the sediment is dried it is ground in the mill, taking care to pre-crush any gravels larger than 7mm with a mortar and pestle. The sediment should be ground to powder, or "rock flour".
3. Carefully weigh (and record) approximately 0.3 – 0.5g of the rock powder into the Teflon reaction vessels of the Microwave Extraction Unit.
4. Using the pipettor, add 5.0mL DI water to the sediment in the reaction vessel. The water is added before the acids in order to avoid a vigorous reaction with any carbonates.
5. Again, using the pipettor, add 10.0mL HNO_3, followed by 3.0mL HCl. Always work in the fume-hood when using strong acids.
6. Insert the reaction vessels into the Microwave Extraction Unit, and secure for heating.
7. Run the "Soils-Environment-Aqua Regia" program. This program takes eight minutes to heat the microwave to 190°C, and holds it at this temperature for six minutes prior to cooling down.
8. When the microwave has cooled down, remove the reaction vessels.
9. In the fume-hood, open the vessels and transfer the contents to the 1oz containers. Use 2 × 3.0mL aliquots of DI water to rinse all of the digestion products from the vessel.
10. If the samples will be stored prior to analysis, cover the lids with Parafilm to help minimize any atmospheric interactions.

A3.4 Summary of Key Issues for Determining Elemental Composition of Sediment

In order to conduct a total elemental analysis on a nonhomogeneous sediment sample, the sample must be brought into a homogeneous solution (Hossner, 1996). Sediment can be brought into solution using either acid digestion or fusion agents.

Acid digestion is achieved by combining sediment samples with mixtures of strong inorganic acids which decompose the sample. Fusion agents tend to be used for the decomposition of samples that are insoluble in acids. It is mainly high temperatures that cause the decomposition effect on the fusion agents.

Key advantages associated with acid digestion include: rapid, high-purity acids that are readily available, and low salt matrix in final solution. Disadvantages include: using dangerous acids (especially if HF is used), corrosive acids, and low recovery of chromium and titanium is typical. Advantages of fusion include: corrosive and potentially explosive acids not required, Teflon-lined digestion bombs not required. Disadvantages of fusion are: high salt matrix in final solution, high potential for contaminants in fusion salts, relatively slow, and loss of volatiles. Acid digestion is typically preferred over fusion decomposition on account of the lower concentrations of extraneous material in the final solution and reduced interference when determining the solution composition. For this project, acid digestion was used.

A3.4.1 Microwave Acid Digestion

Acid digestion of sediment can be conducted in closed Teflon vessels in a microwave unit. This enables the dissolution of the sediment at relatively low temperatures and pressures. This allows for a shorter dissolution time, smaller acid volume requirements, decomposition of relatively insoluble components, and retention of volatile compounds (Hossner, 1996).

A3.4.2 Digestion with Aqua Regia

Aqua regia is a mixture of concentrated nitric and hydrochloric acids. It is effective in decomposing many minerals present in a sediment sample. Silicates are the only major mineral constituent in typical sediment samples that are not decomposed in aqua regia. In order to treat this issue, hydrofluoric acid can also be added to the

digestion acid mixture. This acid is known to break down silicates. The major downfall associated with the use of hydrofluoric acid is that it is one of the most dangerous mineral acids used in a laboratory setting. It attacks calcium in the body and forms a complex with bones. Boric acid is also required when hydrofluoric acid is used, to prevent the volatilization losses of SiF_4 gasses.

A3.4.3 Sources of Error Associated with Acid Digestion

Sampling error, sample heterogeneity, chemical changes and contamination of the sample during preparation for digestion all represent potential sources of error for the decomposition of sediment samples for analysis (Hossner, 1996). There is also the possibility of contamination through impurities present in reagents or by leaching of contaminants from the walls of the reaction vessel. Incomplete dissolution, losses of volatile components, formation of sparingly soluble compounds and complex compounds, and reactions with the vessel walls all present further sources of error associated with this method.

A4.0 Analysis by ICP-MS

A4.1 Objective

Inductively Coupled Plasma Mass Spectrometry (ICP-MS) is an accurate technique used to determine the elemental composition of various solutions. In this experimental program, types of solutions to be analyzed include groundwater, mineral leachates, and digested sediment samples.

A4.2 Materials

The following reagents, glassware and equipment are required to complete this analytical procedure:

- Analytical balance
- 50mL plastic centrifuge tubes
- Deionized water
- Perkin Elmer Multi-Element Standard (10mg/L Ag, Al, As, Ba, Be, Bi, Ca, Cd, Co, Cr, Cs, Cu, Fe, Ga, K, Mg, Mn, Mo, Ni, P, Rb, Se, Si, Pb, Sb, Sr, Ti, Tl, U, V, Zn)
- Pipettors with disposable tips
- Transfer pipettes
- Elan 9000 ICP/MS system
- ICP/MS autosampler tubes

A4.3 Method

This method is based on US EPA method 6020.

1. Prepare blank and standards (50mL each) in plastic centrifuge tubes. Standards should be prepared to concentrations of 2, 10, and 100µg/L. For ultimate

precision, these dilutions should be done gravimetrically, as compared to volumetrically. The matrix used for the blank and standards should be consistent with that of the samples to be analyzed. For example, if the sample matrix is water, the blank and standard matrix should be deionized water. Or if it is a digested sediment sample prepared in nitric acid, the blank and standards should be prepared in an equivalent concentration of nitric acid. If at all possible, care should be taken to avoid the use of hydrochloric acid (HCl) in the matrix as the chlorides cause many isobaric interferences in this analytical method. In the case of the digested sediment samples however, a small amount of HCl is present in the Aqua Regia solution.

2. The samples must also be prepared. They should also be prepared to exactly 50mL. This is important later, when the internal standard is added, such that it is consistent between each of the samples and standards. A concentrated sample (such as digested sediment) should be diluted between 100 and 1000 times. In this research program, these samples were run at both 100 and 1000 times dilution in order to determine the more dilute elements (100X) and to determine the more concentrated elements with less interferences (carryover, contamination) from other concentrated elements (1000X). If further dilutions (or more concentrated samples) are required they can be prepared later. It is better to start off with samples that are dilute, rather than concentrated samples that may contaminate the instrument.
3. Add 50ppb of internal standard to each sample, standard, and blank. This is equivalent to 0.25mL of 10ppm internal standard (Li, Sc, Ge, In, Tb, Y).
4. Pour the standards and samples into the autosampler tubes and insert into their designated positions.
5. Optimize and tune the Elan 9000 as per manufacturers directions (in manual).
6. The ICP/MS is run by the Elan (Version 2) software. Set the autosampler to run the standards and samples according to the US EPA Method 6020. The blank and standards are run first, immediately prior to running the samples. After inspection of the counts/concentrations of the various elements of interest, further dilutions or concentrations of the samples can be made and rerun.

7. Calibration verification standards should be run every 10 samples to ensure that the system is operating properly and generating accurate results. This should be a 10µg/L multi-element standard, preferably of a different stock solution than the calibration standards so that any mistakes in the preparation of these standards will also be caught.

A4.4 Results

A calibration curve is created for each individual element. The linear regression of this curve gives an indication of how well the instrument detects and measures each element. Typically the regression for major cations (Ca, Mg, Na, K, etc,) is not good, however these elements are more accurately measured using ion chromatography, so the measured values from this method are disregarded for these elements. Iron is another element that also did not calibrate particularly well. This is due to the occurrence of many isobaric interferences. For other elements, the software corrected these interferences very effectively, but not for iron. Iron analyses were conducted at an external laboratory in order to obtain meaningful results. In cases where more than one isotope of a particular element was measured, the regression value of the calibration curve must be taken into account to determine which isotope yields the most accurate results.

The peak intensity for each element in a sample is compared to the calibration curve for that element. The software then determines the concentration of each element relative to their calibration curves and outputs this measured value, along with the associated standard deviation.

A5.0 Analysis by Ion Chromatography

A5.1 Objective

Ion chromatography (IC) is a technique used to determine the concentration of major ions in solutions. The principle of this technique is that the solutions to be analyzed are pumped through a resin-bead column. The different cations and anions each have a characteristic retention time in the column. As the ions elute through the column, they then pass through a conductivity detector, which translates the conductivity reading into a concentration, based on calibration curves for each ion.

In this experimental program, types of solutions to be analyzed include groundwater, mineral leachates, and digested sediment samples.

A5.2 Materials

The following reagents, glassware and equipment are required to complete this analytical procedure:

- Analytical balance
- 50mL plastic centrifuge tubes
- Deionized water
- Dionex Six-Cation Standard (50mg/L lithium, 200mg/L sodium, 250mg/L ammonium, magnesium, 500mg/L potassium, calcium)
- Dionex Seven-Anion Standard (20mg/L fluoride, 100mg/L chloride, nitrite, nitrate, bromide, sulfate, 200mg/L phosphate)
- Pipettors with disposable tips
- Transfer pipettes
- Dionex ICS-2000 system (equipped with CS12A and AS14 columns)
- Dionex 10mL IC autosampler vials
- Cation eluent (20mN H_2SO_4)

- Anion eluent (10mN sodium carbonate/bicarbonate solution)

A5.3 Method

1. Prepare standards (at least 10mL each) in plastic centrifuge tubes. Standards should be prepared to concentrations of 2, 10, and 100mg/L (with respect to sodium for cations six-element standard and chloride for anions seven-element standard). For ultimate precision, these dilutions should be done gravimetrically, as compared to volumetrically.
2. Pour the standards and samples into the auto sampler vials and insert into their designated positions. If the samples are of a completely unknown nature, or if they are known to be relatively concentrated with respect to one or more ions, they should be diluted between 10 and 100 times. If this is to dramatic to still be able to detect other ions the samples can be rerun in a more concentrated form to measure the more dilute ions.
3. The IC system is run by Chromeleon software.
4. Let the system equilibrate itself with the appropriate eluent (cations or anions) being pumped through it for at least one hour prior to running any standards or samples. Be sure that the conductivity is within the appropriate range (<20μS/cm for anions and <1μS/cm for cations).
5. Set the auto sampler to run the standards for calibration, immediately prior to analyzing the samples.
6. Ensure that a good quality calibration has been achieved by checking the correlation coefficients. These should be as close as possible to 100 for each element if they are properly calibrated. Most elements typically calibrate very well with correlation coefficients of ~99.99%, however magnesium and ammonium are exceptions to this. Because ammonium is not an element of importance in this particular research program, this is of little consequence. Magnesium is a key element however, with the dissolution of dolomite. Because magnesium tends to have a lower correlation coefficient of ~96%, there is a greater source of experimental error associated with the measurement of this

element. This effect is reflected in the 20% margins of error applied to the magnesium measurements, compared to the <10% error associated with most other elements. .

7. A calibration verification standard should be run every 10 samples. This can be a sample of any composition within the calibration limits, of known or unknown composition. Each time it is run, the measured values should be within 5% of the original value for each element. When they begin to drift beyond those limits the system should be recalibrated. Typically there is little drift, and the system can run for several days before requiring recalibration.

A5.4 Results

A calibration curve is created for each individual element, based on the inputted concentrations and measured conductivities. The correlation coefficient of this curve gives an indication of how well the instrument measures each ion. The conductivity of each ion in a sample is compared to the calibration curve for that particular ion. The software then determines and outputs the concentration of each element based on the measured conductivity levels, relative to their calibration curves.

APPENDIX B

DETAILED MINERALOGY

1.	Classification: Color: Shape: Diameter:	Chert conglomerate Light grey Overall angular, "corners" sub-angular 20mm	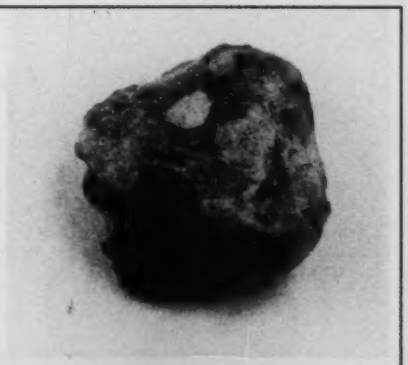
2.	Classification: Color: Shape: Diameter:	Granite – quartz, feldspar (albite?), biotite, potassium feldspar Grey, with reddish-brown and black flecks Sub-rounded 20mm	
3.	Classification: Color: Shape: Diameter: Other:	Dolomite Light grey Angular fragment (possibly a drilling relict) Effervesces in hot HCl (10%)	

4.	Classification: Color: Shape: Diameter: Other:	Calcite/limestone white, buff rounded (a) 22mm, (b) 27mm, (c) 12mm Effervesces strongly in cold HCl	 a b 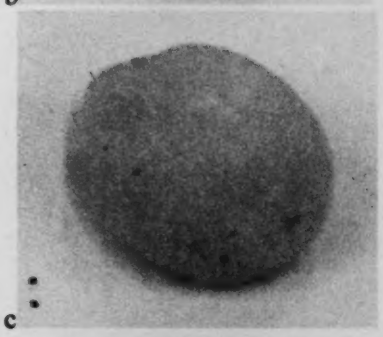 c
5.	Classification: Color: Shape: Other:	Coal Black Rounded Prominent joint surfaces (cleats) on dry samples. Bedding planes clearly visible. Red/brown layer (or deposits) on fractured surfaces.	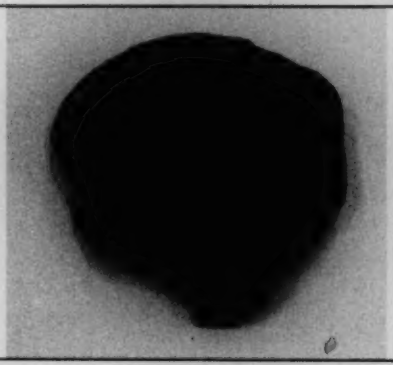

6.	Classification: Color: Shape: Diameter:	Granite, quartz, feldspar White, with iron staining Sub-rounded 32mm	
7.	Classification: Color: Shape: Diameter:	Granite, quartz, feldspar, trace biotite White Rounded 25mm	
8.	Classification: Color: Shape: Diameter:	Quartzite, trace biotite Grey Rounded 25mm	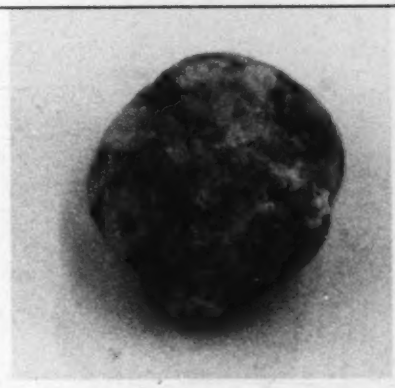

9.	Classification:	Chert	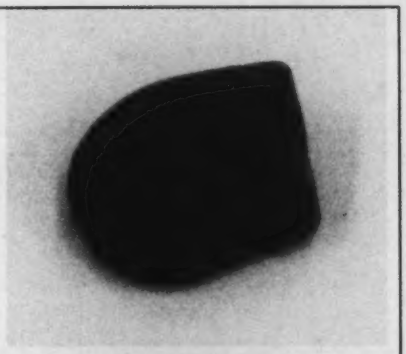
	Color:	Olive grey	
	Shape:	Rounded	
	Diameter:	10mm	
10.	Classification:	Carbonaceous – extremely fine grained	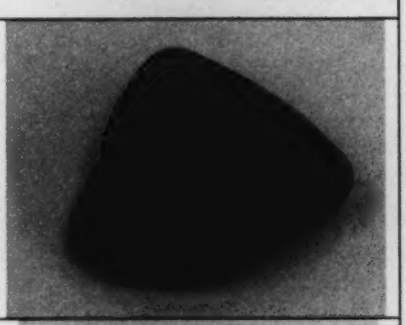
	Color:	Grey	
	Shape:	Rounded	
	Diameter:	30mm	
	Other:	Effervesces vigorously in cold HCl	
11.	Classification:	Carbonaceous – fine grained (dolomite?)	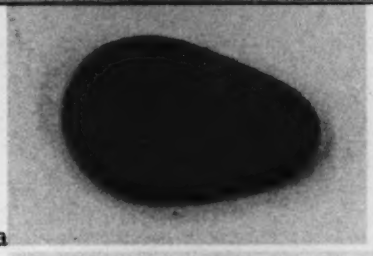 a
	Color:	Grey	
	Shape:	Rounded	
	Diameter:	(a) 24mm, (b) 10mm	
	Other:	Effervesces weakly in hot HCl	b

12.	Classification:	Quartzite	a 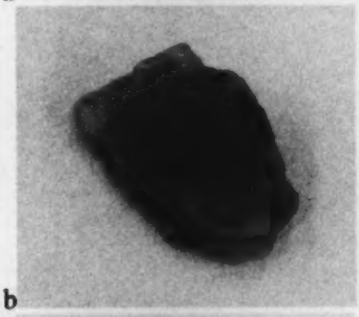 b c
	Color:	(a,c) Yellow/tan, (b) grey, translucent	
	Shape:	(a,c) Rounded, (b) angular	
	Diameter:	(a) 18mm, (b) 13mm, (c) 28mm	
13.	Classification:	Quartz, trace mica, non-calcareous, (quartzite?)	
	Color:	Dark grey	
	Shape:	Rounded	
	Diameter:	10mm	

14.	Classification:	Chert	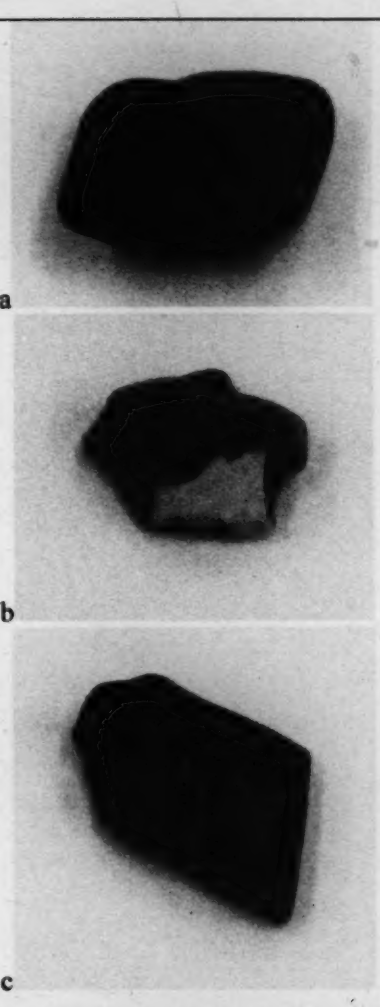
	Color:	(a) Brown/black, mottled, (b) olive brown, with white non-calcareous concretion, (c)grey	
	Shape:	(a,b) Sub-angular, (c) angular	
	Diameter:	(a) 17mm, (b) 13mm, (c) 18mm	
15.	Classification:	Quartzite, fine grained	
	Color:	Dark grey, with trace white flecks	
	Shape:	Flat, rounded	
	Diameter:	21mm	
	Other:	Does not effervesce in hot HCl	

16.	Classification: Color: Shape: Diameter:	Quartzite, trace biotite white/yellow white (a) angular, (b) sub-angular (a) 12mm, (b) 13mm	 a b
17.	Classification: Color: Shape: Diameter: Other:	Calcite, with a calcareous coating Grey, with a yellowish coating Flat, rounded 20mm Effervesces in cold HCl	
18.	Classification: Color: Shape: Diameter: Other:	Calcareous (limestone fragment in calcite cement) Grey. Fractured surface coated with rust/white colored concretion (breccia) Rounded, broken fragment 18mm Effervesces strongly in cold HCl	

19.	Classification:	Calcite/limestone, fine grained
	Color:	Whitish buff
	Shape:	Rounded - sub-angular
	Diameter:	8 - 20mm
	Other:	Strongly effervesce in cold HCl

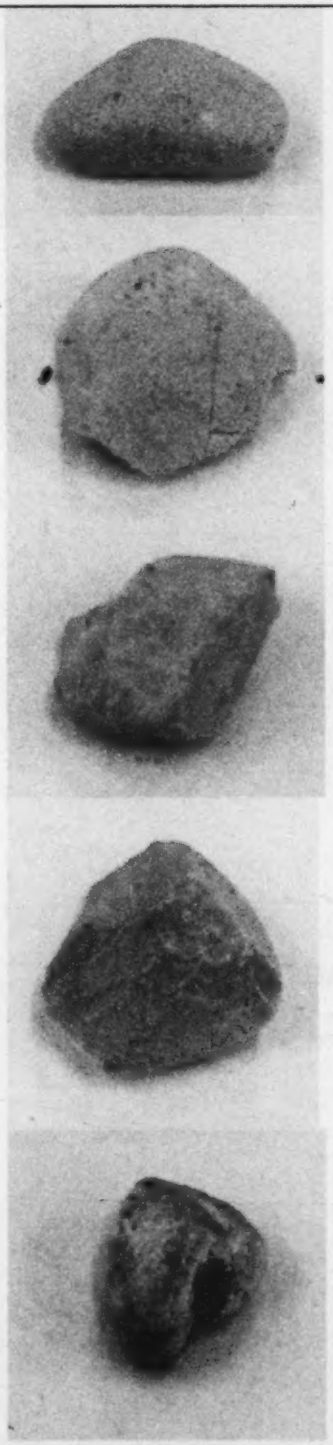

20.	Classification: Color: Shape: Diameter:	Quartzite White/grey Rounded 10mm	
21.	Classification: Color: Shape: Diameter:	Feldspar White and pink, mottled (flat surfaces) Angular 8mm	
22.	Classification: Color: Shape: Diameter:	Quartzite – quartz, trace biotite Grey Rounded 13mm	

23.	Classification:	Limestone
	Color:	Buff
	Shape:	Rounded - sub-angular
	Diameter:	9mm – 20mm
	Other:	Weakly effervesce in cold HCl

APPENDIX C

ADDITIONAL LEACHING TEST RESULTS
(600 & 1200mg CO_2/L SYSTEMS)

C1.0 Leaching Test Results for 600 mg CO_2/L Reactions

		Concentration [ug/g]						
		Day 1	2	4	8	16	32	64
Calcium	Ca	6.77E+00	6.70E+00	8.89E+00	8.90E+00	1.35E+01	1.32E+01	2.58E+01
Magnesium	Mg	6.15E-01	0.00E+00	1.27E+00	0.00E+00	1.97E+00	2.28E+00	2.89E+00
Sodium	Na	1.30E+00	8.72E-01	3.48E+00	1.41E+00	4.82E+00	6.42E+00	3.57E+01
Potassium	K	0.00E+00	0.00E+00	3.41E-01	0.00E+00	3.96E-01	0.00E+00	0.00E+00
Carbonate	CO3	0.00E+00	0.00E+00	0.00E+00	0.00E+00	0.00E+00	0.00E+00	0.00E+00
Bicarbonate	HCO3	0.00E+00	0.00E+00	0.00E+00	0.00E+00	0.00E+00	0.00E+00	0.00E+00
Sulphate	SO4	-2.50E+00	-2.37E+00	-1.68E+00	-1.67E+00	-7.55E-01	1.73E+00	5.96E+00
Chloride	Cl	-1.13E+01	-1.08E+01	-3.69E-01	-1.43E+00	1.02E+01	1.73E+01	3.52E+01
Nitrate - Nitrite	NO3, NO2 + NO3	0.00E+00	0.00E+00	0.00E+00	0.00E+00	0.00E+00	0.00E+00	0.00E+00
Total Iron	Fe	1.49E-02	1.03E-01	1.28E-01	1.94E-01	1.93E-01	1.52E-01	1.94E-01
Aluminum	Al	-8.64E-02	-8.27E-02	-7.94E-02	-8.15E-02	-8.71E-02	-8.18E-02	-8.50E-02
Antimony	Sb	-1.45E-04	-1.36E-04	-1.43E-04	-8.90E-05	-1.40E-04	-5.05E-05	-9.00E-05
Arsenic	As	9.17E-04	8.78E-04	3.71E-04	-4.77E-04	-4.80E-04	-5.00E-04	-5.29E-04
Barium	Ba	3.93E-02	5.25E-02	5.93E-02	6.27E-02	1.05E-01	9.59E-02	8.94E-02
Berryllium	Be	0.00E+00	0.00E+00	0.00E+00	0.00E+00	0.00E+00	0.00E+00	0.00E+00
Bismuth	Bi	0.00E+00	0.00E+00	0.00E+00	0.00E+00	0.00E+00	0.00E+00	0.00E+00
Cadmium	Cd	7.33E-06	1.17E-05	8.15E-06	1.02E-05	9.86E-06	7.32E-06	9.89E-06
Cesium	Cs	0.00E+00	0.00E+00	0.00E+00	0.00E+00	0.00E+00	0.00E+00	0.00E+00
Chromium	Cr	0.00E+00	0.00E+00	0.00E+00	0.00E+00	0.00E+00	0.00E+00	0.00E+00
Cobalt	Co	0.00E+00	0.00E+00	0.00E+00	0.00E+00	0.00E+00	0.00E+00	0.00E+00
Copper	Cu	-2.79E-04	3.06E-05	2.01E-04	-2.79E-04	-3.05E-05	3.35E-04	1.19E-04
Gallium	Ga	4.72E-05	0.00E+00	0.00E+00	1.00E-04	2.99E-04	2.83E-04	0.00E+00
Lead	Pb	-1.20E-04	-1.20E-04	-1.20E-04	-1.20E-04	-1.20E-04	-7.25E-05	-1.20E-04
Lithium	Li	-3.29E+00	-3.57E+00	-9.49E-01	-1.94E+00	3.22E-01	1.91E+00	-1.05E+01
Manganese	Mn	7.56E-04	5.68E-04	0.00E+00	0.00E+00	0.00E+00	0.00E+00	0.00E+00
Molybdenum	Mo	-5.56E-03	-5.74E-03	-5.05E-03	-5.85E-03	-6.51E-03	-6.70E-03	-6.95E-03
Nickel	Ni	3.42E-03	4.70E-03	3.73E-03	3.08E-03	1.41E-03	2.62E-03	2.06E-03
Phosphorus	P	0.00E+00	0.00E+00	0.00E+00	0.00E+00	0.00E+00	0.00E+00	0.00E+00
Rubidium	Rb	-1.51E-04	-9.84E-05	5.06E-05	3.37E-05	2.82E-05	3.74E-05	1.28E-04
Selenium	Se	1.32E-03	1.34E-03	1.06E-03	2.00E-03	1.99E-04	1.42E-04	0.00E+00
Silicon	Si (soluble)	-4.11E-03	-4.11E-03	-4.11E-03	-4.11E-03	-4.11E-03	-3.92E-03	-4.01E-03
Silver	Ag	0.00E+00	0.00E+00	0.00E+00	0.00E+00	0.00E+00	0.00E+00	0.00E+00
Strontium	Sr	9.44E-02	1.08E-01	1.64E-01	1.49E-01	2.02E-01	2.28E-01	2.56E-01
Sulfur	S	3.29E+01	4.75E+01	3.62E+01	4.30E+01	4.25E+01	3.40E+01	4.25E+01
Tellurium	Tl	0.00E+00	0.00E+00	0.00E+00	0.00E+00	0.00E+00	0.00E+00	0.00E+00
Titanium	Ti	-4.27E-04	1.59E-03	8.32E-04	3.40E-03	-1.00E-03	-2.84E-03	8.50E-04
Uranium	U	-9.69E-05	-1.90E-04	3.47E-04	2.94E-04	2.87E-04	3.28E-04	8.83E-05
Vanadium	V	0.00E+00	0.00E+00	0.00E+00	0.00E+00	0.00E+00	0.00E+00	0.00E+00
Zinc	Zn	1.63E-02	1.28E-02	1.17E-02	8.74E-03	6.47E-03	3.81E-03	1.15E-03

C2.0 Leaching Test Results for 1200 mg CO_2/L Reactions

		Concentration [ug/g]						
		Day 1	2	4	8	16	32	64
Calcium	Ca	1.53E+01	8.34E+00	1.07E+01	1.37E+01	9.26E+00	1.77E+01	3.25E+01
Magnesium	Mg	1.44E+00	9.13E-01	1.69E+00	2.22E+00	0.00E+00	3.21E+00	3.98E+00
Sodium	Na	3.96E+00	2.12E+00	4.78E+00	6.75E+00	-1.23E+00	8.16E+00	4.49E+01
Potassium	K	0.00E+00	2.75E-01	0.00E+00	0.00E+00	6.11E-01	4.03E-01	0.00E+00
Carbonate	CO3	0.00E+00	0.00E+00	0.00E+00	0.00E+00	0.00E+00	0.00E+00	0.00E+00
Bicarbonate	HCO3	0.00E+00	0.00E+00	0.00E+00	0.00E+00	0.00E+00	0.00E+00	0.00E+00
Sulphate	SO4	-1.60E+00	-2.15E+00	-1.20E+00	-6.08E-01	4.78E-01	1.55E+00	5.64E+00
Chloride	Cl	2.97E+00	-6.58E+00	8.26E+00	1.81E+01	1.94E+01	2.22E+01	3.78E+01
Nitrate - Nitrite	NO3, NO2 + NO3	0.00E+00	0.00E+00	0.00E+00	0.00E+00	1.29E-02	0.00E+00	0.00E+00
Total Iron	Fe	1.42E-02	6.17E-02	9.59E-02	1.67E-01	1.75E-01	1.83E-01	1.77E-01
Aluminum	Al	-8.27E-02	-8.50E-02	-7.78E-02	-7.13E-02	-8.41E-02	-6.08E-02	-8.29E-02
Antimony	Sb	-9.42E-05	-1.40E-04	-1.43E-04	-1.43E-04	-1.42E-04	-9.21E-05	-1.42E-04
Arsenic	As	1.30E-03	1.10E-03	3.81E-04	-1.53E-04	-3.92E-04	-3.87E-04	-4.88E-04
Barium	Ba	6.20E-02	5.56E-02	6.25E-02	8.38E-02	1.07E-01	8.20E-02	9.39E-02
Berryllium	Be	0.00E+00	0.00E+00	0.00E+00	0.00E+00	0.00E+00	0.00E+00	0.00E+00
Bismuth	Bi	0.00E+00	0.00E+00	0.00E+00	0.00E+00	0.00E+00	0.00E+00	0.00E+00
Cadmium	Cd	8.50E-06	9.58E-06	8.51E-06	8.39E-06	8.71E-06	9.19E-06	-3.99E-05
Cesium	Cs	0.00E+00	0.00E+00	0.00E+00	0.00E+00	0.00E+00	0.00E+00	0.00E+00
Chromium	Cr	0.00E+00	0.00E+00	0.00E+00	0.00E+00	0.00E+00	0.00E+00	0.00E+00
Cobalt	Co	0.00E+00	0.00E+00	0.00E+00	0.00E+00	0.00E+00	0.00E+00	0.00E+00
Copper	Cu	-1.34E-04	1.17E-04	-2.79E-04	-1.83E-04	-3.63E-05	2.61E-04	-2.79E-04
Gallium	Ga	0.00E+00	4.95E-05	4.84E-05	4.83E-05	5.83E-04	1.96E-04	0.00E+00
Lead	Pb	-7.13E-05	-7.02E-05	-1.20E-04	-1.20E-04	-1.20E-04	-1.20E-04	-1.20E-04
Lithium	Li	-1.38E-01	-2.36E+00	5.86E-01	2.19E+00	2.35E+00	3.44E+00	-1.05E+01
Manganese	Mn	6.78E-04	4.95E-04	2.42E-04	0.00E+00	0.00E+00	0.00E+00	0.00E+00
Molybdenum	Mo	-5.13E-03	-5.77E-03	-5.52E-03	-5.86E-03	-6.58E-03	-6.86E-03	-7.01E-03
Nickel	Ni	6.82E-03	7.63E-03	4.45E-03	4.00E-03	3.64E-03	1.28E-03	2.14E-03
Phosphorus	P	0.00E+00	0.00E+00	0.00E+00	0.00E+00	0.00E+00	0.00E+00	0.00E+00
Rubidium	Rb	1.53E-04	-2.55E-05	5.63E-05	1.99E-04	1.08E-04	1.16E-04	1.58E-04
Selenium	Se	7.74E-04	1.29E-03	7.74E-04	1.50E-03	4.86E-04	1.96E-04	0.00E+00
Silicon	Si (soluble)	-4.11E-03	-4.11E-03	-4.11E-03	-4.11E-03	-4.11E-03	-3.86E-03	-3.96E-03
Silver	Ag	0.00E+00	0.00E+00	0.00E+00	0.00E+00	0.00E+00	0.00E+00	0.00E+00
Strontium	Sr	1.80E-01	1.35E-01	1.69E-01	2.52E-01	2.75E-01	3.52E-01	3.17E-01
Sulfur	S	3.74E+01	4.09E+01	3.76E+01	3.75E+01	3.88E+01	4.03E+01	3.90E+01
Tellurium	Tl	0.00E+00	0.00E+00	0.00E+00	0.00E+00	0.00E+00	0.00E+00	0.00E+00
Titanium	Ti	-3.18E-04	4.23E-04	4.09E-04	1.32E-03	-1.55E-03	9.96E-04	3.24E-04
Uranium	U	2.58E-04	-8.54E-05	2.10E-04	3.52E-04	4.57E-04	2.24E-04	1.18E-04
Vanadium	V	0.00E+00	0.00E+00	0.00E+00	0.00E+00	0.00E+00	0.00E+00	0.00E+00
Zinc	Zn	2.21E-02	2.62E-02	2.13E-02	1.85E-02	1.68E-02	6.55E-03	9.29E-04

APPENDIX D

PHREEQC INPUT/OUTPUT FILES

```
SOLUTION_SPREAD
    -temp      20
    -units     mg/l
      Alkalinity  583mg/l as CaCO3
      Cl          667mg/l
      S(6)        121mg/l
      Ca          74mg/l
      Mg          31.9mg/l
      Na          580mg/l
      K           6.6mg/l
      Al          645ug/l
      Mn          0ug/l
      Fe(2)       0.33mg/l
      Zn          0.6ug/l
      Ba          11.6ug/l
      Si          8.63mg/l
      pH          7.60
      Description day 0

      Alkalinity  2500mg/l as CaCO3
      Cl          650mg/l
      S(6)        115mg/l
      Ca          520mg/l
      Mg          87mg/l
      Na          600mg/l
      K           19.5mg/l
      Al          250ug/l
      Mn          7ug/l
      Fe(2)       215mg/l
      Zn          15ug/l
      Ba          100ug/l
      Si          10mg/l
      pH          5.48
      Description after study


PHASES
   CH2O
   CH2O = 0.5CO2 + 0.5CH4
   log_k  0


INVERSE_MODELING 1
    -solutions      1        2
    -uncertainty    0.05     0.05
    -phases
        Calcite
        Dolomite
        Siderite          pre
        CO2(g)
        Gibbsite
        Goethite          dis
        K-feldspar        dis
        CH2O
        Fe(OH)3(a)
```

```
    Hematite
    SiO2(a)
-balances
    Cl          0.05      0.05
    K           0.05      0.05
    Na          0.05      0.05
    S           0.05      0.05
-range              1000
-tolerance          1e-010
-force_solutions    true true
-mineral_water      true
```

APPENDIX E

CALCULATIONS

E1.0 Buffer Capacity

E1.1 Original Groundwater

The first bracketed term is the contribution of water and dissolved carbonate species. The second term in brackets is the calcite contribution.

$$\beta = 2.3\left[(H^+)+(OH^-)+\frac{C_T 10^{10.3}(H^+)[10^{16.7}(H^+)^2+10^{7.0}(H^+)+1]}{[10^{16.7}(H^+)^2+10^{10.3}(H^+)+1]^2}\right] + 2.3\left[\frac{10^{8.5}(H^+)}{C_T}(2H^+ +10^{-6.4})\right]$$

$$C_T = (HCO_3^-) = 11.7\frac{meq}{L}, (CO_3^{2-}) = 0\frac{meq}{L}$$

$$\beta = 1.6\frac{meq}{L\ pH}$$

E1.2 Groundwater in pressurized column in equilibrium with calcite

$$\beta = 2.3\left[(H^+)+(OH^-)+\frac{C_T 10^{10.3}(H^+)[10^{16.7}(H^+)^2+10^{7.0}(H^+)+1]}{[10^{16.7}(H^+)^2+10^{10.3}(H^+)+1]^2}\right] + 2.3\left[\frac{10^{8.5}(H^+)}{C_T}(2H^+ +10^{-6.4})\right]$$

$$C_T = (HCO_3^-) = 49.2\frac{meq}{L}, (CO_3^{2-}) = 0\frac{meq}{L}$$

$$(H^+) = 10^{-pH} = 10^{-5.5}$$

$$\beta = 11.2\frac{meq}{L\ pH}$$

E1.3 Groundwater in pressurized column in equilibrium with clays

$$\beta = 2.3\left[(H^+) + \frac{K_w}{(H^+)} + 10^{6.5}(H^+)\right]$$

$$(H^+) = 10^{-pH} = 10^{-5.5}$$

$$\beta = 23.0\frac{meq}{L\ pH}$$

E2.0 Siderite Formation

The following equilibrium relationships apply to the formation of the carbonate mineral siderite:

$Fe^{2+} + HCO_3^- \leftrightarrow FeCO_3 + H^+$

$$K = \frac{[H^+]}{[Fe^{2+}][HCO_3^-]} \qquad K = 1.66, \log K = 0.22$$

$[HCO_3^-] = 0.0516 mol/L$

$$\log K = -pH - \log[Fe^{2+}] - \log[HCO_3^-]$$

$$\begin{aligned} pH &= -\log K - \log[Fe^{2+}] - \log[HCO_3^-] \\ &= -0.22 - \log[Fe^{2+}] - \log[0.0516] \\ &= 1.067 - \log[Fe^{2+}] \end{aligned}$$

For pH = 5.4 (approximate conditions in column), what $[Fe^{2+}]$ is required to be within the siderite stability field?

$$\begin{aligned} \log[Fe^{2+}] &= 1.067 - pH \\ &= 1.067 - 5.4 \\ &= -4.333 \end{aligned}$$

$$\begin{aligned} [Fe^{2+}] &= 4.65 \times 10^{-5} \frac{mol}{kg} \\ &= 4.65 \times 10^{-5} \frac{mol}{kg} \times \frac{56g}{mol} \times \frac{1000mg}{L} \\ &= 2.6 \frac{mg}{L} \end{aligned}$$

The iron concentration in solution exceeds this concentration many times. Because the redox conditions of the water are not known precisely, the following calculation was performed in order to determine if the Fe(II) rich clay minerals could have contributed enough iron to be within the siderite stability field.

47282μg/g Fe in fines before column study
33774μg/g Fe in fines after column study

ΔFe = 13508μg/g in fines over the duration of the column study

1.07kg of fines, based on particle size distribution and total mass of solids in the column.

Therefore, the total amount of iron that has gone into solution from the fines is:

$$13508\frac{\mu g}{g} \times 1.0kg \times \frac{1000g}{kg} = 14453mg\ Fe$$

The total volume of water in the column (and reservoir) is 10.9L, therefore the concentration of iron in solution can be determined:

$$[Fe] = \frac{14453mg}{10.9L} = 1326\frac{mg}{L}$$